The magmatic architecture of continental flood basalts I : Observations from the Deccan Traps

Tushar Mittal [1,2], **Mark A. Richards**[2,3], **Isabel M. Fendley**[2,4]

[1]Department of Earth, Atmospheric and Planetary Sciences, Massachusetts Institute of Technology, Cambridge, Massachusetts, USA
[2]Department of Earth and Planetary Science, University of California, Berkeley, California, USA
[3]Department of Earth and Space Sciences, University of Washington, Seattle, Washington, USA
[4]Department of Earth Sciences, University of Oxford, Oxford, UK

Key Points:

- We compile diverse observations from geochronology, geochemistry, volcanology for the Deccan Traps to constrain magmatic architecture.
- These different datasets consistently suggest large, frequent eruptions for Deccan Traps (and potentially other CFBs).
- Constraints from Deccan eruptive tempo, geophysics, and geochemistry are inconsistent with the large crustal magma reservoir model.

Corresponding author: Tushar Mittal, tmittal2@berkeley.edu

Abstract

Flood basalts are some of the largest magmatic events in Earth history, with intrusion and eruption of millions of km^3 of basaltic magma over a short time period ($\sim$ 1-5 Ma). A typical continental flood basalt (CFB) is emplaced in hundreds of individual eruptive episodes lasting decades to centuries with lava flow volumes of 10^3- 10^4 km^3. These large volumes have logically led to CFB models invoking large magma reservoirs ($> 10^5$-10^6 km^3) within the crust or at Moho depth. Since there are currently no active CFB provinces, we must rely on observations of past CFBs with varying degrees of surface exposure to develop and test models. In the last few decades, significant improvements in geochronological, geochemical, paleomagnetic, volcanological, and paleo-proxy measurements have provided high-resolution constraints on CFB eruptive tempo - the volume, duration, and frequency of individual eruptive episodes. Using the well-studied Deccan Traps as an archetype for CFB systems, we compile multiple lines of evidence - geochronology, eruption tempo, dike spatial distribution, intrusive-extrusive ratio, geochemical variations, and volcanological observations - to assess the viability of previous models. We find that the presence of just a few large crustal magma reservoirs is inconsistent with these constraints. Although observations from the Deccan Traps primarily motivate our model, we discuss constraints from other CFBs to illustrate that this conclusion may be broadly applicable, with important implications for interpreting CFB geochemical datasets as well as the timing and volumes of climate-altering volatile emissions associated with CFBs.

1 Introduction

Continental flood basalt provinces (CFBs) are cataclysmic magmatic events, whose brief "main-phases" (durations $\sim$ 1 Ma; V. E. Courtillot & Renne, 2003; Bryan et al., 2010; V. Courtillot & Fluteau, 2014; R. E. Ernst & Youbi, 2017; H. Svensen et al., 2018) are associated with eruption of millions of km^3 of dominantly pāhoehoe basaltic lava flows over vast areas (e.g., Self et al., 1998; J. J. Mahoney & Coffin, 1997; Bryan & Ferrari, 2013; R. E. Ernst, 2014, and references therein). CFBs are commonly associated with a large degree of mantle melting due to the arrival of a deep mantle plume head at the base of the lithosphere (e.g., M. A. Richards et al., 1989; Campbell & Griffiths, 1990; Farnetani & Richards, 1994; R. E. Ernst, 2014; R. E. Ernst et al., 2019). Typically, full CFB sequences have an overall duration of about 5-15 Ma (V. E. Courtillot & Renne, 2003; V. Courtillot & Fluteau, 2014; H. Svensen et al., 2018), with the much briefer main-phase eruptions accounting for the majority of the erupted volume (e.g., $>$ 60% for the Deccan Traps, M. A. Richards et al. (2015), $\approx$ 87 % for the Columbia River Basalt, Kasbohm and Schoene (2018)). CFBs are also important events for solid earth-climate interaction, since they are frequently temporally correlated with significant environmental perturbations on a global scale, including major mass extinctions and rapid climate change (e.g., Wignall, 2001; M. T. Jones et al., 2016; R. E. Ernst & Youbi, 2017; Clapham & Renne, 2019; Torsvik, 2020).

The main phase of each CFB is composed of hundreds of individual eruptive episodes, each representing almost continuous eruptions from a single or set of connected vents (Self et al., 2014). In the field, each eruptive episode comprises a flow-field built up of one or several lava flows (See Thordarson & Self, 1998; Self et al., 1998; Jay et al., 2009, for more discussion of the terminology). Analysis of typical CFB flow fields, especially for the well-studied Columbia River Basalt province, suggest that they were emplaced over at least a decade, and likely over multiple centuries (Vye-Brown, Self, & Barry, 2013). Individual flow fields in CFBs have lava volumes ranging from 10^3- 10^4 km^3 (Self et al., 2008; Bryan et al., 2010; Self et al., 2014).

By comparison with present-day basaltic volcanism (e.g., Kilauea, Laki, Piton de la Fournaise), individual CFB eruptive episodes represent a separate class of basaltic

volcanism in terms of both volume (1000s of km^3 vs. 19.6 km^3 for Eldgjá 939 eruption, the largest known lava eruption in human history) and areal extent (10^5 km^2 vs. 780 km^2 for Eldgjá 939 eruption) (Thordarson et al., 2001; Oppenheimer et al., 2018). Hence, the term "flood" basalt. *These huge erupted volumes, combined with relatively homogeneous magma compositions during eruptive episodes, pose significant challenges to understanding crustal magma transport, underscoring two fundamental questions: What are the geophysical conditions, with respect to melt generation and transport, that are required for CFBs ? What is the crustal plumbing system of these CFBs that permits large, repeated individual eruptive events? This magmatic architecture is related to a key question: why do flood basalts erupt persistently in such large eruptive episodes?*

In this set of papers, we explore the hypothesis that the unique character of "flood" basalt eruptions is a consequence of extraordinarily large mantle melt flux distributed over a broad region at the base of the lithosphere. This magma flux in turn establishes a distinct crustal magmatic architecture (compared to modern Ocean Island Basalts), which acts as the transfer function between the quasi-continuous mantle melts and the spatially and temporally localized individual eruptive episodes. Melt transport through the mantle lithosphere may act as an additional control on this behavior of melt focusing. However, once the melt pathways (dikes or two-phase channelization instabilities) are established, the timescale for magma transport through this system is expected to be relatively fast, continuous, and long-lived (Lister & Kerr, 1991; Rubin, 1995; Fowler, 2011).

The CFB magmatic system must consist of an interconnected network of sills or magma reservoirs (layered mafic intrusions) throughout the crust, Moho depth (magmatic underplating), and within the mantle lithosphere (R. E. Ernst et al., 2019, and references therein). This magmatic plumbing network transports millions of km^3 of magma from the underlying mantle plume sources and distributes it as intrusions, and onto the Earth's surface as flood basalts (e.g., R. E. Ernst, 2014). However, there is significant uncertainty on how large these components are and how they combine into a crustal magma system geometry that enables efficient transfer of large magma volumes from a mantle plume source to the surface (Jerram & Widdowson, 2005; R. E. Ernst, 2014; Cruden & Weinberg, 2018; Coetzee & Kisters, 2018; Magee et al., 2018; Magee, Ernst, et al., 2019). The only quantitative models for CFB magmatic architecture (Karlstrom & Richards, 2011; Black & Manga, 2017, see more description in Section 2.2) assume that the large eruptive episodes are fed from correspondingly large magma reservoirs ($> 10^4$-10^6 km^3) within the crust and/or at Moho depth through dikes. As we show in later sections of this paper, this assumption is not well-founded in terms of available constraints.

In order to test possible models, we must rely upon observations of erupted CFBs since there is no modern-day active CFB province where the magmatic architecture can be inferred from direct geophysical methods. However, one of the primary difficulties with this approach is that we seldom have exposure of both the sub-crustal magmatic system and the overlying lava flow system in the same setting. For example, layered mafic intrusions (e.g., the Bushveld complex) and giant radiating dike swarms (e.g., McKenzie dike swarm) are interpreted to represent the crustal magma system and the feeders for massive overlying volcanic provinces (R. Ernst et al., 2010; Buchan & Ernst, 2019; R. E. Ernst et al., 2019). However, in most of these cases, there are either no remaining lava flows or geochronologic constraints on the eruptive fluxes or volumes of lava flows (e.g., Bushveld complex Lenhardt & Eriksson, 2012). Additionally, there is the additional complexity that we are observing the final integrated system after solidification, and it is difficult to infer the temporal history vis-a-vis surface eruptions.

Conversely, for most Phanerozoic flood basalts with good temporal constraints on eruption rate for individual flow units, there are limited direct observations (exposures) of the trans-crustal magmatic system. In a few CFBs such as the Siberian

Traps, North Atlantic Magmatic Province, and Karoo-Ferrar Traps (all with a thick sedimentary basin overlying the basement and underlying the lavas), multiple studies have analyzed the numerous interconnected stacked sill-dike complexes to provide constraints on very shallow (< 3 km) CFB plumbing systems (e.g., H. Svensen et al., 2012; S. M. Jones et al., 2019; Hoggett, 2019; Magee, Ernst, et al., 2019, and references therein). Analogously, extensive geophysical and geochemical analysis of the dike swarms feeding surface lava flows has helped develop our understanding of the shallow CFB plumbing system (e.g., Vanderkluysen et al., 2011; Rivalta et al., 2015; Kavanagh, 2018; Magee, Ernst, et al., 2019; Buchan & Ernst, 2019). However, the magma transport relationship between dike swarms, sills, mid-crustal, and Moho depth magma reservoirs, and the mantle melt generation region remains unclear due to limited observational constraints (e.g., D. H. Elliot & Fleming, 2018, and references therein for the Karoo CFB). The primary direct observational support for the large magma reservoir model comes from the presence of thick ($\sim$ 5-15 km) high-velocity features above the Moho location in multiple CFBs (Emeishan, Deccan, Siberian, and Columbia River flood basalt provinces K. G. Cox, 1993; Ridley & Richards, 2010) as expected from the presence of solidified olivine- and clinopyroxene-rich cumulates in deep magma reservoirs (Farnetani et al., 1996). However, it is difficult to distinguish lower velocity crustal magma bodies from seismic data alone. Similar to layered mafic intrusions, geophysically observed mafic-ultramafic bodies represent the final time-integrated igneous evolution of mantle-generated melts with no information whether the features represent a single magma reservoir that was molten at the same time or was constructed incrementally (R. B. Larsen et al., 2018; Robb & Mungall, 2020).

An alternative method to test the validity of models for CFB magmatic architecture is to use the tempo of eruptive episodes. Specifically, this requires constraints on three key variables: the duration, volume, and frequency of individual eruptive episodes. *The primary process that controls the eruptive tempo must be the magmatic architecture of CFBs.* For example, the analysis by Black and Manga (2017) shows that in a magmatic architecture consisting of two large magma reservoirs (Moho and shallow-crustal levels), buoyancy overpressure is the primary mechanism for triggering CFB eruptions. This buoyancy overpressure is, in turn, controlled by the volatile content of the primary magmas. Due to the incompatible nature of magmatic volatiles (CO_2 and H_2O) during mantle melting, the initial low degree partial melts will be volatile-rich and are expected to erupt in frequent, low volume eruptive episodes. By contrast, subsequent higher degrees of partial melts will accumulate in a large magma reservoir and become eruptible by volatile buoyancy over 10^5 - 10^6 years. Thus, the expected eruptive tempo during the main volumetric phase of CFBs is a few brief ($\sim 10^4$ yr) eruptive episodes with long (10^5 - 10^6 year) hiatuses in surface eruptions in-between them, again incompatible with observations, as discussed in detail below.

In this study, we use a compilation of recent datasets from the Deccan Traps CFB to estimate the eruptive tempo of eruptive episodes, in order to test the models for CFB magmatic architecture. The Deccan Traps (DT) are a continental flood basalt province (primarily tholeiitic) occupying an area of over 500,000 sq. km. in Western India, whose main-phase eruptions spanned $\sim$1 Ma beginning at about 66.3 Ma (e.g., Sprain et al., 2019; Schoene et al., 2019). The primary source of erupted magma was likely decompression melting in a large plume head (hundreds of km across) marking the arrival of the Réunion plume (M. A. Richards et al., 1989; Campbell & Griffiths, 1990). Due to extensive research over the past few decades, there are high-resolution constraints on eruption rate based on geochronology (Renne et al., 2015; Schoene et al., 2015; Sprain et al., 2019; Schoene et al., 2019), paleomagnetic directional groups (Chenet et al., 2008, 2009), as well as Hg chemostratigraphy (Percival et al., 2018; I. M. Fendley, Mittal, Sprain, et al., 2019) along with extensive geochemical characterization of the lava flows (e.g., K. G. Cox & Hawkesworth, 1984; Beane et al., 1986; Lightfoot & Hawkesworth, 1988; J. J. Mahoney, 1988; Z. Peng et al., 1994, 1998; Sano

et al., 2001). Additionally, the many geophysical datasets from gravity, seismic, and magnetotelluric observations provide constraints on the sub-surface magmatic structure feeding the lava flows (e.g., Patro et al., 2018). The Deccan Traps have a clear geophysical, as well as geochemical (and isotopic) signature associated with melt production from a mantle plume head, which also provides some constraints on the rate of melt input into the crustal column.

In aggregate, the available data sets constraining eruptive tempo for the Deccan Traps are unique among all CFBs. The closest CFB with comparable data sets is the Miocene Columbia River Basalts (CRB) with extensive geochemical and volcanological studies (P. Hooper, 1988a; P. Hooper & Hawkesworth, 1993; Barry et al., 2013; Wolff & Ramos, 2013). However, the total erupted volume of the CRB ($\geq$ 210,000 km^3; S. P. Reidel et al., 2013) is much smaller than for other CFBs. Additionally, the onset of the largest phase of Deccan volcanism, responsible for about 2/3 of the total erupted known DT volume, is coincident, within Ar-Ar age precision, with the Cretaceous-Paleogene boundary (M. A. Richards et al., 2015; Sprain et al., 2019). This temporal coincidence makes understanding the magmatic architecture of the Deccan Traps of special interest, given the recent hypothesis that this most voluminous phase of Deccan eruptions were accelerated ("triggered") by the strong ground motion from the Mw$\sim$11 Chicxulub impact (M. A. Richards et al., 2015).

In Section 2, we review published conceptual and physical models for CFBs to illustrate the predictions from previous models. In Section 3, we provide a summary of the various observational constraints from the Deccan Traps (along with some additional data sets from other well studied flood basalt provinces such as the Columbia River Basalts and Siberian Traps) for eruptive tempo constraints. This is followed by a discussion of the stratigraphic geochemical variations (Section 4), exposed magmatic architecture (dikes and sills, Section 5), and geophysical observations (Section 6) as constraints on the magmatic plumbing system of CFBs. Finally, in Section 7, we summarize the results of our observational analysis and comparison with previous models.

2 Proposed Models for CFB magmatic architecture

Upon reviewing the literature on CFBs it becomes apparent that there have been remarkably few quantitative, much less well-accepted, models proposed to explain the uniquely large total erupted volumes (typically $> 10^6$ km^3), or the large volumes of individual eruptive episodes, compared to contemporary basaltic volcanism. To first order, it has been proposed that CFBs are just a consequence of the larger mantle melt flux from a mantle plume head with this melt erupting to the surface through some process. Nevertheless, we feel that it is important here to review the basics of the models that have been put forward previously in order to provide a fuller context for understanding our focus on the question: How are the processes of melt generation and lithosphere-crustal melt transport different for CFBs compared to other, much less voluminous, forms of basaltic volcanism?

Regarding melt generation, the conclusion based on a large number of studies analyzing extensive geochemical data sets for major CFBs, seismic imaging, plate reconstruction models, and geodynamic models is that CFB melts are derived from three potential sources: partial melting of hot mantle plume heads (e.g., M. A. Richards et al., 1989; J. J. Mahoney, 1988; R. White & McKenzie, 1995; Lassiter & DePaolo, 1997; S. A. Gibson, 2002; Sobolev et al., 2011; G. Sen & Chandrasekharam, 2011; Jennings et al., 2019, and references therein), melting of the overlying metasomatized lithospheric mantle material due to the plume thermal anomaly (Arndt & Christensen, 1992; J. S. Marsh, 1987; Lightfoot & Hawkesworth, 1988; Mckenzie & Bickle, 1988; Lightfoot et al., 1993; Turner & Hawkesworth, 1995; Natali et al., 2017; Black &

Gibson, 2019; S. A. Gibson et al., 2020, and references therein), and other crustal-asthenospheric melting processes (e.g., Arndt, 1989; J. S. Marsh, 1989; Lassiter & DePaolo, 1997; Kempton & Harmon, 1992; H. C. Sheth, 2005). Of these, the plume head model is by far the most widely accepted. Nevertheless, irrespective of the specific source, the large volume of buoyant partial melts must migrate through the lithosphere via a combination of dikes and/or two-phase channelization instabilities to feed the crustal CFB magmatic system (Rabinowicz & Ceuleneer, 2005; Schiemenz et al., 2011; Solano et al., 2012; T. Keller et al., 2013; Madrigal et al., 2015; Yarushina et al., 2015; Schmeling et al., 2018, 2019).

Rising CFB melts encounter a rheological contrast at or above the Moho since, depending on the geotherm and the fluid saturation state, the lower crust is either weaker than the upper crust, and lithospheric mantle or is stronger than the underlying lithospheric mantle (e.g., Bürgmann & Dresen, 2008; K. G. Cox, 1993; Fyfe, 1992). In both cases, the CFB magmas are expected to accumulate at Moho depth by magmatic underplating. Additionally, depending on the volatile content of the melt, the Moho may also be a density barrier leading to melt accumulation at these depths. Thus there are physical reasons to expect the formation of magmatic reservoirs at Moho depths beneath flood basalt provinces. These conclusions are further supported by various geophysical observations for crustal underplating in flood basalts (K. G. Cox, 1993; Bryan et al., 2010; Ridley & Richards, 2010; M. A. Richards et al., 2015; Farnetani et al., 1996, See Section 6.1 for more discussion). Finally, melt accumulated in these Moho-depth magma reservoirs, as well as additional shallow crustal magma bodies, feed large, dike-fed fissure eruptions (e.g., R. Ernst et al., 2001; R. E. Ernst et al., 2019; Magee et al., 2018, and references therein).

Besides this general framework, it remains unclear how the large individual magma reservoirs are if they also exist at shallower depths, and how the magmatic system supplies vast volumes of magma to large individual eruptions (e.g., Morrison et al., 1985). So far, only a few models have been advanced for crustal magmatic processes specific to CFBs despite decades of geochemical studies on these systems. These models are primarily conceptual in nature, and largely motivated by petrological observations. There are only two published (to the best of the authors' knowledge) quantitative or physical models for crustal magmatic processes specific to CFBs, which seems curious for the largest eruptions of igneous rock on our Earth.

In this study, our focus is on the crustal magma transport system for CFBs. Hence we are largely agnostic about the actual source of primary melting as well as the processes of melt transport through the lithosphere.*Additionally, we use the term "magma reservoir" to refer to a well-mixed magma body which can be represented by a volume-averaged temperature, melt and volatile composition.* We choose this definition not to imply that individual magma bodies of any size must necessarily be compositionally, thermally, and rheologically well mixed (see discussion in B. D. Marsh (2013) about the relevant processes), but rather for model consistency. Typically, most petrological models and magma physics models (including the new models in this Paper II), assume that the magma bodies have a single representative temperature, pressure, and melt composition, such that a single very large magma chamber with significant spatial variations in thermal, chemical, and rheological properties (e.g., mush zones) will be represented as multiple magma reservoirs with a high degree of connectivity in between them.

In the following, we first describe the various conceptual CFB models followed by a description of the two published quantitative models. We specifically highlight the magmatic architecture proposed by these models, especially the size of individual magma reservoirs, along with the observational motivation.

2.1 Conceptual Models

The first conceptual magmatic models for continental flood basalts was proposed by K. G. Cox (1980). He envisioned that the CFB magmatic system consists of a large (multi-km thick) crustal sill complex at/or close to Moho depth as the primary melt accumulation location, along with an elaborate network of dikes and sills for feeding surface lava flows. In the K. G. Cox (1980) model, the parental picritic magma (MgO >15 wt.%) undergoes extensive fractional crystallization in the lower crustal sill complex with progressive fractionation of an ultramafic cumulate phase, and with a residual lower density evolved basaltic magma (MgO contents <8 wt.%, also see K. G. Cox & Hawkesworth, 1984). If the density of this magma were sufficiently lower than the overlying crustal column, the consequent buoyancy overpressure was hypothesized to lead to surface eruptions with some short-duration storage in an upper sill complex. A key feature of this model is that the relatively homogeneous composition of flood basalts is explained as a consequence of compositional buffering due to the crystallization of olivine, clinopyroxene, and plagioclase. In addition,K. G. Cox (1980) proposed that the observed small scale variation within this relatively homogeneous basaltic composition can be explained by small contributions of trans-crustal polybaric fractionation during magma ascent through the dike-sill network (See also K. Cox and Hawkesworth (1985), and H. Sheth (2016) for variants of this model).

More recently, R. E. Ernst et al. (2019) proposed a similar structural model for a CFB magmatic system with an extensive primary underplated magma reservoir(s) spanning hundreds of km laterally and up to 20 km in thickness. The magma is then envisioned to ascend both laterally outward and vertically through the crust via a large number of dikes (radiating, linear, or circumferential). During this transport, the magma can periodically accumulate in mafic-ultramafic intrusions of various shapes (e.g., multiple-km wide dikes: 2580 Ma Great dike of Zimbabwe; multiple km thick upper-to-mid crustal sills: 2060 Ma Bushveld and 2710 Ma Stillwater complexes; funnel-shaped intrusions: Rum and Skye igneous complexes associated with 56 Ma North Atlantic Magmatic province), and in sill complexes in sedimentary basins.

Another class of related models has been proposed by Heinonen et al. (2019a), and Neumann et al. (2011) (and references cited therein) for CFB magma transport, specifically focused upon explaining the range of lava major and trace element compositions and mineralogy. These studies use a combination of Assimilation Fractional Crystallization (AFC) and energy-constrained AFC (EC-AFC) models (Spera & Bohrson, 2001; Bohrson & Spera, 2001; Spera & Bohrson, 2002; Bohrson & Spera, 2007) to assess what P-T conditions can match measured compositions. They suggest that the flood basalt magmatic plumbing system consists of a two-stage network wherein the magma undergoes AFC first at deep crustal depths ($\sim$ 10-30 km), followed by Fractional Crystallization (FC) in a shallow magma reservoir (3-5 km depth). A vital feature of this model is that of order 10-20 % assimilation of crustal material into the parental magma only occurs at a deeper depth. The Heinonen et al. (2019b) study proposes that the lack of shallow crustal assimilation is a consequence of sufficiently limited melt transport in individual dikes emplaced in a cold upper crust so as to prevent significant wall-rock melt back as required by observations of CFB dikes (H. L. Petcovic & Dufek, 2005; H. Petcovic & Grunder, 2003; H. C. Sheth & Cañón-Tapia, 2015). Additionally, if the same dike is used again for vertical melt transport, the chilled margins in the dike would provide a chemical barrier to reduce mixing between deep crustal melts and country-rock. Finally, the overall magmatic system is hypothesized to be in a quasi-steady state through active RTF processes (periodically Replenished and Tapped, continuously Fractionating O'Hara & Mathews, 1981). This model is essentially equivalent to REFC - Recharge FC model, (DePaolo, 1981; C.-T. A. Lee et al., 2014) in individual magma reservoirs. This provides a mechanism for

buffering magma compositions to explain the relative homogeneity of flood basalt lava compositions (e.g., K. Cox, 1988; Luttinen & Furnes, 2000).

Yu et al. (2015) proposed a very similar conceptual CFB magmatic architecture model to explain the variations in lava compositions in continuous stratigraphic sequences (Also see Potter et al., 2018, for a similar model). They propose that since the earliest magmas of a magma reservoir are emplaced in the colder crust, they will rapidly cool and form a compositional boundary plating layer (a high crystallinity solidification front B. D. Marsh, 2013), which progressively helps reduce crustal assimilation for subsequent magmas emplaced into the reservoir. Similar to other models, Yu et al. (2015) find that REAFC (REFC with crustal Assimilation C.-T. A. Lee et al., 2014) processes are necessary to explain the range and pattern of lava flow compositions (See discussion in Section 4).

A final class of conceptual models for LIP systems describe the long-term evolution of the CFB magmatic system from the initiation of the flood basalt province to its termination. As a representative example, we briefly describe a model presented by S. R. Krans et al. (2018) based on the petrological analysis of continuous 1635 m-thick lava flow sequence of the Ethiopian Traps. The principal observational basis for this model is relative changes in phase assemblages (specifically olivine, clinopyroxene, ortho-pyroxene, and plagioclase) as a function of depth (e.g., Morse, 1980; Albarede, 1992; M. Richards et al., 2013). S. R. Krans et al. (2018) propose that initially, the parental mantle melts accumulate in the Moho depth magma reservoirs that periodically feed ol-phyric surface flows with minimal intermediate storage. Over time, a shallower magmatic plumbing system is established, leading to magma stalling and differentiation, as evidenced by a higher fraction of plag-phyric lava flows. This evolution in the magmatic plumbing network naturally leads to polybaric crystal fractionation (as argued by other conceptual models discussed above). Eventually, decreasing partial melt flux from the lithosphere leads to freezing of an increasing fraction of crustal magma reservoirs and increasing fractionation of the magmas that do erupt. Finally, the termination of the flood basalt activity in Ethiopian Traps is followed by a transition to much lower volume, localized shield building (Kieffer et al., 2004). S. R. Krans et al. (2018) posited that atop this general evolution of the magmatic system, there are variations in magmatic flux into the shallow crustal system. These include multiple pulses of magma recharge and brief hiatuses (as indicated by weathering horizons). Since there are no evident systematic mineralogical or volcanological variations on a flow-by-flow scale to these variations, they propose that the complex response is indicative of a complex magma plumbing system with multiple reservoirs. Depending on their pathway through the magmatic system, different melt batches will have varying storage times before eruption and hence experience different amounts of magma mixing and fractionation.

As additional evidence for this inference, S. R. Krans et al. (2018) interpret the occurrence of the few plagioclase-megacrystic basalt flows as indicative of a well established shallow magmatic mush zone. Based on the presence of complex zoning patterns and high An-content in plagioclase megacrysts, they propose that frequent recharge of deep melt into the magma reservoirs is required to explain these flows, with some of the larger influxes leading to large scale re-mobilizing the mush zone and eruption. A critical feature of this class of conceptual models is the presence of a complex magmatic plumbing network and the presence of multiple magma reservoirs and eruptive pathways in the system.

In summary, the various conceptual models all propose the presence of a deep crustal/Moho depth magma reservoir as well as some significant upper crustal plumbing network, which is continuously replenished in order to explain both the overall geochemical homogeneity as well as inter-flow variations in a stratigraphic section. Although these models do not explicitly discuss the size of individual magma reser-

voirs, it appears to be generally assumed that they are large enough to feed individual eruptive episodes (a size concomitant with volumes in excess of 1000 km^3 per eruption). The one exception to this is H. C. Sheth and Cañón-Tapia (2015) who explained geochemical variations within composite dikes in Deccan Traps with a model wherein individual CFB eruptive episodes are fed by multiple interacting magma reservoirs.

2.2 Quantitative Models

2.2.1 Recharge-crystallization model

A first quantitative model for CFB magmatic systems was proposed by Karlstrom and Richards (2011). Akin to the conceptual models described above, they assumed that the parental ultramafic melt forms ellipsoidal intrusions at Moho depth or in the lower crust, since they are denser than the overlying crust. With subsequent fractional crystallization (up to $\sim$ 30% crystallinity), CO_2 exsolution from the melt makes the melt - volatile mixture buoyant and eruptible. Using thermo-mechanical models, they showed that during the early phases of a CFB, melt in a magma reservoir of volume comparable to the size of a single eruptive episode (10^3 - 10^4 km^3, $\sim$ 10-30 km semi-major axis horizontal length, 1-5 km vertical length) cools sufficiently to become buoyant on a timescale shorter than the viscous stress relaxation timescale. Consequently, buoyant melt from each of these reservoirs feeds an individual surface eruption through dikes initiated by elastic stresses in the lower crust caused by the growth of the magma reservoirs (recharge). Continued magma flux will progressively heat the lower crust, leading to faster viscous stress relaxation and dominantly intrusive magma bodies instead of surface lava flow eruptions. For representative melt fluxes and crustal rheology, Karlstrom and Richards (2011) found that this transition occurs on a timescale of order 1 Ma, which is comparable to the duration of the main phase of CFB emplacement.

The Karlstrom and Richards (2011) model envisions the formation of a dense network of intrusions in the lower crust. Due to melt buoyancy and background tectonic stresses, these magma reservoirs are expected to progress upward into colder, more elastic crust. The model also proposes that the maximum size of individual reservoirs is similar to the depth from the surface. This restriction is a consequence of free-surface shear stress and dike initiation at the edges of reservoirs for laterally extensive CFB magma bodies. Based on analog experiments and seismic datasets for sill complexes in Karoo Basin and North Atlantic magmatic province, the typical total diameter of sills is 1.5- 15 times the depth of the emplacement (e.g., Hoggett, 2019, and references therein), with a median value of 2.5 consistent with theoretical expectations (Malthe-Sørenssen et al., 2004; Manga & Michaut, 2017; Galland et al., 2009). We would however note that there are some very large sills (e.g., Basement Sill with $\sim$ 10,000 km^2 area, 400 m thickness) exposed in a 3-4 km deep surface section of the magmatic plumbing structure of the Karoo-Ferrar CFB in McMurdo Dry Valleys, Antarctica (B. D. Marsh, 2004). Thus, in practice, the concentration of free-surface shear stress may not be a strong limit on the spatial size of magma bodies due to visco-plastic deformation processes (Schofield et al., 2012; Galland et al., 2019). Finally, the eruption frequency is controlled by the melt recharge timescale, which determines the rate of deviatoric stress buildup in the lower crust and cooling timescale for buoyancy production by CO_2 exsolution. Since the lower crustal temperature will rapidly increase during the course of a CFB event, the first-order prediction from this model is that the time period between individual eruptive episodes will increase during generation of a CFB province, potentially with larger eruptive volumes later (e.g., Deccan Traps) due to expanding magma reservoirs.

2.2.2 Buoyancy overpressure model

Another quantitative model for CFBs was proposed by Black and Manga (2017) with a focus on explaining the available geochronological constraints and paleo-proxy inferred environmental changes for the Siberian Traps. They model the CFB plumbing architecture as composed of two magma chambers, one at Moho-depth and another at upper crustal depth. The reservoir sizes dynamically evolve in the model with melt influx from the underlying magma reservoir (mantle) and outflux to surface eruptions (overlying chamber) for the crustal-depth (Moho-depth) reservoir. The critical feature of this model is that the brittle tensional failure of large magma reservoirs is hypothesized to be a consequence of the buoyancy of the magma-volatile mixture. This buoyancy with respect to the surrounding country rock (δ_{rho}) leads to a buoyancy overpressure ($\Delta P_{buoy} = \delta_{rho} g h$; h is the magma reservoir thickness). This buoyancy overpressure cannot be relaxed by the viscous stress relaxation. Hence, ΔP_{buoy} can slowly accumulate over time without dissipation except by fluid flow into the surrounding crust.

Black and Manga (2017) used a 1D thermo-chemical model of the two magma reservoirs with thermal evolution, volatile exsolution, crustal assimilation of carbon-rich crust, bubble coalescence, and diffusive volatile escape into the country rock, and found that buoyancy overpressure alone is sufficient for the failure of large magma reservoirs. With regard to the eruptive tempo of CFBs, they find three primary eruptive regimes. At the start of a flood basalt sequence, the low-degree melts are volatile-rich and hence highly buoyant due to volatile exsolution during decompression. Consequently, the melt rises rapidly from the Moho-depth magma reservoir to surface eruptions with minimal storage in the crustal reservoirs. Additionally, the size of individual magma reservoirs is small ($\sim$ 1-2 km in height) since most of the mantle melt erupts rather than accumulating. With time, volatile content in the higher-degree mantle melts decreases, reducing magma buoyancy. As buoyancy slowly builds up slowly with volatile-exsolution as well as thicker/larger magma chambers (since $\Delta P_{buoy} \propto h$, the typical thickness is 8-15 km), the eruption frequency decreases along with a larger volume of individual eruptions. The eruptions are further inhibited by volatile loss to the surrounding medium during this accumulation phase. As a result, crustal permeability around the magma reservoir needs to be reduced sufficiently by thermal annealing of fractures, and crustal compaction before overpressure can build up and lead to crustal failure. These processes are repeated in the upper-crustal reservoir, which has an additional source of volatiles from the assimilation of carbon-rich crust (typically organic sediments in sedimentary basins, e.g., Karoo sills and Siberian Trap Sills H. H. Svensen et al., 2018), but also higher crustal permeability (Ingebritsen & Manning, 2010; Mittal & Richards, 2019). Finally, in the third stage, the decrease in parental flux prevents the buildup of sufficient ΔP_{buoy} in the magma reservoirs, and the reservoirs remain molten with some overpressure for 10^5 - 10^6 yr before eventual solidification.

During the second eruptive regime, Black and Manga (2017) found that the eruptive tempo of surface volcanism is very pulsed with perhaps just 2-4 eruptive events. Each eruptive pulse is expected to last 10^3 - 5x10^4 yrs with long hiatus of 2x10^5 - 5x10^5 yrs. Since each failure event at the Moho depth transfers a large volume of magma to the upper crustal system, the size of the upper crustal magma reservoirs feeding each eruptive episode is large (typical thickness is 2-4 km). Extrapolating from the 1D calculations, Black and Manga (2017) propose that a full continental flood basalt sequence is fed by order 1-10 pairs of Moho and upper crustal magma reservoirs each with a melt source in the mantle of order 100-300 km (compaction lengthscale). Thus, on a province scale, the hiatuses between eruptive pulse may be shorter of order 10^5 - 5x10^5 yrs, whereas individual stratigraphic sections would have

longer hiatus since the erupted lava is expected to have been sourced from the same localized eruptive plumbing system in the crust.

2.2.3 Difficulties associated with large magma reservoirs

Although assuming that each large eruptive episode is fed from a correspondingly large magma reservoir makes logical sense, at least as a starting point, the description of the two models described above (Black & Manga, 2017; Karlstrom & Richards, 2011) illustrate that both the assembly and eruption of large magma reservoirs is challenging. In addition, the results illustrate that the presence of larger magma reservoirs naturally leads to more prolonged hiatus between eruptive episodes.

Among the two primary mechanisms for triggering eruptions, the efficiency of recharge associated overpressure decreases for a large reservoir for the following reasons. First, since the recharge associated overpressure is inversely proportional to the volume of the magma reservoir, it becomes progressively harder to erupt large magma bodies (Jellinek & DePaolo, 2003; Karlstrom et al., 2010; Townsend et al., 2019). Second, with the progressive assembly of lower crustal magma bodies, the increasing crustal temperature leads to faster visco-elastic stress relaxation of any accumulated recharge associated overpressure (Jellinek & DePaolo, 2003; Karlstrom et al., 2017). Additionally, in order to assemble the large magma bodies in the first place, the magma recharge rate needed to be low enough to prevent an eruption. Thus, using recharge-induced over-pressurization for the assembled larger magma bodies requires the special, likely unreasonable, co-incidence of significant changes in melt influx into the magma reservoir. Although there may be some physical feedbacks for melt focusing (e.g., Karlstrom et al., 2009, 2015), it would seem unlikely that these would counteract the negative feedbacks described above.

As a consequence, recharge associated elastic stresses alone become inefficient as triggers for the eruption of large magma bodies, so that additional mechanisms such as buoyancy overpressure (e.g., Caricchi et al., 2014; Black & Manga, 2017) or roof failure (e.g., de Silva & Gregg, 2014; Gudmundsson, 2016) are required. However, if buoyancy overpressure is the eruption trigger, a long eruption hiatus is a natural consequence due to the timescale for vertically assembly of the magma body (which would be slowed by lateral viscous flow), the timescale for crustal permeability reduction, and the timescale for sufficient solidification for volatile exsolution (Karlstrom et al., 2010; Black & Manga, 2017; Mittal & Richards, 2019). Thus, we contend that if individual eruptive episodes are indeed fed by large magma reservoirs, the eruptive tempo is naturally expected to be very pulsatory with hiatus of order 10^5 - 10^6 yrs, completely contrary to observations. Additionally, a large magma reservoir will lead to large melt fluxes into the upper crustal reservoir when crustal failure does happen, and hence naturally leads to very large crustal magma reservoirs. Finally, since crustal assimilation of carbon rich country rock is an important source of volatiles for the upper-crustal magma reservoir, the eruptive tempo will be expected to be different for CFBs emplaced into a granitic upper crust instead of a thick sedimentary basin (e.g., Siberian Traps). Specifically, one would expect that the hiatus time between eruptive episodes is longer for CFBs with granitic upper crust (e.g.,Deccan Traps) along with overall reduced likelihood of eruption.

3 Observational constraints on magmatic architecture

In order to test the predictions from the previous models for CFB architecture, we use the Deccan Traps flood basalt as a representative example. Since the 1980s, the DT has been extensively studied and consequently has the most extensive geochemical, geochronological, and volcanological datasets among the large ($>$ 1 Million km^3 erupted volume) CFBs. In the following, we first give a brief geological overview of

the Deccan Traps with a special emphasis on the chemo-stratigraphic framework and contribution of different crustal, lithospheric, and mantle sources to the erupted lava flows. We then summarize the direct constraints on the eruptive tempo of individual eruptive episodes for the DT main phase using geochronology, paleomagnetic secular variation, Mercury proxy records, and lava flow morphology. Although our primary focus for this study is the DT, we include some complementary observations from other CFBs, layered mafic intrusions, and modern flood basalt analogs (e.g., the 1783 Laki eruption) to assess whether our DT observations are representative of CFBs in general.

3.1 Geological Background - Deccan Traps

The Deccan Traps is a late Cretaceous–Paleogene continental flood basalt province covering more than 500,000 km^2 of peninsular India (J. J. Mahoney, 1988; Verma & Khosla, 2019; Kale et al., 2020; Manu Prasanth et al., 2019; Krishnamurthy, 2020, and references therein). The Deccan Traps mark the beginning of the Réunion hotspot track and are associated with partial melting due to the arrival of a deep mantle plume under the Indian subcontinent (presently beneath Réunion) (e.g., M. A. Richards et al., 1989); see Peters et al. (2017) for discussion of isotopic evidence). The present-day subaerial volume of the DT lava flows is about 600,000 km^3 (Jay & Widdowson, 2008; M. A. Richards et al., 2015) along with a significant volume offshore in the Arabian Sea (Gombos Jr et al., 1995; Calvès et al., 2011; D. Pandey et al., 2011; P. Kumar & Chaubey, 2019; Fainstein et al., 2019), and some small-volume Deccan-related intrusions in Seychelles (Devey & Stephens, 1991; Ganerød et al., 2011; T. M. Owen-Smith et al., 2013; Shellnutt et al., 2017). Estimates of the total pre-erosional DT lava flow volume range from 1 to 2 x 10^6 km^3 (Sukheswala, 1981; G. Sen, 2001; Jay & Widdowson, 2008).

Based on observed structural discontinuities as well as different geochemical and isotopic compositions of the lava flows, the Deccan Traps CFB is typically subdivided into four separate subprovinces each with potentially different eruptive history and corresponding magmatic system (Figure 1). These four subprovinces are the Western Ghat-Central Indian Volcanic province (WVP), the Mandla Lobe province, the Malwa plateau province (including the volcanic sequences in the Narmada-Tapti rift zone which may be a separate sub-province), and the Saurashtra-Kutchh province (Z. X. Peng et al., 2014; Kale et al., 2020). Among these, the WVP hosts some of the thickest continuous basalt flow sections for DT along the Western Ghats Escarpment (WGE) along the Western Coast of India (J. J. Mahoney, 1988). With a $\sim$ 3.5 km composite section of 10-50 m thick basalt flows emplaced atop Neoarchean basement (e.g., 1251 m thick Koyna core Mishra et al., 2017) easily logistically accessible, WGE sections have been extensively studied geochemically with detailed analysis of major and trace elements and isotopic composition (Sr, Pb, and Nd).

3.1.1 Western Ghats Geochemical Formations

On the basis of these measurements and volcanological features, the Western Ghats (WG) section has been grouped into three subgroups which are further subdivided into 12 geochemical formations each with several hundred meter thicknesses (Deshmukh, 1977; J. Mahoney et al., 1982; K. Cox & Hawkesworth, 1985; Basu, Saha-Yannopoulos, & Chakrabarty, 2020; Devey & Lightfoot, 1986; Beane et al., 1986; K. V. Subbarao, 1988; K. Subbarao et al., 1988; Beane & Hooper, 1988; Bodas et al., 1988; Khadri et al., 1988; Lightfoot, Hawkesworth, et al., 1990; C. Mitchell & Widdowson, 1991; Z. Peng et al., 1994; Choudhary & Jadhav, 2014; Hegde et al., 2014). The three subgroups of the WG (Wai, Lonavala, and Kalsubai, top to bottom) together represent more than 70 % of the total erupted volume of the DT and hence

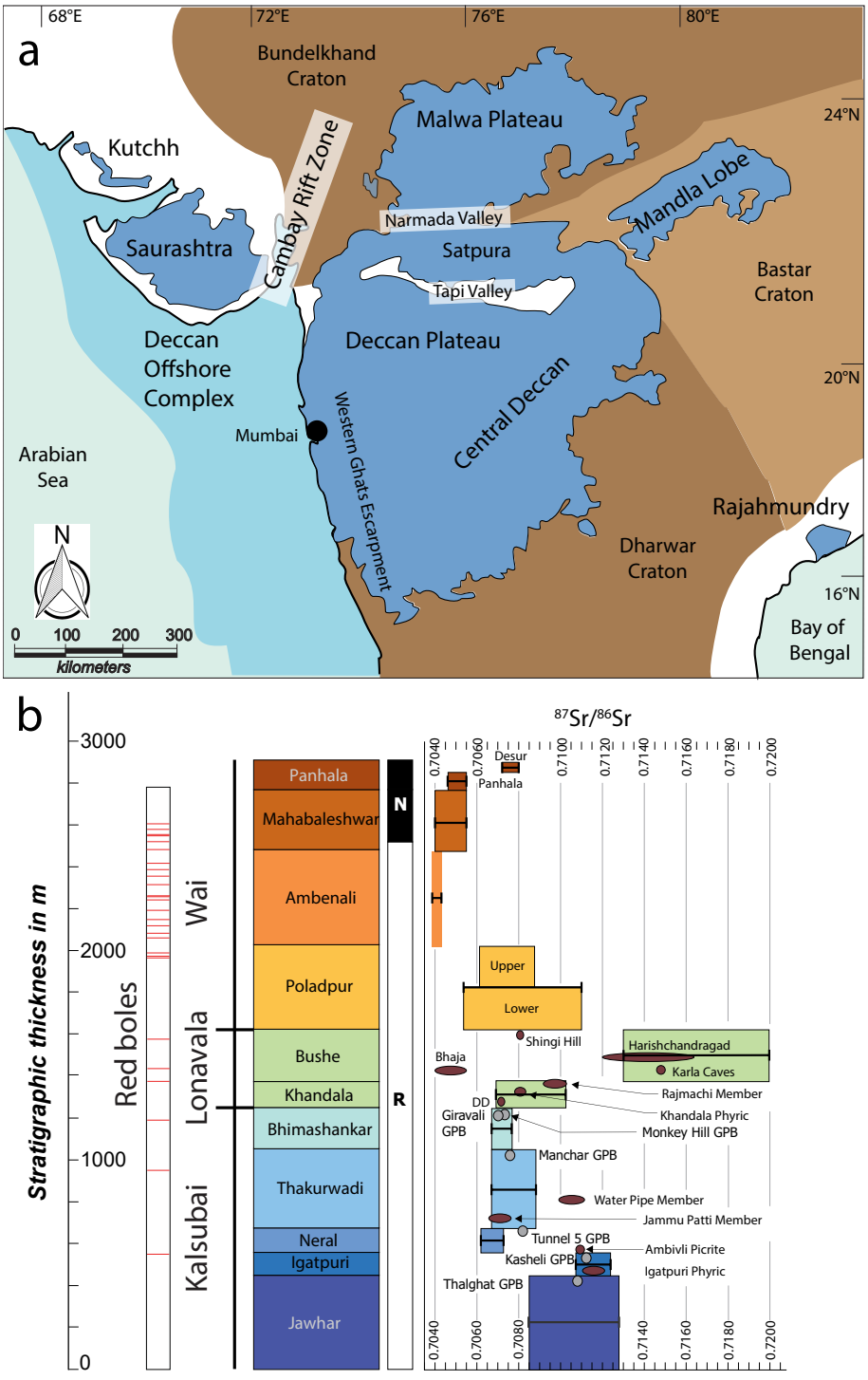
a
68°E
72°E
76°E
80°E
24°N
20°N
16°N
Bundelkhand Craton
Malwa Plateau
Kutchh
Cambay Rift Zone
Narmada Valley
Mandla Lobe
Saurashtra
Satpura
Tapi Valley
Bastar Craton
Deccan Offshore Complex
Deccan Plateau
Central Deccan
Mumbai
Western Ghats Escarpment
Arabian Sea
Rajahmundry
Dharwar Craton
Bay of Bengal
N
0 100 200 300
kilometers
b
Stratigraphic thickness in m
3000
2000
1000
0
Red boles
Wai
Lonavala
Kalsubai
Panhala
Mahabaleshwar
Ambenali
Poladpur
Bushe
Khandala
Bhimashankar
Thakurwadi
Neral
Igatpuri
Jawhar
N
R
87Sr/86Sr
0.7040
0.7060
0.7080
0.7100
0.7120
0.7140
0.7160
0.7180
0.7200
Desur
Panhala
Upper
Lower
Shingi Hill
Harishchandragad
Karla Caves
Bhaja
Rajmachi Member
DD
Giravali GPB
Khandala Phyric
Monkey Hill GPB
Manchar GPB
Water Pipe Member
Jammu Patti Member
Tunnel 5 GPB
Ambivli Picrite
Kasheli GPB
Igatpuri Phyric
Thalghat GPB

Figure 1 *(previous page)*: A) : Outline of the Deccan Traps Volcanic Province India including the offshore Deccan complex (based on data from Kale et al., (2019) and Jay & Widdowson (2008)). The whole subaerial Deccan province is subdivided into four main subprovinces : Western Ghat-Central Indian Volcanic province (WVP), the Mandla Lobe province, the Malwa plateau province (including the volcanic sequences in the Narmada-Tapti rift zone), and the Saurashtra-Kutchh province. The southern edge of the Malwa province is typically the Narmada Tapi zone though some of the lava flows in the Satpura region may have been sourced from the central Deccan region. The Saurashtra-Kutchh and the Malwa subprovinces are divided by the Cambay rift zone. B) : A composite stratigraphic sections for the Western Ghats region showing the chemostratigraphic formations, magnetostratigraphic with the chron C29N and C29R boundary, and the locations of red boles in the section (following Sprain et al., 2019; Chenet et al., 2008). We show the range of $^{87}Sr/^{86}Sr$ for each geochemical formation (using compilation from Vanderkluysen et al., 2011; Sheth et al., 2016). The gray ellipses show the values for some selected Giant Plagioclase basalts while the brown ellipses show the values of some other Central Deccan chemical types (Figure modified from Kale et al., 2019).

are the "main volumetric component" (M. A. Richards et al. (2015) and references therein).

The Kalsubai subgroup, consisting of the Jawhar, Igatpuri, Neral, Thakurwadi, and Bhimashanker formations, exhibits a large range of compositions ranging from picritic flows to evolved flows (Mg # <36, Beane et al. (1986)). The Lonavala subgroup, consisting of the Khandala and Bushe formations, includes flows in the Bushe formation with significant crustal assimilation. Finally, the Wai subgroup, comprising the Poladpur, Ambenali, Mahabaleshwar, Panhala, and Desur formations, are the most evolved lavas with regards to fractional crystallization. The Ambenali Formation records the lowest $^{87}Sr/^{86}Sr$ and the highest εNd values among the WG flows, indicative of minimal crustal assimilation (J. J. Mahoney, 1988; Lightfoot & Hawkesworth, 1988; Z. Peng et al., 1994). Geochemical analysis of lava flow sections in the Indian Deccan plateau has shown that the WG geochemical formations can potentially be extended 100s of km laterally into the central Deccan (e.g., the Khandala and Poladpur formations Z. Peng et al., 1998; Melluso et al., 2004), the south-eastern Deccan (e.g., the Poladpur, Ambenali, and Mahabaleshwar formations C. Mitchell & Widdowson, 1991; Jay & Widdowson, 2008; Kaotekwar et al., 2014), and the Rajamundry Traps (about 1000 km from the WG Baksi, 2001; Self et al., 2008; I. M. Fendley et al., 2020). These results illustrate that the DT was typically associated with individual lava flows 100s of km long, and hence large individual eruptive episodes of order 1000s of km^3.

In the other DT subprovinces, lava flow major and trace element compositions similar to the WG geochemical formations have been found. For example, Z. Peng et al. (1998) (also see J. J. Mahoney, 1988; J. Mahoney et al., 2000) found Poladpur formation type lava flows in a Malwa plateau province section about 1000 km from the WG Poladpur outcrops. However, these Poladpur-like lava flows have a very different Pb isotopic composition than the WG Poladpur geochemical formation. Thus, they could not be fed overland by the same magmatic plumbing system as the Poladpur flows. Instead, they must have a different crustal magmatic eruptive system interacting with different crustal assimilant (see discussion in the next section). There are similar examples of lava flows from the Saurashtra and Mandla lobe provinces, which have isotopic mismatches with WG formations despite similar major and trace element characteristics (e.g., Z. Peng et al., 2014; Vanderkluysen et al., 2011; H. Sheth et al., 2018). In addition to isotopic mismatches, there are also temporal differences between

similar geochemical chemo-type lava flows across the different DT subprovinces (e.g., H. Sheth et al., 2018, and references therein). A particularly illustrative case is the presence of the Bushe chemo-type (both isotopic and major/trace element composition) in lava flows and dikes in Saurashtra (Melluso et al., 1995, 2006; H. C. Sheth et al., 2013), the Mandla Lobe (Shrivastava et al., 2014), the Malwa Plateau subprovinces (Z. Peng et al., 1998; P. Hooper & Subbarao, 1999; J. Mahoney et al., 2000; H. Sheth et al., 2004), and Seychelles Island dikes (Devey & Stephens, 1991). However, given the chronostratigraphic and volcanologic constraints, these flows can not represent the same Bushe Formation of the Western Ghats (See the cited references for details). As described in Section 3.2.2, these subprovinces erupt over a multiple Ma time-period with some provinces predating the WG sequence (e.g. Saurashtra, Malwa Plateau though some of the uppermost Malwa flows may be coveal with WG), while the other post-dating the WG Bushe flows (Mandla Lobe). In aggregate, these observations illustrate that the magmatic plumbing system for these subprovinces, at least the upper crustal transport network, is different.

Nevertheless, the repeated occurrence of lava chemically similar to the WG formations suggests a common sub-continental magma source and that specific petrologic processes occurred multiple times across the CFB magmatic system (Z. Peng et al., 1998; J. Mahoney et al., 2000; Haase et al., 2019). Because of the complexities in magmatic architecture across multiple DT subprovinces described above, in this study we principally focus on the most voluminous Western Ghat-Central Deccan province. There is a broad consensus that most of this province represents eruptions from a single magmatic plumbing system, barring some components of the Central Deccan Plateau in the Narmada-Tapi rift valley (See Fig.1, discussion in Kale et al., 2020).

3.1.2 Magma composition and melt components

The dominant lava flow composition in the Deccan Traps is tholeiitic ($> 95\%$ of the exposed area) with minor volumes of carbonatitic, felsic, and alkaline eruptive products and intrusions (e.g. , Krishnamurthy, 2020; Krishnamurthy & Cox, 1977, 1980; Devey & Cox, 1987; J. J. Mahoney, 1988; K. V. Subbarao, 1988; Z. Peng et al., 1994; Shrivastava & Pattanayak, 2002; Melluso et al., 2002; Jay & Widdowson, 2008; Talusani, 2010; A. Ray et al., 2010; Chandra et al., 2019; Prasanth et al., 2019; Sheikh et al., 2020, and references therein). Picritic lava flows are most abundant in the Saurashtra region and the northern part of the WG (Krishnamurthy & Cox, 1977; K. Cox & Hawkesworth, 1985; Beane & Hooper, 1988; Melluso et al., 1995; Sano et al., 2001). These olivine-phyric picritic lava flows are generally erupted in the early part of the lava flow sequence along with some alkali basalts (e.g., Krishnamurthy et al., 2000, and references therein). In the Western Ghats section, picritic basalts constitute less than 10% of the total volume and are mostly reported in the lower formations (Igatpuri, Neral, Thakurvadi, Bushe, and Poladpur Beane & Hooper, 1988; Krishnamurthy et al., 2000). The reduced occurrence of picritic flows in younger DT sections has been typically interpreted as a sign of a steady-state magmatic plumbing system with progressively more fractionation and ponding of picritic magmas (Krishnamurthy et al., 2000). The rhyolitic/silicic flows associated with Deccan are minor volume ($<$ a few percent of total Deccan volume) with limited present day exposures primarily in Saurashtra region (and adjoining parts of Narmada-Tapi rift zone and Barmer rift zone) (Sheikh et al., 2020; A. Pandey et al., 2017; Dolson et al., 2015).

The geochemical diversity of WG lava flows (and silic complexes) suggests a complex petrologic evolution, involving significant fractional crystallization of plagioclase, clinopyroxene, and olivine as well as crustal assimilation and magma mixing (J. Mahoney et al., 1982; J. J. Mahoney, 1984; K. G. Cox & Hawkesworth, 1984; Ganguly et al., 2014; K. Cox & Hawkesworth, 1985; J. J. Mahoney, 1988; Chatterjee & Bhattacharji, 2008; Basu, Chakrabarty, et al., 2020). The initial parental magma

for the WG lava flows (the Ambenali Formation end-member) is a high-degree partial melt from the Réunion plume source along with some asthenospheric and lithospheric mantle contributions (Z. Peng et al., 1994; Z. Peng & Mahoney, 1995). K. G. Cox (1980) proposed that these high degree partial melts are initially picritic but undergo extensive fractional crystallization in the crustal system to form basalts with < 8 % MgO before surface eruptions (K. G. Cox & Hawkesworth, 1984; Herzberg & Gazel, 2009). Based on rare-earth element (REE) inversions (McKenzie & O'nions, 1991; S. Gibson & Geist, 2010), M. A. Richards et al. (2015) concluded that the top of the asthenospheric melt column was at about 60 km depth during the WG eruptive sequence.

Several different assimilates have been proposed for the DT lavas, including granitic upper crust (J. Mahoney et al., 1982; K. G. Cox & Hawkesworth, 1984; Lightfoot & Hawkesworth, 1988; Lightfoot, Hawkesworth, et al., 1990; Z. Peng et al., 1994; Dessai et al., 2008), lower granulitic continental crust (K. G. Cox & Hawkesworth, 1984; Z. Peng et al., 1994; Peters et al., 2017), and partial melting of subcontinental lithospheric mantle (Lightfoot & Hawkesworth, 1988) either individually or in sequence (Z. Peng et al., 1994). Some of the geochemical variations in lava flows have also been suggested to be indicative of partial melt from the lithospheric, asthenospheric, and deep plume components (e.g., J. J. Mahoney, 1988; K. V. Subbarao, 1988; Jennings et al., 2017; Hari, Swarnkar, & Prasanth, 2018; R. E. Ernst, 2014, and references therein). Furthermore, the crust beneath each subprovince is compositionally different due to the pre-Deccan structure of the Indian craton (See Figure 1). For instance, the WG region is underlain by continental crust similar to the Western Dharwar craton while the central DT is emplaced atop Archaen Eastern Dharwar Craton and the Bastar craton (Dessai & Vaselli, 1999; Y. B. Rao et al., 2017; Kale et al., 2017). In contrast, the Mandla subprovince is underlain by the Bastor craton and some Proterozoic mobile belts (J. S. Ray & Parthasarathy, 2019; Kale et al., 2020, and references therein) while the crust under the Malwa province includes the Bundelkhand craton, Proterozoic Vindhyan Supergroup (sandstone, shale, and carbonates), and a Late Archean-Proterozoic collisional mobile belt (R. Ray et al., 2008; Ramakrishnan & Vaidyanadhan, 2010; L. Ray et al., 2016). As a consequence, the isotopic and geochemical composition of the crustal contaminants in each of the DT subprovinces can vary significantly.

It is clear that the assimilates can vary rapidly between geochemical formations, despite their uncertain composition, or even their crustal vs. lithospheric–mantle nature (e.g., (J. J. Mahoney, 1988; Lightfoot, Hawkesworth, et al., 1990; Gallagher & Hawkesworth, 1992; Arndt et al., 1993; Hawkesworth & Gallagher, 1993; Z. Peng et al., 1994; Turner & Hawkesworth, 1995; Lassiter & DePaolo, 1997; H. Sheth & Chandrasekharam, 1997; Allegre et al., 1999; G. Sen, 2001; Chandrasekharam et al., 2000). For instance, the crustal assimilation component for the highly contaminated Bushe Formation is isotopically different from the assimilate for the Mahabaleshwar Formation (e.g., K. Cox & Hawkesworth, 1985; Beane et al., 1986; Lightfoot & Hawkesworth, 1988; Z. Peng et al., 1994; J. Mahoney et al., 2000; Gangopadhyay et al., 2003; Melluso et al., 2006). Similarly, the main WG geochemical formations show abrupt changes in $^{87}Sr/^{86}Sr$ ratios, sometimes across even a single sheet lobe. These changes are indicative of rapid changes in the source components for the erupted magma (Beane et al. (1986), Figure 1b modified from Kale et al. (2020), Haase et al. (2019) for Mandla Lobe). Hence, the magmatic plumbing system for the DT is complex, with multiple assimilates, but also dynamic, with the ability to rapidly switch magma compositions. The geochemical memory of the magmatic system is relatively small. This is difficult to reconcile with a magmatic plumbing system composed of only a few large well stirred magma chambers where each eruptive episode typically integrates magma compositions over multiple 100s of kyr (Black & Manga, 2017).

719 ## 3.2 Deccan Traps Geochronology

720 The total DT eruptive sequence lasted about 10 Ma, with the oldest alkalic lava
721 flows in Pakistan around 72-73 Ma (Khan et al., 1999; J. Mahoney et al., 2002), and
722 the youngest lava flows around 60-61 Ma in the Mumbai sequence (H. C. Sheth et al.,
723 2001a, 2001b; Pande, Yatheesh, & Sheth, 2017). However, the majority ($> 90\%$) of
724 volcanism occurred during a $\sim$ 1 Ma time-interval from 66.3 to 65.3 Ma (Renne et
725 al., 2015; Schoene et al., 2015; Parisio et al., 2016; Sprain et al., 2019; Schoene et al.,
726 2019). This interval includes almost all of the Western Ghats eruptive sequence and
727 hence constitutes the "main phase" of DT volcanism (Sprain et al., 2019; Schoene et
728 al., 2019).

729 In the following section, we first discuss the geochronological datasets from the
730 Western Ghats, since they represent the primary volumetric component of the Deccan
731 Traps and have the best constraints on eruptive tempo. We then briefly describe the
732 available geochronological constraints for the DT subprovinces, with a focus on their
733 implications for the overall magmatic activity of the DT flood basalt province.

734 ### *3.2.1 Western Ghats geochronology*

735 Our best direct constraints on the eruptive rates for the Deccan Traps comes
736 from the high-precision $^{40}Ar/^{39}Ar$ dating of lava flows and U-Pb dating of inter-flow
737 horizons in the Western Ghats region (Renne et al., 2015; Schoene et al., 2015; Sprain
738 et al., 2019; Schoene et al., 2019). Using their new ages with previously published
739 high-precision dates, Sprain et al. (2019) concluded that the DT lava flows in the
740 Western Ghats-Central Deccan province erupted continuously (within age precision)
741 for a total duration of 0.991 Ma from $\sim$ 66.413 Ma (Jawahar Formation) to $\sim$ 65.422 Ma
742 (Upper Mahabaleshwar Formation). This time period spans the Cretaceous-Paleogene
743 Boundary (KPB; 66.052 Ma Sprain et al., 2018) with more than 75 % of the DT
744 volume erupted within 650 kyr of the KPB. The zircon U-Pb dates in Schoene et al.
745 (2019) are consistent with the ^{40} $Ar/^{39}Ar$ results with respect to the overall duration
746 of the WG although their exact location of the KPB within the WG section is slightly
747 different.

748 However, these recent studies do differ with respect to eruptive tempo. Sprain
749 et al. (2019) found no evidence for a long hiatus (> 150 kyr) between individual lava
750 flows or geochemical formations, and the mean magma eruption rate for the Kalsubai
751 and Lonavala (0.4 ± 0.1 km/year) subgroups is statistically similar to that of the Wai
752 subgroup (0.6 ± 0.2 km/year). In contrast, Schoene et al. (2019) proposed multiple
753 hiatuses within the WG stratigraphy: a $\sim$ 100 kyr hiatus between Poladpur and Am-
754 benali, and a $\sim$ 250 kyr hiatus between Ambenali and Mahabaleshwar formations.
755 Correspondingly, they conclude that the eruptive rates were also pulsed with the Am-
756 benali and Poladpur Formations each having an eruptive pulse of 6-10 km^3/year with
757 a $\sim$ 100 kyr duration.

758 Although ascertaining why the results of the two studies differ is an area of
759 ongoing work, we can use volcanological features to assess if there is any evidence for
760 the proposed long hiatuses. Since sub-continental India was located in the equatorial
761 belt around 66 Ma with potentially high rainfall and weathering rates (e.g., Dessert
762 et al., 2003; Johansson et al., 2018), a long hiatus would be expected to correspond to
763 a thick weathering horizon in between basaltic flows. Indeed, multiple Western Ghats
764 sections have red weathering horizons (red boles, typically $\leq$ 1 m thick) in between
765 basaltic flows (e.g., stratigraphic sections in Jay, 2005, Steve Self personal comm.).
766 However, there is no evidence of a stratigraphically continuous, extraordinarily thick
767 red-bole between the Poladpur and Ambenali formations (Jay, 2005; Jay et al., 2009;
768 Chenet et al., 2009). Furthermore, some of the Ambenali-Poladpur transition sections
769 do not have any red boles (Jay et al., 2009; Chenet et al., 2009; Sprain et al., 2019, ;

also See Figure 1). Finally, red boles are frequently found between lava flows within the Ambenali formation, suggesting some hiatus time-period between individual eruptive episodes. Thus, we conclude that the eruptive tempo of the Western Ghats sequence does not show any evidence for multiple 100 kyr hiatuses between eruptive time-periods contrary to expectations of a large magma reservoir model (See Section 2.2.3).

3.2.2 Constraints for other DT subprovinces

Volcanism in the Saurashtra-Kutchh province (including some erupted products in Rajasthan) is generally considered to be the oldest in the Deccan stratigraphy. The largest silicic complexes in the DT - Barda Hills and Alech Hills in Saurashtra - and the overlying basalts in the region were emplaced between 69.5- 68.5 Ma based on the $^{40}Ar/^{39}Ar$ ages and field relationships (Dave, 1971; "Acid ring dykes and lava flows in Deccan trap basalt, Alech hills, Saurashtra, Gujarat", 1984; Shukla et al., 2001; A. Sen et al., 2012; Cucciniello et al., 2015, 2019). We would note that some recent U-Pb dates from the Alech, Barda, Girnar (also Ar-Ar), Rajula, and Phenai Mata intrusions suggest that these silicic-alkaline complexes were emplaced between 66.2 - 65.7 Ma, coincident with the main Deccan eruptive phase (Basu, Chakrabarty, et al., 2020; Sahoo et al., 2020). More work is needed to reconcile the various age constraints, and whether the different dating methods are sampling different parts of a long lived igneous complex (Basu, Chakrabarty, et al., 2020; Sahoo et al., 2020; Pande, Cucciniello, et al., 2017). Additionally, although $^{40}Ar/^{39}Ar$ dates on two alkaline complexes (Sarnu-Dandali and Mundwara) in the Cambay graben suggest a multi-phase emplacement spanning 90 to 60 Ma (H. Sheth et al., 2017; Pande, Cucciniello, et al., 2017), the oldest DT associated components have ages of 69.62 ± 0.08 Ma and 69.58 ± 0.16 Ma (Basu et al. (1993); recalculated to Renne et al. (2011) standards by Parisio et al. (2016)). Finally, there were subaerial/submarine eruptions on the Saurashtra Volcanic Platform between 75-68 Ma (Calvès et al., 2011; G. Bhattacharya & Yatheesh, 2015) and the Anjar Traps in Kutchh erupted between 67.47 ± 0.30 and 67.67 ± 0.60 (V. Courtillot et al. (2000); recalculated to Renne et al. (2011) standards by Parisio et al. (2016)). It is noteworthy that Central Saurashtra mafic dikes have $^{40}Ar/^{39}Ar$ ages spanning 66.6 Ma to 62.4 Ma (Cucciniello et al., 2015), younger than any published ages of the lava flows in the region. Additionally, Paul et al. (2008) used paleomagnetic data to conclude that magmatism in the Kutchh basin (dominantly tholeiitic, though with a significant alkaline component) occurred across chrons C30N, C29R, and C29N (i.e., across the KPB boundary) although the data do permit older ages. In summary, the available geochronological datasets suggest that the magmatic activity in the Saurashtra-Kutchh province is among the oldest in any DT province and may have had large time-gaps between periods of activity (G. Sen et al., 2009). Nevertheless, it may also have partially overlapped in time with the Western Ghat main phase volcanism.

For the Malwa plateau subprovince, Parisio et al. (2016) found that the alkaline and tholeiitic rocks were emplaced around the same time (within the age precision) with $^{40}Ar/^{39}Ar$ ages between 66.60 ± 0.35 to 65.25 ± 0.29 Ma for the Phenai Mata intrusive complex (also Basu et al. (1993) found similar ages) and 66.40 ± 2.80 to 64.90 ± 0.80 Ma for the Mount Pavagadh region. Based on paleomagnetic data as well as some $^{40}Ar/^{39}Ar$ dates (Schöbel et al., 2014, oldest date of 67.73 ± 0.22 Ma), the volcanism in the Malwa plateau may have been long-lived, spanning the chron C30N-C29R-C29N transitions.

In contrast to both the Saurashtra-Kutchh and Malwa Plateau provinces, the lava flows in the Mandla lobe are generally younger, with ages around 64.42 ± 0.33 Ma (Shrivastava et al., 2015; Pathak et al., 2017). However, some of the dikes in the region are older than published lava flow ages (e.g., 66.56 ± 0.42 Ma Shrivastava et al., 2017) suggesting the potential presence of older lava flows in the sequence. Some

of the dikes in the eastern-most extension of the Mandla lobe (in the Damodar valley region) have Deccan associated mafic dikes with ages ranging from 70.5 to 65.5 Ma, potentially indicating a long duration magmatic activity in the Narmada-Tapi rift zone associated structures (Srivastava et al., 2020).

The youngest section in the DT is the Mumbai sequence in the WG (along with some intrusive dikes in Goa) with some subaqueous lavas (Duraiswami et al., 2019). The Mumbai sequence includes a much wider compositional diversity than the rest of the DT, containing tholeiitic basalts, rhyolites, trachytes, and pyroclastics (Melluso et al., 2002). The $^{40}Ar/^{39}Ar$ ages for this sequence are typically between 61.5 and 63 Ma (Widdowson et al., 2000; H. C. Sheth et al., 2014; Samant et al., 2019; Duraiswami et al., 2019) with some volcanism ranging from 64.55 Ma to 60.8 Ma (H. C. Sheth et al., 2001b, 2001a; P. Hooper et al., 2010; Basu, Chakrabarty, et al., 2020). The main phase of Laxmi Ridge-India-Seychelles continental rifting and voluminous offshore magmatism (Misra et al., 2014; Pande, Yatheesh, & Sheth, 2017; Samant et al., 2019) as well as intrusions in Seychelles (Shellnutt et al., 2017), also have an age around 62.5 Ma, suggesting a possible association.

In summary, there is a general progression of younger Deccan Trap ages moving southward, consistent with the northward motion of the Indian plate over a quasi-stationary mantle plume head. With a typical Indian plate motion of $\sim$ 15-20 cm/yr during Late Cretaceous-Early Paleogene (Cande & Patriat, 2015), the northward plate motion over 2 Ma is 300 - 400 km comparable to the distance between the Saurashtra region and the Mumbai-Pune region. However, the geochronology also suggests additional complexities, principally associated with the role of pre-existing tectonic features on the Indian sub-continent such as the Narmada-Tapi and the Cambay rift zone (See Figure 1). Petrologically, observations from each subprovince show that the silicic lavas and intrusions were typically emplaced after the local primary flood basalt sequence (e.g., Mount Pavagadh, Parisio et al. (2016); Mumbai : H. C. Sheth et al. (2014)). With a few exceptions, the alkaline rocks in the DT are generally emplaced both prior to and post the main phase of tholeiitic lava flows (e.g., Parisio et al., 2016), analogous to some other CFBs (e.g., S. Gibson et al., 2006; R. E. Ernst & Bell, 2010; R. B. Larsen et al., 2018). This is consistent with an initial lower degree melt that quickly traverses the crust, potentially with minimal assimilation (e.g., Malwa plateau, Haase et al., 2019). This is followed by an increasing degree of partial melting in the mantle plume head and more extensive fractionation (K. G. Cox & Mitchell, 1988). Eventually, the system reverts back to a lower degree, alkalic melt, along with some silicic melts, coincident with progressive plate motion away from the plume (M. A. Richards et al., 1989).

With regards to eruptive tempo, the subprovinces appear to typically have a much more extended period of volcanic activity compared to the Western Ghats sections. However, with the available geochronological constraints, it is unclear whether the eruptive activity is pulsed with long hiatuses in between or if the typical time between individual eruptive episodes is simply longer.

3.2.3 Geochronological Constraints for other CFBs

Most CFBs, including the DT, show evidence for a short duration $\sim$ 0.5-1 Ma long "main phase" of volcanic activity wherein the majority of the CFB volume is erupted (e.g., V. E. Courtillot & Renne, 2003; Bryan et al., 2010; R. E. Ernst & Youbi, 2017; Wilkinson et al., 2017; H. Svensen et al., 2018, and references therein). However, most of them lack a robust chemostratigraphic framework, or as abundant surface exposure of lava flows as the DT. Thus, at present, it is unclear based on geochronology alone whether the majority of eruptive episodes in other CFBs are further clustered into pulses within the main phase volcanism.

The two exceptions to this are the Columbia River Basalts (CRB) and the Siberian Traps. For the CRB, Kasbohm and Schoene (2018) used high precision zircon U-Pb geochronology on volcanic ash beds between basaltic flows to constrain the duration of the main volcanic phase (> 95% of CRB volume) to about 800 kyr (16.7 to 15.9 Ma). These results, in combination with the magnetostratigraphy, show no evidence for a > 50-100 kyr hiatus between eruptions.

For the Siberian Traps, high-resolution U-Pb geochronology (S. D. Burgess & Bowring, 2015; S. Burgess et al., 2017) suggests that the volcanic sequence should be divided into three stages. More than two thirds of the extrusive volume was erupted in the first stage, which lasted 700 kyr (252.2 to 251.9 Ma). This was followed by a $\sim$ 420 kyr period of emplacement of mostly intrusives across the Siberian platform (also see Jerram et al., 2016; Augland et al., 2019), potentially due to the volcanic load of the overlying lava flows (S. Burgess et al., 2017). Finally, in stage 3, a combination of extrusive and intrusive volcanism occurred for another 300-500 kyr. As there are only four dates for the basaltic lavas (two in Stage 1, and one each in Stage 2 and 3), it is not possible to assess if there were any eruptive hiatuses within each stage of extrusive lava flows. The intrusions continued throughout Stage 2 without any resolvable hiatus (> 100 kyr). It is important to note that the U-Pb dates are from intrusions emplaced within the lava flow stratigraphy or exposed on the periphery of lavas and volcaniclastic rock. This suggests that these intrusions were likely emplaced at shallow depths (< 2 km, also see Tomshin et al. (2005, 2014) for petrographic data suggesting shallow emplacement). Consequently, we would argue that the Stage 1-Stage 2 transition from extrusive eruptions to shallow intrusive magmatic activity for $\sim$ 420 kyr does not represent a hiatus for the crustal magmatic system. In addition, the sill complex does not correspond to a single well-mixed large magma reservoir, as the intrusions have varying geochemical compositions and emplacement ages (e.g., N. A. Krivolutskaya et al., 2018, see Description of a magma reservoir in Section 2). Hence, the frequency of crustal diking will be controlled by the timescale of pressure buildup in the upper crustal magma reservoir, regardless of whether each dike feeds a shallow sill complex or eruptions at the surface.

In conclusion, there is no clear evidence of long (> 100 kyr) eruptive (including shallow sill emplacement) hiatuses for either the Siberian Traps or Columbia River Basalts given the available datasets. These observations are inconsistent with the expectations of the large magma reservoir model (See Section 2.2.3).

3.3 Paleomagnetic constraints on eruptive tempo

Although there have been significant improvements in analytical techniques and consequent improvements in the precision of geochronological age precision to order 0.1 - 0.01%, the geochronological methods still have an absolute age uncertainity of order 10,000 kyr (for KPB age samples Sprain et al., 2019; Schoene et al., 2019). In order to obtain a higher resolution eruptive tempo, multiple studies have utilized the record of paleo-secular variation recorded in successive lava flows (directional groups, DGs) to constrain lava flow eruption rates at $\sim$ 100 yr resolution (Riisager et al., 2003; Knight et al., 2004; Chenet et al., 2008, 2009; V. Courtillot & Fluteau, 2014; Moulin et al., 2017; Pavlov et al., 2019). The Earth's magnetic field experiences secular variation, i.e. it naturally moves slightly over time. The paleomagnetic directions recorded in rocks accordingly display these variations in field position. Sets of lava flows with indistinguishable or very similar field directions (typically 5-10 $\circ$)are assigned to a directional group, which is commonly assumed to have been emplaced very rapidly (within $\sim$ 400 years) based on estimates of modern secular variation (Pavlov et al., 2019). The number and distribution of directional groups is thus an estimate of the temporal frequency of eruptions.

Based on a large study in the Western Ghats region, Chenet et al. (2009) concluded that the whole WG stratigraphy erupted as a combination of 30 major eruptive periods along with 41 additional individual lava units. Using the available geochemical stratigraphy, they estimated that each eruptive period had a volume of 1000 to 20,000 km^3 while individual lava flows were $\sim$ 1300 km^3 (based on analogy with Roza flow field in the Columbia River basalt (Thordarson & Self, 1998). Using similar secular variation timescale arguments as described in the previous section, they concluded that each of these 71 units had a duration of 10-100 years. In conclusion, Chenet et al. (2008, 2009) estimated that a very short active eruptive period of 1000 to 7000 years for the Western Ghats Deccan lava flows with the rest being hiatuses. If correct, this would suggest very pulsed eruption tempo consistent with the large magma reservoir model. However, the relationship between the correlation of paleomagnetic directions to eruptive timescales has been based on strongly simplifying assumptions about secular variation. In particular, the quasi-cyclic nature of paleosecular variation (with a time scale of order 10 kyr, (Panovska et al., 2019)) can introduce spurious correlations wherein lava flows separated by multiple secular variation cycles still have a small difference in paleomagnetic directions.

We addressed these challenges by developing a generalized forward modeling approach to compare synthetic eruptive histories with field datasets in a Bayesian inversion framework (Mittal et al., 2019). Since the real paleomagnetic field has a complex temporal structure with excursions and changing timescales for secular variation, we use a multi-million year long, low latitude deep sea sedimentary record of field variations for our forward model (Ohneiser et al., 2013). Additionally, we utilize the full statistical properties of the flow-by-flow records (e.g., fraction of lava flows in DGs and mean number of lava flows in DGs) instead of just the number of DGs to constrain permissible models. Using the same paleomagnetic dataset as Chenet et al. (2008, 2009), we find that the observations for the WG composite section (spanning Kalsubai, Lonavala, and Wai subgroups) is most consistent with continuous eruptions every 6,000-12,000 years (Figure 2). We find that the key characteristic of the "spurious" DGs is that each DGs only has 2-3 lava flow members. Additionally, a substantial fraction of lava flows from the full stratigraphy aren't part of a DG. When only considering DGs for a single physical stratigraphic section in the Western Ghats, the Deccan lavas satisfy both these characteristics with only $\sim$ 50% flows part of a unique DG in the Wai-Panchgani section spanning the Wai subgroup. Our new analysis results are further supported by the observation that many of the Deccan DGs as defined by Chenet et al. (2008, 2009) have weathering horizons (red boles) in between flows of a single DG from detailed stratigraphic logs (Jay, 2005). Since it is commonly assumed that 10cm - 1m red boles take at least a few 1000 years to form (Sheldon, 2003), a few hundred years time scale for emplacement of Deccan DG is unlikely. In conclusion, we find no evidence for a long ($>$ 50 kyr,Figure 2) eruptive hiatus in the Western Ghats region contrary to the large magma chamber model predictions.

3.4 Hg eruptive tempo estimates

Another indirect method to estimate the eruptive tempo of the DT at a 100-1000 yr resolution is the use of mercury (Hg) chemostratigraphy (e.g., Sial et al., 2013; Font et al., 2016; G. Keller et al., 2018; Percival et al., 2018; I. M. Fendley, Mittal, Sprain, et al., 2019). The primary source of Hg in the geological Hg cycle is emission from volcanism (See I. M. Fendley, Mittal, Sprain, et al. (2019) for more discussion). Hg, a highly [volatile??] species, is emitted as a vapor during individual LIP eruptions and potentially during passive degassing of LIP intrusives. Since Hg has a long atmospheric lifetime (order 6 month-2 years, Horowitz et al. (2017)) it can be globally distributed by atmospheric transport. Thus, large changes of the global Hg budget due to flood basalt eruptions will lead to increases in Hg concentration in sediments globally.

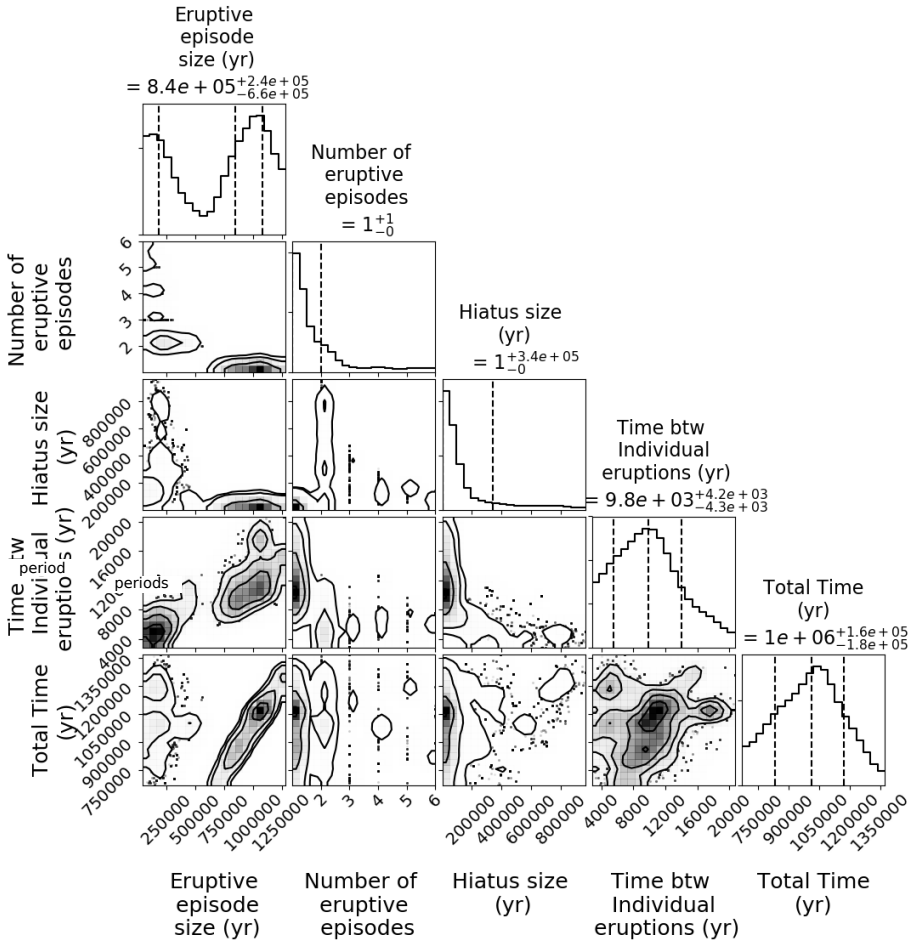

Figure 2: Bayesian parameter estimates for paleo-secular variation analysis for Eruptive period size (yr), Number of eruptive periods, Hiatus size (yr), Time between individual eruptive episodes (yr), and the Total time for the Composite Deccan Section. We use the flow-by-flow dataset from Chenet et al. (2008), and Chenet et al. (2009) for this analysis

However, to compare Hg concentration records from different locations and depositional environments, one must account for differences in sedimentation rate, sampling resolution, and sedimentary conditions such as organic carbon and sulfur concentration. I. M. Fendley, Mittal, Sprain, et al. (2019) used an environmental Hg cycle box model (Amos et al., 2013) to estimate eruptive rates and volumes by quantitatively evaluating the changes in the global mercury budget indicated by varying concentrations in sedimentary records. To do this analysis, they used a variety of eruptive rates and durations as inputs into the Hg cycle box model Amos et al. (2013). The inversion includes a time-smoothing step to account for sedimentation rate, bioturbation and diffusion, as well as the physical sample size. These synthetic model histories are then compared with the calculated Hg enrichment factors for many eruptive parameters with those from an actual sedimentary terrestrial Hg record (I. M. Fendley, Mittal, Renne, & Marvin-DiPasquale, 2019). For sedimentary Hg records from the time-period near the KPB boundary IRA-NV section ($\sim$ 40kyr before and $\sim$ 80kyr after the KPB boundary), I. M. Fendley, Mittal, Sprain, et al. (2019) find that the best-fit model parameters suggest eruptive episodes which lasted approximately 100 to 1000 years, occurred at least every 5-10 thousand years, and erupted around 40-240 cubic kilometers of basalt per year (I. M. Fendley, Mittal, Renne, & Marvin-DiPasquale, 2019). All of these estimates are averaged over the duration of the eruptive episode. Other longer sedimentary Hg records spanning the DT eruptive period also do not have pronounced hiatuses in peaks, after controlling for lithological effects and sampling resolution (Percival et al., 2018; G. Keller et al., 2018). Thus, to first order, Hg results do not find any support for a long ($>$ 50 kyr) hiatus throughout the "main-phase" DT volcanism, between $\sim$ 66.3 - 65.6 Ma.

We would emphasize that at present, the available Hg datasets do not have sufficiently uniform high resolution to reconstruct a time-varying eruptive history for the DT. Consequently, it is unclear if the IRA-NV section eruption rates are representative of the whole Wai subgroup, or just the Khandala-Bushe-Poladpur formations. Based on the available datasets (e.g., Percival et al., 2018; I. Fendley et al., 2019), individual eruptive episodes during the Ambenali formation had similar eruptions rates as the full DT main phase interval results, but with a longer eruption duration. However, more data are needed to confirm this preliminary conclusion. Nevertheless, we do not find any evidence for a significant increase in the time-period between eruptive intervals with the Hg dataset. This is in direct contrast to the model expectations for a larger magma reservoir wherein eruptions are expected to become less frequent during a CFB sequence.

It is also important to note that the Hg proxy integrates eruptions over the whole of the Deccan Traps (at any given time) instead of a single stratigraphic lava flow section. Thus, the results are not biased by local hiatus in a particular lava flow stratigraphic section. Based on modern CFB analogs, a $\sim$ 20 m thick lava flow may not cover the topography uniformly and completely (e.g., Thordarson & Self, 1993; Neal et al., 2019). Consequently, a single stratigraphic CFB section would probably not record all the lava flows in the region, especially for spatially extensive flows, e.g., Wai sub-group flows. We hence naturally expect that the eruptive tempo from paleo-secular variation measurements is slower than that from Hg. This process also helps explain the more frequent occurrence of weathering horizons (red boles) in the Wai subgroup flows vis-a-vis Kalsubai and Lonavala subgroups (Figure 1). In the field (WGE sections), most of the red boles are spatially heterogeneous and are, in most cases, not continuous across 10s of km. Our Hg eruptive rates are thus very compatible with results from geochronology (Section 3.2) and paleo-secular variation analysis (Section 3.3).

Our overall results are also consistent with the lava flow eruption rate estimates (10-200 km^3/year) based on flow morphology from Columbia River basalts (e.g., Vye-

Brown, Self, & Barry, 2013, Section 3.5). In conclusion, Hg chemostratigraphy does not provide any evidence for a prolonged province-wide eruptive hiatus, contrary to expectations from the large magma reservoir model (See Section 2.2.2).

3.5 Eruptive estimates based on lava flow morphology

Every CFB is comprised of 100-1000s of individual eruptive episodes, each of which is associated with a dominantly pahoehoe lava flow field (Self et al., 1998) with exceedingly rare fully developed a'a lava flows (Self et al., 1997; N. R. Bondre et al., 2004; Waichel et al., 2006; Sengupta & Ray, 2006; Passey & Bell, 2007; Duraiswami et al., 2008; Brown et al., 2011; El Hachimi et al., 2011; Vye-Brown, Self, & Barry, 2013; Braz Machado et al., 2015). Early studies of CFB flow fields proposed that individual flow fields were emplaced within a few days to weeks timescale with a correspondingly large eruption rate (Shaw & Swanson, 1970; Mangan et al., 1986; Tolan, 1989). However, extensive work on the lava flow fields in the Columbia River Basalt (Self et al., 1998; Vye-Brown, Self, & Barry, 2013, and references therein) has illustrated a strong similarity between CFB lava flows and modern Hawaiian and Icelandic lava flows despite the significantly different spatial scale. As a consequence, the CFB flows were emplaced as inflated compound pahoehoe flow fields with eruption rates similar to the highest observed for Iceland (e.g., Laki 1783; 8,700 m^3/s Thordarson & Self, 1993; Guilbaud et al., 2005) and Hawaii (e.g., Kilauea 2018: 130-200 m^3/s Neal et al. (2019), Mauna Loa a'a flow: 1,179-1,769 m^3/s Finch and Macdonald (1953)), but sustained over years to decades (e.g., Ho & Cashman, 1997; Keszthelyi & Self, 1998; Self et al., 1998; Anderson et al., 1999; Bryan et al., 2010; Keszthelyi et al., 2006); See S. Reidel et al. (2018) for an alternative viewpoint).

This conclusion is supported by the observations that the typical thickness of individual flow lobes in the Deccan Traps is $\sim$ 15-20 m (Jay, 2005; Jay et al., 2009) with only a few thicker lobes (up to 100 m) in the Wai subgroup formation (Koyna Core Mishra et al., 2017). Although this lobe thickness is larger than the typical value for Hawaiian pahoehoe flow fields ($\sim$ 5 m lobes, HSDP2 core Katz & Cashman, 2003), the Laki 1783 eruptions are associated with 15-25 m thick basaltic flows Thordarson and Self (1993).

Finally, the lack of a'a flow fields in CFBs provides an upper limit for permissible effusion rate. Hawaiian a'a flow fields form when emplacement is rapid (days to weeks, average effusion rates $\geq$10 m^3/s Rowland & Walker, 1990) with open lava channels near the fissure vents (e.g., Lipman & Banks, 1987; Wolff & Ramos, 2013). Since there is no clear evidence of such processes in most CFB flow fields (Self et al., 1998), we conclude that these flow fields (with much larger volumes than Hawaiian flows) must be emplaced over a long time-period (decades-centuries) rather than days-weeks. For the DT in particular, no clear lava tubes have been identified (Duraiswami et al., 2004; Pawar et al., 2015). However, the lack of unequivocally identified eruptive vents potentially allow for more frequent lava tubes and open channels. We also acknowledge that we do not preclude the possibility for some short-lived high effusion rate pulses that have been proposed to explain the rubbly pahoehoe structure in some CFB flows (N. R. Bondre et al., 2004; Duraiswami et al., 2008; B. Sen, 2017). In fact, Rader et al. (2017) have argued that effusive flux variations (of factor $\sim$ 2-5) are a necessary requirement for the formation of inflated sheet lobes. In both Columbia River Flood Basalts and Deccan Traps, the presence of multiple vesicle horizons in a single flow lobe may be evidence of this cyclic inflation (Hon et al., 1994; Cashman & Kauahikaua, 1997).

One potential challenge with using constraints on the effusion rate at the vent location to the estimate the duration of a CFB flow field is that each flow field may be fed by a long fissure system (e.g., $\sim$ 150 km for the CRB Rosa flow Self et al.,

1998). If this fissure is active along a significant fraction of its length, the total time-period for a CFB emplacement will be short despite the restricted effusion rate. This hypothesis can be tested by using the thickness of a flow lobe's upper vesicular crust to constrain the duration of active inflation of the thickest flow lobe in a flow field. For the $\sim$ 1300 km^3 Roza flow field in the CRB, Thordarson and Self (1998) estimated a minimum duration of 5 to 14 years (using the (Hon et al., 1994) $\sqrt{t}$ scaling for the thickness of the flow's upper crust). Using a similar method, Vye-Brown, Self, and Barry (2013) estimated similar minimum emplacement durations for other CRB flow fields: Palouse Falls (233 km^3, 19.3 years), Ginkgo (1570 km^3, 8.3 years), and Sand Hollow (2,660 km^3,16.9 years). These estimates are minimum estimates for the duration of a CFB field since they assume that the thickest flow was inflating throughout an eruption. If instead, different lobes undergo inflation at different times and/or have some time-hiatus between them, the total duration of a CFB field would be longer (order centuries) (See Vye-Brown, Self, and Barry (2013) for a more detailed discussion of other model uncertainties). Thus, we can conclude that individual CFB fields are emplaced over a long time-period ($\sim$ centuries) by sustained eruptions.

Another dataset supporting a multi-year to decadal-scale of CFB field emplacement is the low and high-temperature thermo-chronology around CRB dike segments ($\sim$ 1 km long) from the Chief Joseph dike Swarm (H. L. Petcovic & Dufek, 2005; Karlstrom et al., 2019). The active duration of the $\sim$ 10 m thick Maxwell dike is constrained to be 1.4–5.4 years (H. L. Petcovic & Dufek, 2005; Karlstrom et al., 2019) while the $\sim$ 10 m Lee dike was active for 1.7 - 4.1 years with a long flow unsteadiness scale of 3.9 - 11.3 years (Karlstrom et al., 2019). Although more observations are needed to assess how representative these values are for other CRB dikes, as well as DT dikes, the general lack of melt-back in CRB dike swarm (Grunder & Taubeneck, 1997) suggests that analogous to the Laki 1783 eruption, different parts of the fissure may have been active at different times during an eruption (Thordarson & Self, 1993). Summarizing the various observations, we conclude the CFB flow fields were most likely emplaced over a decade to centuries with eruption rates comparable to the peak Laki 1783 eruption rate.

4 Geochemical characteristics of Deccan Flows - Implications for the magmatic system

We can indirectly constrain some of the characteristics of the DT magmatic architecture based on the stratigraphic pattern of geochemical variations in lava flows. Since the Deccan magmas underwent a complex sequence involving fractionation (potentially at multiple depths), assimilation of multiple components, and periodic replenishment of parental magmas before surface eruption, it is difficult to confidently ascertain the volume of cumulate material or their precise P-T histories and storage locations (See discussion in O'Hara and Herzberg (2002) and references therein). However, we can use stratigraphic changes in major, minor, and isotopic compositions to constrain the nature of the magmatic plumbing structure, especially whether an open system with constant recharge is required.

With regards to Deccan magma across all subprovinces, there is a general consensus that the AFC processes occur first in a lower crust reservoir(s) followed by shallow ($<$ 2 kbar) fractionation and mixing (and in some cases assimilation) in upper crustal magma reservoir(s) (K. Cox & Devey, 1987; Devey & Cox, 1987; J. J. Mahoney, 1988; Hawkesworth et al., 1990; Lightfoot, Hawkesworth, et al., 1990; Z. Peng et al., 1994; J. Mahoney et al., 2000; G. Sen, 2001; Chatterjee & Bhattacharji, 2008; H. C. Sheth & Melluso, 2008; Natali et al., 2017). However, within with the general framework, is the magmatic plumbing system primarily a closed system with pulsed inputs of melts into the upper crustal system followed by closed system fractionation and assimilation?

4.1 Open System behavior

Firstly, many geochemical formations (e.g., Ambenali, Beane et al., 1986) as well various individual sections in other DT provinces (e.g., Malwa Plateau, Haase et al., 2019) typically have a restricted major and minor element composition. This observation can be explained by either of the two-model end-members: a quasi-steady state open magmatic system with reservoirs undergoing Recharge, Tapping via eruptions, Fractionation, and Assimilation (RTF, O'Hara & Mathews, 1981; Leeman & Hawkesworth, 1986; K. Cox, 1988; Arndt et al., 1993), or a thermally buffered, quasi-closed magma reservoir undergoing minimal chemical evolution (as suggested in Black & Manga, 2017). Similarly, continuous stratigraphic changes (e.g., from Poladpur to Ambenali) in ratios between incompatible elements (e.g., Ba and Zr) and isotopes can be explained by either of the scenarios since the observation-only requires some form of mixing between different magma bodies (K. Cox & Hawkesworth, 1985). However, if the system undergoes a sudden change in lava composition (e.g., Bushe to Poladpur), a model with large lower and upper crustal reservoirs will have challenges since it is difficult to change bulk compositions with a large volume of pre-existing melt without drastic amounts of contamination. Instead, it is easier to explain these transitions in a magmatic system with multiple chambers coupled with changes in lower crustal magma compositions (K. Cox & Hawkesworth, 1985).

Finally, the Black and Manga (2017) style model predicts an increasing contribution from crustal assimilation with increasing thermal maturity of the upper crust. In contrast, the least contaminated DT lava flows are the Ambenali formation, which erupts towards the end of the sequence. We note that over time, the increasing size of the crustal magma reservoir due to the addition of lower crustal melt (Black & Manga, 2017) will partly modulate this effect. However, without quantitative calculations, it is unclear how much this will buffer compositions. For the DT, multiple authors have proposed that minimal crustal assimilation of the Ambenali flows (even though they have undergone extensive fractionation) is a consequence of geochemical buffering due to plating of the reservoir by previous solidification zones (e.g., J. J. Mahoney, 1988; Devey & Cox, 1987). If this process were to be relevant for the large magma reservoir also, it could explain the Ambenali formation composition within that model context. However, it will also further increase the hiatus time between eruptive episodes since the crustal volatile source will be removed unless the parental magma has sufficient volatile content to be buoyant.

4.2 Intra-geochemical formation variability

Another avenue to distinguish among the two model end-members is to use the small but resolvable geochemical (e.g., Sr isotopes, Ni and Ti, Cr and Zr, Mg and Fe; J. J. Mahoney, 1988, and references therein) and petrological variations (e.g., phenocryst fraction and modal percentages of ol, plag, and cpx; Beane et al., 1986; Pattanayak & Shrivastava, 1999; G. Sen, 2001; Krishnamurthy, 2020; Basu, Saha-Yannopoulos, & Chakrabarty, 2020) within a geochemical formation. As illustrated by almost all sections in WG, the stratigraphic variation in a formation is not smooth even after accounting for possible biases due to surface alteration and lava flow fractionation (J. J. Mahoney, 1988; K. Cox & Hawkesworth, 1985; Krishnamurthy, 2020; Basu, Saha-Yannopoulos, & Chakrabarty, 2020). In Figure 3, we show a few representative sections from the Deccan Traps illustrating this behavior. In Figure 3a, we show the $^{87}Sr/^{86}Sr$ variation for a composite WG section with geochemical formations from Neral to Mahabaleshwar as well as an inset with just Ambenali, Mahabaleshwar, Panhala formations (Beane et al., 1986; Lightfoot & Hawkesworth, 1988). Figure 3b shows the dataset for Zr in a 480 m section spanning almost the whole Ambenali Formation section (the Torna hill-fort Devey & Lightfoot, 1986). Both these datasets clearly illustrate quasi-oscillatory variations within a single geochemical formation.

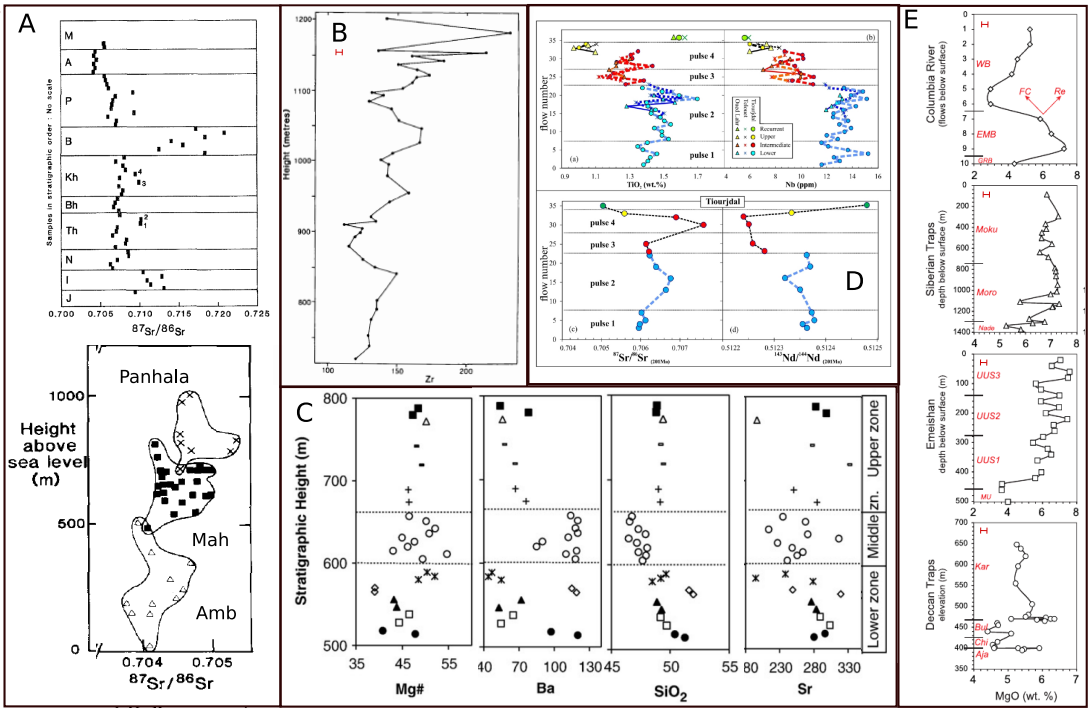

Figure 3: Representative sections showing geochemical variations within a stratigraphic section for Deccan Traps and some other continental flood basalts. A) $^{87}Sr/^{86}Sr$ variation for a composite WG section with geochemical formations from Neral to Mahabaleshwa(from Beane et al., 1986) with a zoomed inset showing the variations for the Ambenali, Mahabaleshwar, Panhala formations (from Lightfoot & Hawkesworth, 1988). B) Variation in Zr in a 480 m section spanning almost the whole Ambenali Formation section (the Torna hill-fort, Devey and Lightfoot (1986); K. Cox (1988)). C) Geochemical data from the Bhir section located about 300 km east of WGE in the Central Deccan province (from Talusani, 2010) with alkalic middle flow (this section has been correlated with the Ambenali formation). D) Geochemical datasets from the CAMP sections from Morrocco. The Nb (ppm), TiO_2 (wt %) data is shown for three sections from the Central High Atlas Mountains - Tiourjdal, Telouet, Oued Lahr while the isotopic dataset are from Tiourjdal section only. The Figure also shows the 4 eruptive pulses defined based on classical Directional Group analysis by Knight et al. (2004)(from Marzoli et al., 2019) E) MgO (wt %) for stratigraphic sections for stratigraphic sections for various flood basalts (from Yu et al., 2015). The dataset for Columbia River basalt include Eckler Mountain Basalt (EMB) and Wanapum Basalt (WB) flows. The Deccan Traps section is from K. V. Kumar et al. (2010) showing the Ajanta (Aja), Buldhana (Bul), Chikhli (Chi) formations (correlative to the Poladpur formation), and Karanja (Kar) formation (correlative to the Ambenali formation). The Yangliuping basaltic sequence from Emeishan large igneous province has been divided into four units by Song et al. (2006). Finally, the Siberian Traps section consists of three formations Mokulaevky (Moku), Morongovsky (Moro), and Nadezhdinsky (Nade) (Lightfoot, Hawkesworth, et al., 1990). The FC and Re arrows indicate the effect of Fractional Crystallization and magma recharge in an REAFC (REcharge Assimilation Fractional Crystallization) model. The typical error bar for each panel is of the size of the symbol unless otherwise specified. All of these datasets clearly illustrate quasi-oscillatory variations within a single geochemical formation across CFBs.

As another example, we show the geochemical data for the 282 m Bhir section located about 300 km east of WGE in the Central Deccan province Talusani (2010) in Figure 3c. Based on the trace element ratios (e.g., Zr/Nb, Ba/Y) most diagnostic of different WG geochemical formations as well as regional stratigraphy (Jay & Widdowson, 2008), the Bhir section lavas have Ambenali-type geochemistry (Talusani, 2010). However, within this section (10 flows), the middle flow is alkalic with a very different composition compared to the other tholeiitic basalt flows in the section. Additionally, the Bhir basalts show a wide range of chemical compositions for incompatible elements (e.g., Nb, Zr, Y, and Rare Earth Elements) between individual flows as well as within a single flow (e.g., the middle alkalic flow). Since the difference between alkalic and tholeiitic basalt is explained as a different degree of partial melt in the mantle, the presence of the flow in the same geochemical formation is indicative of a magmatic plumbing system that does not homogenize the melt in a large magma reservoir (Talusani, 2010).

We show another Central Deccan Trap stratigraphic section in Figure 3e (lowermost panel) where the local geochemical formations are correlative to the Ambenali and Poladpur formations (K. V. Kumar et al., 2010). Similar to the other examples, there is clear evidence of oscillations in MgO concentration within the same formation. We would emphasize that these examples are not unique and are instead representative of a large number of DT studies both within WGE as well as other subprovinces (e.g., K. Cox & Hawkesworth, 1985; Devey & Cox, 1987; Devey & Lightfoot, 1986; Lightfoot, Hawkesworth, et al., 1990; Z. Peng et al., 1998; J. Mahoney et al., 2000; Sengupta & Ray, 2011; S. K. Bhattacharya et al., 2013; Z. X. Peng et al., 2014; Haase et al., 2019). This conclusion is also illustrated by the fact that each geochemical formation typically traces out an extended region (much larger than analytical uncertainty) in the Sr, Pb, and Nd isotope parameter space instead of a single point (e.g., Vanderkluysen et al., 2011).

Our conclusion of continuous magma recharge and mixing during the eruption of a geochemical formation is further supported by the common occurrence of various zoning patterns (normal, oscillatory, reverse, complex) in plagioclase and clinopyroxenes phenocrysts in lavas. These zoning patterns are indicative quasi-continuous mixing between primitive and evolved magmas (Lightfoot et al., 1987; Pattanayak & Shrivastava, 1999; N. R. Bondre et al., 2004; Talusani, 2010). Similar to other geochemical variations, both the type of zoning patterns as well as phenocryst mineral composition (e.g., anorthite content of plagioclase) show clear changes in a stratigraphic section but without any smooth pattern (Lightfoot, Hawkesworth, et al., 1990).

4.3 Geochemical variability - Model

K. Cox (1988) proposed that these kinds of variations can be explained using a RTF-type magma reservoir with stochastic melt influx (z, in units of initial magma reservoir mass/model cycle), eruption rate(y, in units of magma reservoir mass/model cycle), and crystallization rates (x, in units of magma reservoir mass/model cycle) around the steady-state values. K. Cox (1988) showed that a WG Ambenali section (Figure 3c) could be statistically reproduced by the model with $x/y \sim 1$, z random chosen between 0-5, and $x \sim 0.05$ along with a slow increase in x up-section (to produce the long term trend). Each lava flow is considered the output of one model cycle and the lava's trace element composition oscillates around a steady-state value. Although this is a reasonable model to explain the data, it requires that a significant mass influx (up to five times the original magma reservoir mass) into the system throughout the eruption of a geochemical formation (i.e. an open system). This is extremely difficult to do for a large magma reservoir, especially the upper crustal reservoir where the expected influx is expected to be large ($z \sim$ 1-3) but only occur a few times at most during the eruption of a geochemical cycle (Black & Manga, 2017).

In order to explore a broader range of values for z (and corresponding values of x and y) can explain the geochemical datasets, we use a modified version of the Recharge-Eruption-Fractional crystallization model (ignoring assimilation to be consistent with K. Cox, 1988). Although this is not as thermodynamically rigorous as the Magma Chamber Simulator (e.g., Heinonen et al., 2020), this model captures the first order behavior of interest here. Following C.-T. A. Lee et al. (2014); Yu et al. (2015), and K. Cox (1988), the rate of change of the total mass M and elemental mass m_{ch} of a magma reservoir per eruptive cycle (dN_c) is :

$$\frac{dM}{dN_c} = \frac{dM_{re}}{dN_c} + \frac{dM_e}{dN_c} + \frac{dM_{cc}}{dN_c} + \frac{dM_x}{dN_c} \tag{1}$$

$$dm_{ch} = dM_x DC_{ch} + dM_e C_{ch} + dM_{cc} C_{cc} + dM_{re} C_{re} \tag{2}$$

$$\frac{dM_{re}}{dN_c} = z * M_{initial} \tag{3}$$

$$\frac{dM_e}{dN_c} = y * M \tag{4}$$

$$\frac{dM_x}{dN_c} = x * M \tag{5}$$

Here, the magma reservoir mass changes due to eruption (dM_e, negative), assimilation (dM_{cc}, positive), recharge (dM_{re}, positive), and fractional crystallization (dM_x, negative) during an eruptive cycle (dN_c). For the elemental mass balance term, C_{ch} is the element's concentration in the magma reservoir, C_{cc} is the wall-rock composition, and C_{re} is the recharge composition. D is the equilibrium partition coefficient between crystals and melt during fractional crystallization. For our calculations here, we set $dM_{cc} = 0$ to prevent crustal assimilation and x/y =1. Following Yu et al. (2015) and K. Cox (1988), we set bulk partition coefficients for Mg and Zr as 2 and 0.001 respectively. Since the actual composition of the magma recharge is not known, we assume a primitive magma composition with MgO = 9 wt % and Zr = 85 ppm (see K. Cox, 1988; J. J. Mahoney, 1988). We would emphasize our focus with these calculations is to look at broad features and hence the exact parameter choices are not important. For the starting magma composition in the magma reservoir, we set MgO = 5.8 wt % and Zr = 160 ppm, a range typical for the Ambenali formation (Beane et al., 1986; K. Cox, 1988). We randomly choose the value of x,y,and z between 0 and the maximal values x^m,y^m,and z^m.

In Figure 4, we show the results of the calculations for three sets of values : $x^m = y^m$: 0.03 (red), 0.02 (black), 0.01 (blue), and z^m : 0.06 (red), 0.04 (black), 0.02 (blue). The values have been chosen such that the magma reservoir is in quasi-steady state over 100s of eruptive cycles. The key result from this analysis is that sufficiently large values of z^m (and corresponding x^m and y^m) ~ 0.06 are required to produce the amplitude of variations in Figure 3b and 3e (ignoring any long term trends). Although the precise threshold value will be dependent on the exact parameter choice for recharge magma, the result that recharge must be at least a few percentages of the reservoir size is a robust conclusion. In Figure 5A and 5B, we show model results where we have set either recharge (z, Figure 5A) or crystallization (x, Figure 5B) to be zero. We set the other parameters at $x^m = y^m = 0.03$ and $z^m = 0.06$ with the three lines in Figure 5A and 5B showing three model realizations each with the same input parameters. These results clearly illustrate that without all three processes in REFC, we do not get the oscillatory pattern of geochemical variation but instead only a persistent trend.

Based on the model results, there are two primary requirements for explaining the observations: a) a combination of fractional crystallization, recharge, and eruption together in a RTF/REAFC (or a variant of these, see O'Hara & Herzberg, 2002) type magma reservoir, b) a magma recharge volume at least a few percent of the reservoir mass.

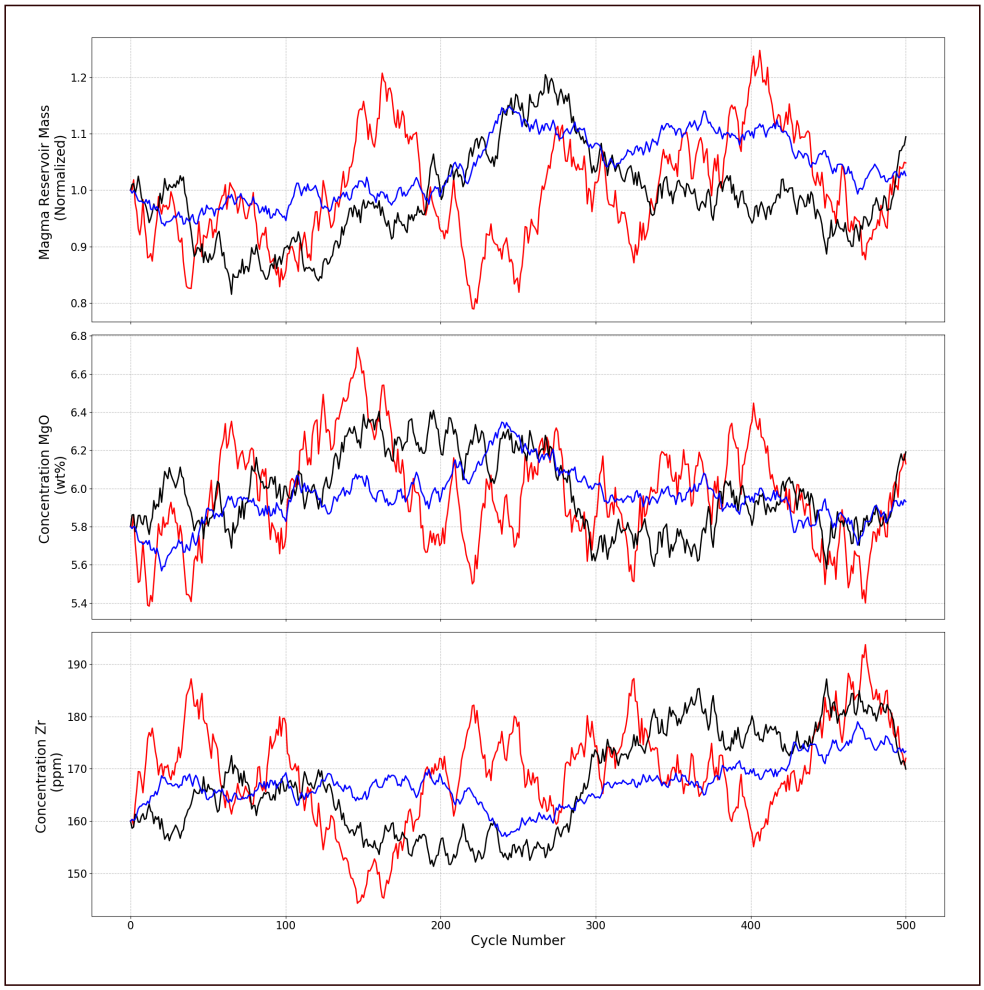

Figure 4: Results of REAFC model for Normalized magma reservoir mass, MgO (wt %), and Zr concentration (ppm). Calculations for three sets of values : $x^m = y^m$: 0.03 (red), 0.02 (black), 0.01 (blue), and z^m : 0.06 (red), 0.04 (black), 0.02 (blue) with stochastic variation around the mean value.

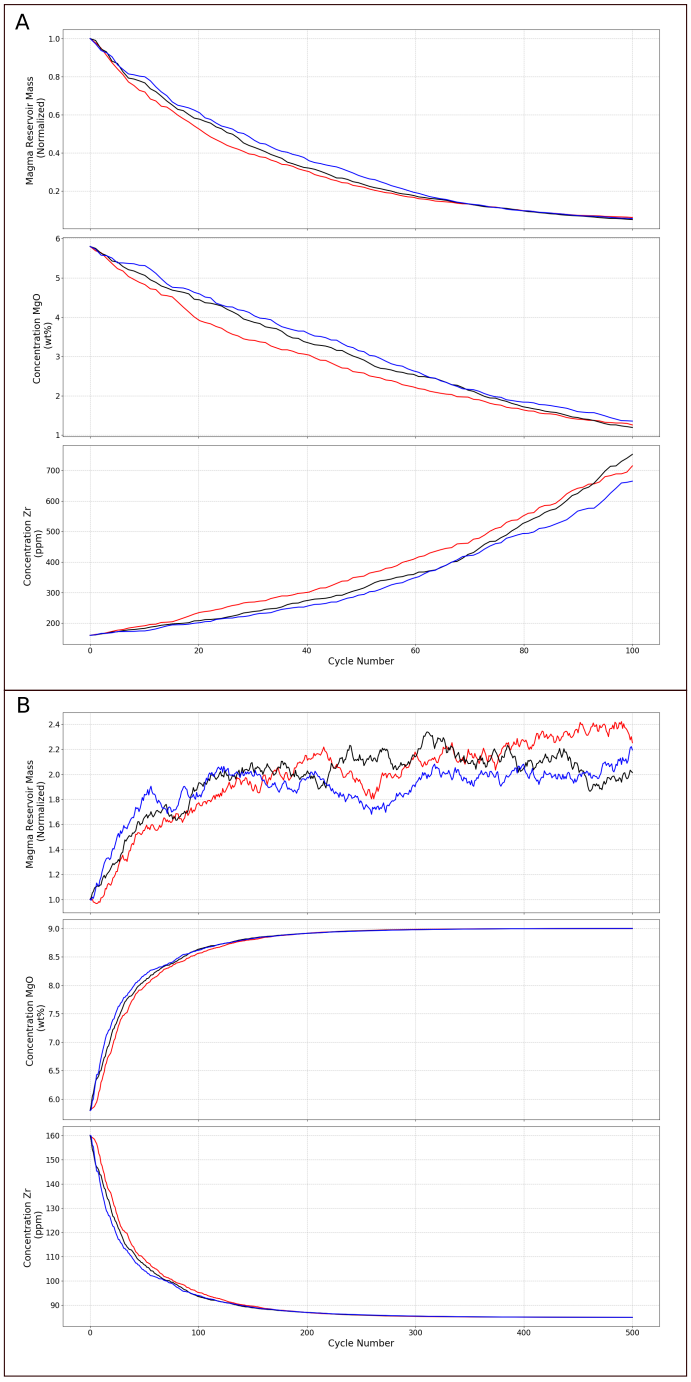

Figure 5: Results of REAFC model for Normalized magma reservoir mass, MgO (wt %), and Zr concentration (ppm). A) Calculations with no recharge (z = 0) B) Calculations with no crystallization (x = 0). We set the other parameters at $x^m = y^m = 0.03$ and $z^m = 0.06$ with the three lines each panel showing three model realizations each with the same input parameters.

4.4 Intra-Flow compositional variations

Although typically individual lava flows in a CFB are considered to be geochemical homogeneous, a few studies have illustrated that this may not always be the case (e.g., Philpotts, 1998; S. P. Reidel, 2005, 1998; N. R. Bondre & Hart, 2008); Passmore et al. (2012) for Laki 1783 eruption). The results of Vye-Brown, Gannoun, et al. (2013) and Vye-Brown et al. (2018) provide especially clear examples of the geochemical variations in products of a single eruption in the Columbia River Basalts.

Through the detailed mapping of the Sand Hollow ($\sim$ 2660 km^3) and Palouse Falls ($\sim$ 233 km^3) flow fields (Vye-Brown, Self, & Barry, 2013), these studies ensured that any observed variations were within a single eruption unit and not due to stratigraphic errors. In both cases (Sand Hallow and Palouse Falls), there is clear geochemical heterogeneity (major and minor elements) within both a single flow lobe, as well as laterally between different flow lobes of a single flow field. Based on the pattern of change across multiple elements, these studies concluded that either chemical weathering or post-emplacement fractionation could not have produced the observed variations. Instead, the intra-lobe and inter-lobe variations are indicative of heterogeneity within the magmatic system feeding the eruption. This conclusion is further supported by variations in $^{187}Os/^{188}Os$ isotopes across a 35 m Sand Hallow flow lobe that require different amounts of crustal assimilation in the erupted melt (Vye-Brown, Gannoun, et al., 2013). These observations are inconsistent with a compositionally homogeneous magma reservoir feeding an individual eruptive episode (See Section 2.2.3). Instead, each eruptive episode is likely sourced from a magmatic system consists of a network of magma reservoirs with more primitive compositions over time (potentially from deeper magma bodies) (Vye-Brown et al., 2018). A counter example of this intra-flow geochemical hetereogeneity is a $\sim$ 2000 km^3 Nadayansky flow in Siberian Traps. Over the flow's few hundred km length, the lava major and trace element composition remains constant, within the analytical uncertainties (N. Krivolutskaya & Kedrovskaya, 2020).

Nevertheless, with the limited number of studies at present, it is unclear how common (or uncommon) intra-flow variations are for CFBs in general, especially isotopic variations which are less sensitive to post emplacement alteration and fractionation. In particular, no systematic stratigraphically controlled analysis of intra-flow variations has been done for lava flows in the Deccan Traps. This is partially due to the challenge of carefully mapping single flow fields over 10s-100s of km physically (Patil et al., 2020; Dole et al., 2020). Nevertheless, there are some potential examples from DT suggestive of geochemical differences within a single eruptive unit. For instance, K. Cox and Hawkesworth (1985) noted that the Kelghar Mafic Unit in the Mahabaleshwar Formation is restricted to only a single WG section. However, less mafic, but geochemically related Mahabaleshwar flows, are present at the same stratigraphic height in sections less than 40 km [away??]. Thus, one potential explanation for the Kelghar Mafic Unit is that it represents a small magma batch within the eruption of a larger, spatially extensive flow field. A similar interpretation has also been proposed for the DT lava flows with large concentrations of multi-cm long plagioclase phenocrysts - giant phenocryst basalts (GPBs P. Hooper, 1988b; Higgins & Chandrasekharam, 2007; H. Sheth, 2016). These flows occur at multiple stratigraphic heights within the WG sections though they are more common during the Kalsubai subgroup (e.g., Beane et al., 1986). They are also found in some of the other Deccan subprovinces (e.g., Talusani, 2012; Alexander & Purohit, 2019). Since GPBs are sometimes not continuous within a single physical eruptive unit, this suggests intra-flow variation within a single eruptive epsiode (Paul Renne and Steve Self, personal comm.).

Other potential evidence for geochemical variations within an eruptive event comes from compositional (including isotopic) differences along a single dike (N. Bondre et al., 2006; R. Ray et al., 2007; H. C. Sheth et al., 2009, 2013; Vanderkluysen et

al., 2011; Cucciniello et al., 2015; H. Sheth et al., 2018). Additionally, closely spaced dikes in a dike swarm don't always have the same chemical compositions (N. Bondre et al., 2006; H. Sheth et al., 2019).

Finally, a substantial fraction of dikes in the Deccan Traps have multiple columnar jointed layers due to several magma injections (H. C. Sheth & Cañón-Tapia, 2015, and references therein). Frequently, each of these layers has a different geochemical composition indicative of a different batch of magma (H. C. Sheth & Cañón-Tapia, 2015; Cucciniello et al., 2015; Gadgil et al., 2019). A typical time-period for the emplacement of these composite dikes can be estimated based on the requirement that dikes need to cool sufficiently between each injection to form and preserve layered columnar joints. Using this principle, H. C. Sheth and Cañón-Tapia (2015) estimated that a multiple large dike (20-m-thick with ten columnar rows) would be emplaced over a minimum of several years and more likely up to a 100 years after accounting for latent heat of crystallization as well as the increasing country-rock temperature after emplacement of each dike segment (Evelyne et al., 2018). We readily acknowledge that there are counter-examples to this with DT dikes that are compositionally homogeneous over 10s of km (e.g., Vanderkluysen et al. (2011), see Kalsbeek and Taylor (1986); R. E. Ernst (2014); Buchan and Ernst (2019) for examples from other CFBs) and that some of the compositional differences may be due to dike-wall rock interactions. With existing literature, we cannot assess how ubiquitous intra-dike geochemical variations are. Still, observations from even a few dikes, along with physical evidence for multiple injections, suggests that a homogeneous, well-mixed magma reservoir does not always feed individual eruptive episodes. Additionally, the presence of multiple dikes in Deccan Traps hints at a long duration ($\sim$ 100 years) for each eruptive episode consistent with other datasets described in this section.

4.5 Geochemical variability - Implications for magmatic architecture

Considering the observations and the model results, we contend that it is very difficult to explain these with a large magma reservoir end-member. Firstly, this model predicts that a single geochemical formation with 10s of eruptive episodes is erupted very rapidly (order 100s to a few 1000 yrs, Black & Manga, 2017). Hence, there is generally not enough time-period between individual eruptive episodes for significant crystal fractionation or assimilation to change magma composition based on diffusion and crystal growth time-scales (Borges et al., 2014; H. Sheth, 2016). The large compositional inertia of the system due to the large magma volume makes this even more challenging. Secondly, the oscillatory stratigraphic, geochemical changes require an influx of some primitive melt input along with fractionation based on our calculations. The recharge into the crustal magma reservoir needs to quasi-continuous, which is contrary to the model results for a large magma reservoir model wherein there are generally very large but very sparse magma inputs for upper crustal reservoirs (Black & Manga, 2017, See description in Section 2.2.2, 2.2.3). The observations are best explained by a smaller (order 5 %) continuous melt input into the magma reservoir (s). Thus, we conclude that the pattern of geochemical variations strongly suggests that the large magma reservoir end-member is not realistic. Instead, these variations are a natural outcome in a RTF/REAFC model with one or multiple magma reservoirs (K. Cox & Hawkesworth, 1985; Yu et al., 2015).

4.6 Observations from other CFBs

The stratigraphic section in many other CFBs shows the same characteristic geochemical variability features as described above for DT (inter and intra-geochemical formation variations). In Figure 3d and 4e, we show a few example cases for the Central Atlantic Magmatic Province (Figure 3d, CAMP Marzoli et al., 2019), Siberian Traps (Lightfoot, Naldrett, et al., 1990), Columbia River Basalts (P. Hooper, 1988a;

P. R. Hooper, 2000), and Emeishan CFB (all Figure 3e, Song et al., 2006). All of these cases have the same oscillatory features within a single geochemical formation as in DT. Many similar examples have been described for most CFBs: CAMP (e.g., Tegner et al., 2019; Marzoli et al., 2019, and references therein) , Karoo-Ferrar CFB (Fleming et al., 1992; D. Elliot et al., 1995; Fleming, 1995; J. Marsh et al., 1997; Luttinen & Furnes, 2000), Siberian Traps (Lightfoot, Naldrett, et al., 1990; Fedorenko et al., 1996; Reichow et al., 2005; N. A. Krivolutskaya & Sobolev, 2016; N. Krivolutskaya et al., 2018; N. A. Krivolutskaya et al., 2018), North Atlantic Magmatic Province (NAMP, Andreasen et al., 2004; Peate et al., 2008; L. M. Larsen & Pedersen, 2009; Millett et al., 2016, 2017), Parana-Etendeka (Peate & Hawkesworth, 1996; Machado et al., 2018), Ethiopian Traps (Kieffer et al., 2004; S. Krans et al., 2018), and Columbia River Basalts (CRB, Brueseke et al., 2007; Wolff & Ramos, 2013; Moore et al., 2018; Potter et al., 2018). The CAMP section shown in Figure 3d is particularly illustrative since the stratigraphic section is divided into four individual pulses based on paleo-secular variation analysis each of which has been interpreted to have been erupted within a few hundred years (Knight et al., 2004; Font et al., 2011; Marzoli et al., 2019, although see the discussion in Section 3.3). Nevertheless, the individual lava flows in a "pulse" have different major and minor elements, as well as Sr and Nd isotopes with the same quasi-oscillatory oscillations as the DT examples. These variations are characteristic of continuous magma mixing, recharge, assimilation, and fractionation (Section 4) and are hence inconsistent with expectations from a single large homogeneous upper crustal magma reservoir (See Section 2.2.2). We readily acknowledge that precise REAFC characteristics (with respect to values of x,y,z) for each CFB province are different and a careful examination of each CFB, and the corresponding magmatic architecture constraints, is beyond the scope of this study. Nevertheless, the general prevalence of flow-by-flow geochemical variations is a robust feature.

In many CFBs, a significant component of the magmatic system is the shallow ($<$ 4 km, See Magee, Ernst, et al., 2019; Hoggett, 2019; S. M. Jones et al., 2019) sill complexes emplaced in cratonic and passive margin sedimentary basins. The typical sill radius, area, and thickness in these complexes as is illustrated by a dataset from NAMP are 1-7.5 km, 1-100 km^2, and 100-500 m respectively (S. M. Jones et al., 2019; Magee et al., 2018; Magee, Ernst, et al., 2019). Nevertheless, the volumes of some of the largest sills can be similar to a single DT eruptive episode e.g., CAMP Palisades Sill (1500- 5000 km^3, Husch, 1990), Karoo-Ferrar associated Peneplain Sill (4750 km^3, Gunn & Warren, 1962), and Basement Sill in McMurdo Dry Valleys (1050 km^3, B. Marsh, 2004; Petford & Mirhadizadeh, 2017), Karoo Basin sills (upto 3000 km^3, H. Svensen et al., 2012), and the Karoo-Ferrar Dufek-Forrestal intrusions (10,200-11,880 km^3, Ferris et al., 1998). Since most sill complexes have been discovered and characterized primarily through seismic datasets (with some boreholes) (e.g., Magee et al., 2018; Galland et al., 2018; Magee, Ernst, et al., 2019), any geochemical variation between individual sills is difficult to ascertain.

The one exception to this is the Karoo Basin where a large number of sills are exposed and accessible. Through careful sampling of 5 sills and a dike over 125 km^2 area (Golden Valley Sill Complex, Karoo basin, South Africa), Galerne et al. (2008, 2011) found that each of the sills, barring two, have different geochemical signatures and hence were fed by a different magma batch. This conclusion is supported by the few studies of larger sills which show evidence for multiple magma injections based on stratigraphic geochemical and petrological analysis e.g., the Beacon Sill (M. Zieg & Marsh, 2012), Palisades Sill (Husch, 1990; Gorring & Naslund, 1995), the Basement Sill (B. D. Marsh, 2004; Bédard et al., 2007), the Doros Complex (T. Owen-Smith & Ashwal, 2015), and the Black Sturgeon Sill (M. J. Zieg & Wallrich, 2018). Thus, these results suggest that large sills and sill complexes were emplaced as multiple magma batches over time (potentially within 10-100s of years to prevent sill solidification) with some of the magma injections having different compositions. We contend that

it is difficult to obtain these eruption characteristics if the magma is sourced from a single, large well-mixed magma reservoir, especially considering the eruption rate results described later in this study.

5 Magmatic Architecture observations - Deccan Traps

The final, direct constraint on the crustal magmatic architecture of continental flood basalts is the exposed magmatic plumbing system - the dike swarms & sills. In CFB provinces, the primary mechanism for magma transport from crustal reservoirs to the surface is a combination of mafic dike swarms, sills - both deep crustal sills (Wrona et al., 2019; Buntin et al., 2019) as well as shallow sill complexes (Maccaferri et al., 2011; Magee, Ernst, et al., 2019). Since the Deccan Traps were emplaced primarily atop Archean cratons, there are no large scale sill complexes hosted within sedimentary basins like many other CFBs e.g., Karoo-Ferrar province, Siberian Traps, North Atlantic Magmatic Province, and Central Atlantic Magmatic Province (See H. Svensen et al., 2018; Magee, Ernst, et al., 2019, and references therein). The sills in Deccan are generally restricted to the outlying regions of the province with sedimentary basins e.g., Jurassic sedimentary rocks in Kutchh (Biswas, 1982, 1987; Karkare & Srivastava, 1990; Duraiswami et al., 2008; Karmalkar et al., 2016) and Gondwana sediments in Central Indian Satpura Range (Crookshank, 1936; Sengupta & Ray, 2011). In addition, a small lopolith is emplaced in an intertrappean at Amboli hill, Mumbai (Tolia & Sethna, 1990), after the main DT eruptive phase (See discussion in Section 3.2.2 about Mumbai section).

The saucer-shaped Mahad sill (Duraiswami & Shaikh, 2013) in the southwestern Deccan Traps is one of the few DT sills within the main DT section along with the olivine-gabbro Khopoli intrusion (Cucciniello et al., 2014). The Mahad sill, the larger of the two, is 7.1 km x 5.3 km long and is intruded into a Bushe Formation flow. Since the sill is geochemically associated with either the Poladpur- or Ambenali Formation, the sill was emplaced at < 1 km depth from the surface (Duraiswami & Shaikh, 2013). Based on existing work, none of these sills feed subaerial lava flows. The only known basaltic sill in DT that may have been responsible for magma transport to an overlying lava flow is the $\sim$ 200 m Chakhla-Delakhari Intrusive Complex (CDIC) in the Central Deccan region (Crookshank, 1936; Shrivastava et al., 2008; H. C. Sheth et al., 2009). CDIC is the largest DT basaltic sill complex with an area of about 150 km^2 and is emplaced primarily in the Gondwana sandstone. The complex stratigraphic shape, spatially variable thickness, the mineralogical as well as chemical heterogeneity, and textural features of the CDIC strongly suggest that it is composed of multiple individual intrusions with different compositions (Crookshank, 1936; H. C. Sheth et al., 2009). Finally, We note that there are a number of small primarily alkaline intrusive complexes in the Saurashtra and Malwa Plateau subprovinces of DT such as Girnar, Osham, Barda (dominantly granophyre), Alech hills (dominantly rhyolite) of Saurashtra as well as the Pavagadh and the Phenai-mata igneous complexes in the Narmada-Tapti Tectonic Zone (Auden, 1949; Greenough et al., 1998; B. Singh et al., 2014a; Cucciniello et al., 2019). Although a number of these intrusions (e.g., Phenai-mata and Pavagadh) are associated with local tholeiitic and alkaline magmatism, there is as yet no geochemical, geochronological, or volcanological evidence suggesting that these intrusive complexes fed large DT lava flow units, especially any of the main phase WG flows.

5.1 Deccan Dike Swarm

The large Deccan Traps eruptive episodes are instead hypothesized to have been fed by tholeiitic dike swarms (Vanderkluysen et al., 2011). There is no concensus if individual eruptive episodes were fed by a single dike (with sequentially active fissure

segments like 1783 Laki eruption, Thordarson & Self, 1993), a set of dikes fed from the same magmatic system, or eruptive centers 100s of km apart that all fed the same flow field (Self et al., 1998; Vanderkluysen et al., 2011; Óskarsson & Riishuus, 2014; Kale et al., 2020). Without a detailed field analysis of individual flow fields along with complementary geochemical and isotopic analyses, each of these models may be applicable for Deccan eruptive episodes with potentially different styles for different DT regions, subprovinces, and/or geochemical formations. The four main DT dike swarms are the Narmada-Tapi dike swarm extending across from Mandla Lobe region to Saurashtra (Sant & Karanth, 1990; Bhattacharji et al., 1996; Melluso et al., 1999; R. Ray et al., 2007; H. C. Sheth et al., 2013; Cucciniello et al., 2015; H. Sheth et al., 2019), the Saurashtra dike swarm (Cucciniello et al., 2020; Chatterjee & Bhattacharji, 2001), the Western Ghats Coastal dike swarm (Widdowson et al., 2000; P. Hooper et al., 2010; H. C. Sheth et al., 2014; Patel et al., 2020), and the Central Dike Swarm (also called Nasik-Pune dike swarm) located to the east of the WGE (N. Bondre et al., 2006; Vanderkluysen et al., 2011; R. Ray et al., 2007; Das & Mallik, 2020) (See Figure 6). Based on similar major and minor element geochemistry as well as Pb-Nd-Sr isotopes, the three (excluding the Saurashtra swarm which feeds that corresponding sub-province) major dike swarms have been correlated with individual geochemical formations across the Deccan Traps (e.g., Vanderkluysen et al., 2011; Patel et al., 2020, and references therein). Vanderkluysen et al. (2011) concluded that lower and middle subgroups were most likely fed by the oriented Narmada-Tapi and Coastal dike swarms while the Upper subgroup lavas were predominantly fed by Nasik-Pune (Central) dike swarm.

Since the spatial pattern of dike emplacement in the upper crust is primarily controlled by the crustal stress field (See M. A. Richards et al., 2015, and references therein), we can use the dike distribution in the Deccan Traps to test the large magma reservoir model. In particular, we are interested in assessing whether there is any clear radial or circumferential dike pattern as expected from a single magma body (R. Ernst et al., 2019; Buchan & Ernst, 2019; Bistacchi et al., 2012; Johnson, 1961). The other possible alternatives are that the dike orientation was controlled by a) overall tectonic extension pattern (especially in the Narmada-Tapi rift zone and the West Coast) in India (O. P. Pandey, 2020), or b) stress field associated with multiple individual magma reservoirs leading to a heterogeneous, and likely time-dependent, stress field. We test these end-members using a new data dataset from a combination of Deccan field mapping by the Geological Survey of India (GSI 1:50k maps, Raju (2016); GSI District Resource Map (2001); GSI Bhukosh (2020 (accessed December 1, 2020))) and joint analysis of satellite image analysis & digital elevation maps (National Geological Lineament Mapping, Jagannathan and members (2010)). Although there is some overlap between the dataset, the majority of the combined dike dataset ($\sim$ 29,000 segments) is from the GSI field mapping ($\sim$ 75 %) and the coverage of the datasets is fairly complementary. Thus, for simplicity, we use the combined dataset for analysis and leave a more careful analysis to remove some of the dike duplicates ¡ 1000 segments based on a preliminary analysis) to future analysis. Since our focus in this study is broad spatial patterns, we do not expect this simplification to introduce an appreciable bias.

In Figures 6 and 7, we show the full dike dataset with the dike segments colored by dike orientations and segment lengths respectively. The highest dike line density (dike number density per km^2 integrated over segment lengths) is in Western Narmada-Tapi rift zone with other local maxima in Saurashtra and Coastal dike swarms. The longest single mapped dike segment is $\sim$ 70 km. We anticipate that there are longer Deccan single dikes in reality but they have been mapped as distinct dike segments due to a combination of erosional breaks and lack of access. Since it is difficult to decide which dike segments are part of the same dike without further analysis, especially geochemistry, we have not merged dike segments here. Consequently, we would advise

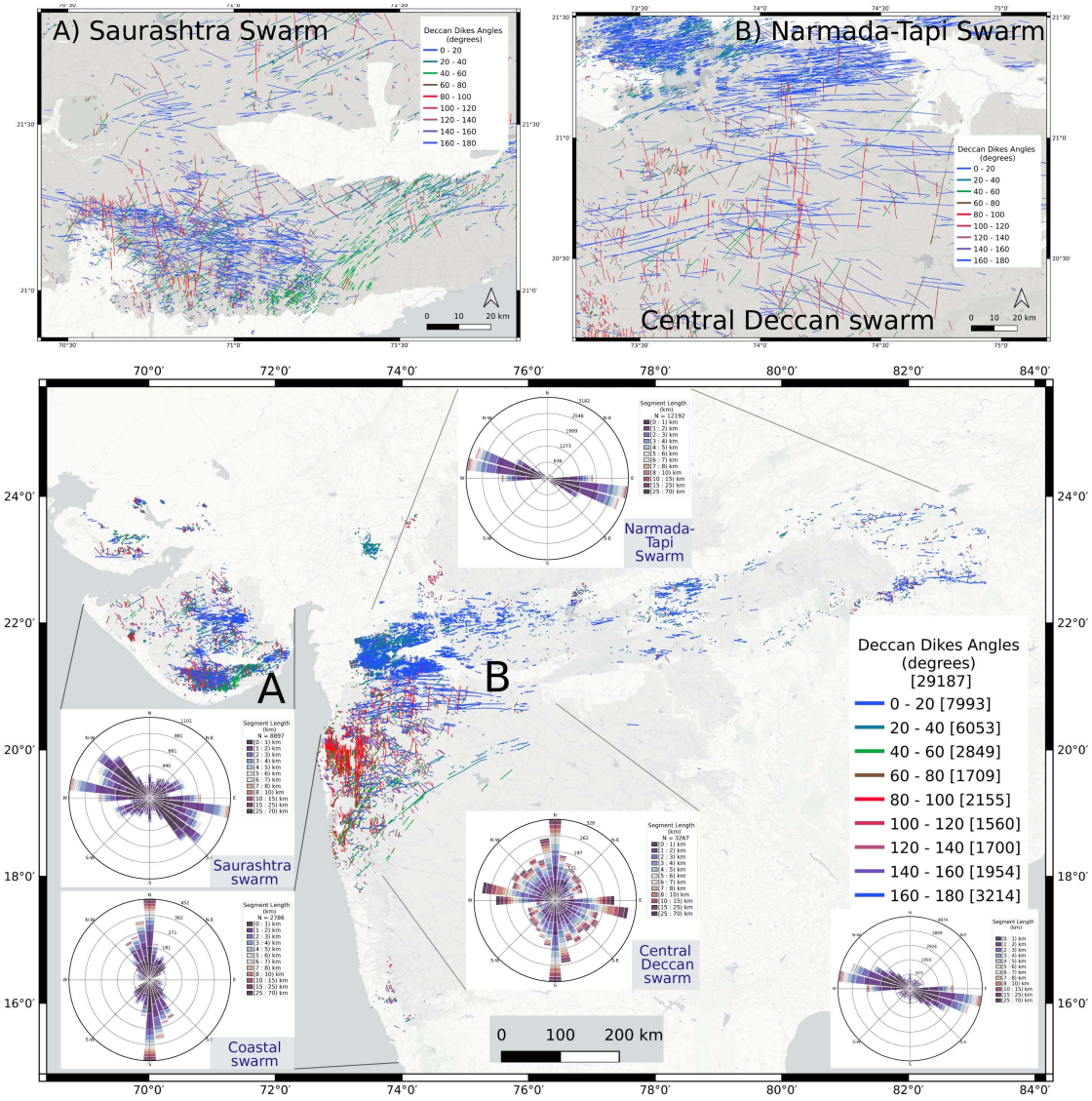

Figure 6: Spatial distribution of ∼29,000 Deccan-associated dike segments (using GSI 1:50 k geologic maps and NGLM dike dataset) with colors denoting dike orientation. Insets A and B show regional zoom-in for Saurashtra and Narmada-Tapi swarms each with multiple overlapping dike orientations. Figure also shows rose diagram for each dike subregion as well as for the whole dataset (in bottom right). For each dike orientation bin in rose diagram, color bars illustrate corresponding dike length distribution histogram.

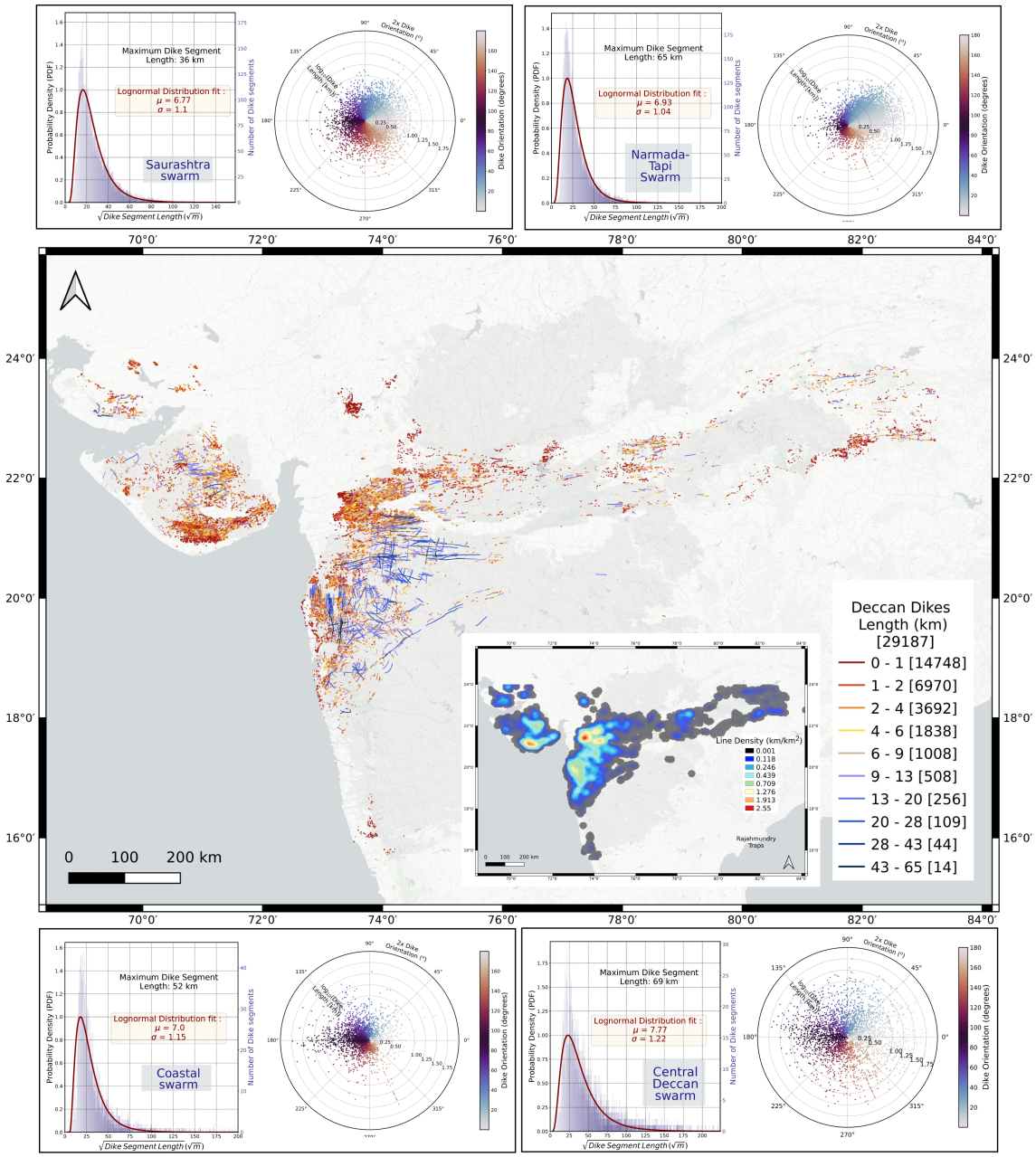

Figure 7: Spatial distribution of ∼29,000 Deccan-associated dike segments (using GSI 1:50 k geologic maps and NGLM dike dataset) with colors denoting dike segment length. Inset in main figure shows spatial map of overall dike density (weighted by dike segment length). For each sub-region, corresponding figure shows PDF of dike length (and best-fit lognormal distribution) as well as polar plot of (2x) dike orientation and (log10) dike segment length.

some caution in interpreting the dike segment length distribution since it is naturally biased against long dikes. Looking at the full dataset, we find that the Deccan dikes overall have a strong ENE-WSW orientation (Figure 6, lower right inset) consistent with previous work (Auden, 1949; Vanderkluysen et al., 2011). However, regionally, the four dike swarms have distinct characteristics with the Narmada-Tapi swarm (Median length – 954 m) generally striking ENE-WSW parallel to the rift-and-graben structure following the Narmada and Tapi rivers (Figure 6 , see top panel B). These dike segment orientations clearly highlight the significance of pre-existing crustal structure for the Deccan crustal magma transport. Next, the Coastal Dike Swarm (from the coast to the WG escarpment, Median length – 990 m) has a strong N-S approximately parallel to the west coast and the India-Seychelles rifting pattern. The Saurashtra dike swarm (Median length - 890 m) is broadly similar to Narmada-Tapi swarm in terms of orientations though there are much more orientation spread with intersecting dikes (Figure 6 , see top panel A). Finally, the Central Deccan swarm, associated with the eruption of the Wai subgroup flows (Median length – 2330m), has weaker preferred directions compared to the other swarms. In addition, the dike segment length is substantially larger than other swarms potentially indicative of a different magmatic overpressure regime and more localization into single dikes (as is evident with the low dike density, Figure 7 main figure inset). Like other CFB dike swarms (e.g. Columbia River Basalts, the log-normal density distribution provides the bestfit to the dike segment length data akin to other LIPs (e.g., CRB Chief Joseph Dike Swarm Morriss et al. (2020)), the log-normal distribution provides the best description of the dike segment length distributions (Figure 7). We expect that systematic under-prediction of the dike length distribution at the small end-member is an artifact of a single dike sub-divided into multiple parallel segments. A full analysis of the dike dataset, and its biases, is beyond the scope of the current study.

Each of the dike swarms is typically composed of a number of sub-swarms of 100s of dike segments each (Vanderkluysen et al., 2011; H. C. Sheth & Cañón-Tapia, 2015) with a wide range of thickness from 1 to 62 m (median of $\sim$ 10-20 m for different subswarms) and lengths (1 km to 79 km R. Ray et al., 2007; N. Bondre et al., 2006; H. Sheth et al., 2019). The only exception is the Goa dike swarm with typically shorter ($<$ 200 m) and thinner (average $\sim$ 6 m) dikes (Gadgil et al., 2019). A significant fraction of these dikes show evidence of multiple magma injections in the form of multiple columnar-jointed rows (2-5 injections) (See discussion in H. C. Sheth & Cañón-Tapia, 2015). Due to surface erosion, the dike tops in DT are generally truncated and thus a clear feeder relationship between lavas and flows is not established. Consequently, it is unclear if the dikes terminated in the crust/lava flow pile or if they fed lava flows directly.

We can compare the expectations of the dike spatial pattern with those from a large magma reservoir by computing the intersection points between dike segments. In order to reduce any biases due to missing/unmapped dike segments, we extended each dike segment by 50 km on either side before computing the intersection points. The results of this analysis (with a total $\sim$ 32,000,000 intersection points) are shown in Figure 8 with a few zoom-in insets for the Coastal dike swarm, Narmada-Tapi dike swarm, and Saurashtra swarm. The key result of note here is that there is no preferred location of dike intersection as would be expected for the case of a central magma reservoir (and a clear circumferential or radial dike swarm). Instead, the dike intersections form multiple local maxima within each sub-swarm as clearly seen for the Coastal dike swarm (Figure 8).

In conclusion, we find that the spatial pattern of Deccan dikes is inconsistent with the predictions of the large magma reservoir model. Instead, the dike distribution is more consistent with a combination of strong tectonic control and variations in small-scale crustal stress field due to small magma bodies. This conclusion is particularly true

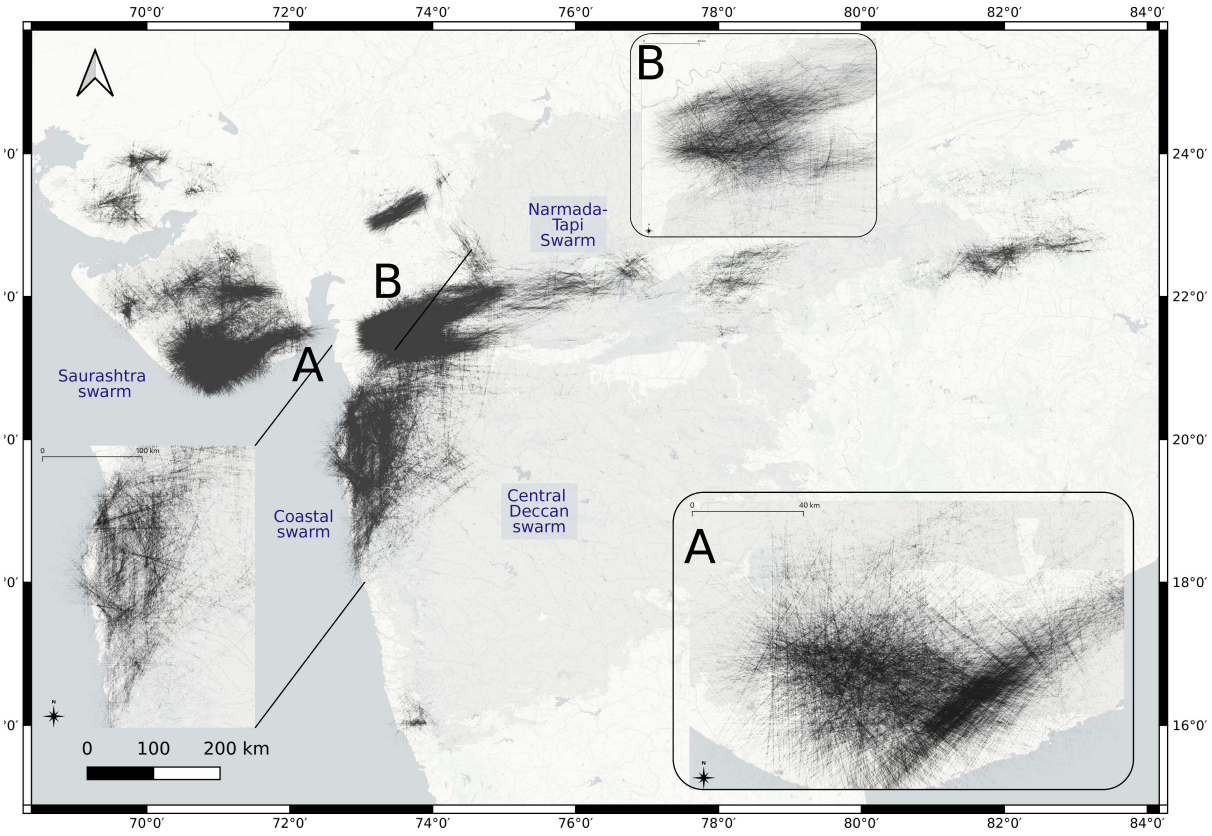

Figure 8: Spatial distribution of intersection points between the ∼29,000 Deccan-associated dike segment with each segment extended by 50 km on either site. The insets show zoom-in regions for the Coastal, Narmada-Tapi, and Saurashtra dike swarms.

for the Central Deccan swarm which shows much larger orientation spread vis-a-vis other dike swarms and geochemically, represents the most likely feeder for voluminous Upper subgroup Deccan lavas (Vanderkluysen et al., 2011). We would note that our conclusion from the dike dataset analysis is completely consistent with the analysis in M. A. Richards et al. (2015) based on a more restricted dataset. Analogous to their interpretation, we posit that the Deccan crustal stress field transitions over time from regional extensional stress dominated (e.g., Narmada-Tapi Swarm) to un-oriented crustal magma intrusion dominated (due to regional-scale lower crustal intrusion; e.g., Central Dike Swarm).

Our conclusion of a lack of large magma reservoir is further supported by the large number of dike segments mapped in Deccan. In typical shield volcanoes, only 30 % of the dikes are feeders (Galindo & Gudmundsson, 2012). Even if the number is higher for DTs (e.g., 50-50 ratio, H. C. Sheth & Cañón-Tapia, 2015), a large number of observed dike segments (e.g., Misra et al., 2014; Misra & Mukherjee, 2017) suggests magma reservoir failed even more frequently to form dykes (Kavanagh, 2018) than the rate of eruptive episodes. This observation makes it even more difficult for a single large magma reservoir to feed the surface eruptions given the various constraints on eruptive tempo described above (See Section 2.2.3).

6 Deccan Traps Intrusive structure - Geophysical Observations

Given the lack of direct observations of intrusive structures in Deccan Traps, we compiled results from various studies using a variety of geophysical methods (gravity, magnetics, magnetotelluric, and Deep seismic sounding) to constrain the crustal intrusive structure. Since the 1980s, geophysical methods have been used to image continental crustal structures, especially in Saurashtra and the Narmada-Tapi Rift zone, along with a few studies across the central Deccan Plateau and the WGE. If mafic magmatic bodies are emplaced at deep depths, they can be converted to a basic garnet-pyroxene-plagioclase-bearing granulite facies assemblage, which are good seismic reflectors (e.g., K. G. Cox, 1980). Similarly, the higher density of intrusive mafic bodies, especially mafic and ultra-mafic cumulates, would naturally lead to a signal in the gravity field as well as the change in seismic velocity (Ridley & Richards, 2010; M. Richards et al., 2013). We note that the high density of the mafic and ultramafic intrusions can lead to post-emplacement deformation and downward crustal flow and potentially crustal delamination if the surrounding crust has sufficiently low viscosity (Roman & Jaupart, 2016, 2017; Gorczyk & Vogt, 2018). However, the presence of the upper crustal Bushveld complex (Eales & Cawthorn, 1996) and the lower crustal Seiland Igneous Province (R. B. Larsen et al., 2018) suggests that this process does not completely remove the crustal intrusives. Thus, the present-day geophysically imaged intrusive bodies represent a lower bound on the total DT intrusives, especially at the Moho depth.

Overall, the shear wave velocity structure of the Indian crust (e.g., Maurya et al., 2016; Sharma et al., 2018; Saha et al., 2020, and references therein) suggest a thick crust (with an underplated mafic layer) in parts of the Indian subcontinent influenced by the Deccan Traps. This signature is particularly strong for parts of the Kutch-Saurashtra region (with the various intrusive complexes), Cambay rift, Narmada-Tapi rift, and the Western Ghat/Western Coastal region and much less for the Eastern/Central Deccan. There is an analogous signature of Deccan plume melting in the lithosphere thickness for India with a much thinner (100 - 120 km) lithosphere under the same regions vis-a-vis $>$ 200 km under Central-Eastern Deccan (Maurya et al., 2016; Saha et al., 2020). Interestingly, this pattern in lithosphere thickness variations and crustal underplating is similar to the spatial (though not necessarily the number density) distribution of Deccan Dikes (Figure 6). This observation suggests that the Deccan crustal magmatic system follows the regional extent of Indian

lithosphere-Réunion plume interaction. However, there is no evidence in these analysis of a large single/few upper or mid crustal magma reservoirs.

To test this conclusion further, we use only high resolution crustal datasets, preferentially local to regional scale in our compilation. This reduces any biases due to spatially variable data coverage in Indian continent scale seismic velocity studies, which typically have 50 km (or larger) spatial resolution. For our analysis, we have mostly followed the interpretation of the original studies to delineate the extent of intrusive mafic bodies vis-a-vis continental crust and sediments. Ideally, a re-analysis of all the datasets using the same model and set of assumptions would lead to more robust results. However, in most cases, the raw datasets are not publicly available for us to be able to do the analysis. In order to reduce biases, we have filtered our compilation only to include studies that utilize more than a single geophysical dataset, and preferably other geological observations, in the model inversion in order to reduce the non-uniqueness of the solutions. Another challenge with the available datasets is that they typically are for 2D sections except for some MT studies. Consequently, our results are not very informative about the full 3D geometry of intrusive bodies. Finally, we expect our calculated volumes to typically be a lower limit for the true intrusive volumes since geophysical methods may not detect small crustal intrusive bodies below the typical model resolution of 1-5 km (e.g., Patro & Sarma, 2016a). Although we have a complementary reduction in the volume of the surface lava flows due to erosion, we expect this would to be a smaller bias than the undetected small intrusive bodies.

The other, potentially much larger error in our compilation, comes from the interpretation of the inversion results with respect to the presence of an intrusive body vis-a-vis crustal faults, fluids, and background crustal structure. We refer the reader to individual studies in our compilation for the inversion method and interpretation of the results. In the end, we use results from 19 individual studies for a total of 53 individual measurements (Table 1). In Figure 9, we show the distribution of estimated Intrusive/Extrusive ratio for datasets with only large scale Moho-depth underplating (median of 5.5, 25th to 75th percentile of 2.5-8.5, 18 measurements), datasets include only upper crustal magma bodies (median of 1.3, 25th to 75th percentile of 0.5-2.0, 17 measurements), and datasets which include magmatic bodies throughout the crustal column (median of 8.5, 25th to 75th percentile of 5-14.0, 17 measurements). The primary result of this compilation is the absence of significant upper crustal magma bodies in the Deccan Traps with most of the intrusive volume in the lower crustal region. In the following, we describe the results of this analysis for Deccan Traps as well as some supporting datasets from other CFBs.

6.1 Mafic Underplating

In almost all the DT sections with geophysical datasets, we find significant (multiple km thick) layers of underplating in the lower crust. Typically, the Extrusive to Intrusive ratio is an average value of 6 and a large range between $\sim$ 0.5 to 15.5. Even in datasets with some upper crustal magma bodies (full crustal column, Figure 9), most of the mafic intrusives are still at Moho depth (except the Phenaimata and Pavagardh intrusion described in the next section). A large value for Moho depth intrusions is consistent with the models of K. G. Cox (1980) as well as Black and Manga (2017) who proposed that at least 30-40 % of the parental melt is emplaced at the base of the crust as mafic cumulates. Existing gravity and seismic data suggest that similarly, thick Moho/lower-crust mafic underplates are common for both oceanic and continental flood basalts (Furlong & Fountain, 1986; K. G. Cox, 1993; R. White & McKenzie, 1989; Coffin & Eldholm, 1994; Ridley & Richards, 2010; M. Richards et al., 2013; Mammo, 2013; Thybo & Artemieva, 2013; Deng et al., 2016). Thus, there is significant observational support for models of flood basalt volcanism (See Section 2.1

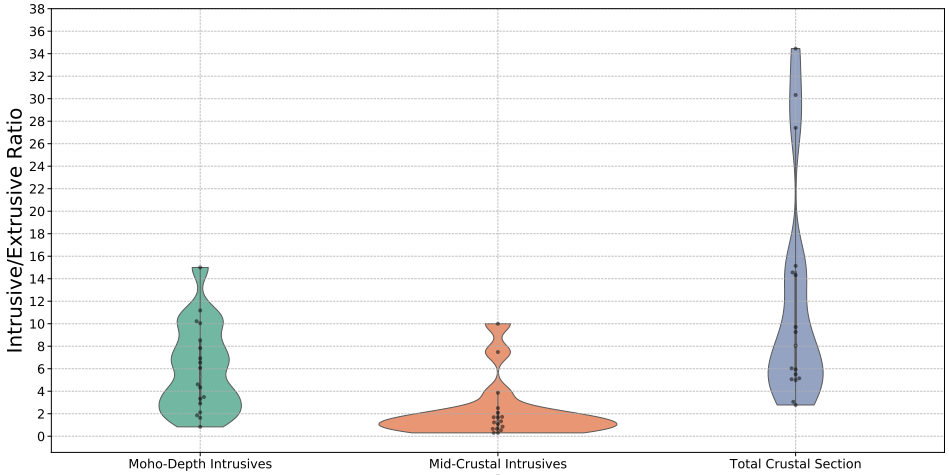

Figure 9: Kernel density estimates of Intrusive to Extrusive (I/E) Ratio for Deccan Traps using a literature compilation of gravity, seismic, and MT observations spanning the Western Ghats, Saurashtra, and Narmada Rift Valley in India (Table 1). The observations are divided into three groups based on whether the compiled datasets observed only Moho-depth intrusives, only mid/upper crustal intrusives, or mafic/ultramafic bodies across the whole crustal section (Moho plus crust). For each category, the individual measurements are plotted as circles while the bar plot shows the 25th to 75th percentile range. The high values for the I/E ratio (>20) are the Phenai-mata and Pavagadh intrusive complexes. The range of I/E ratio for the whole crustal sections is approximately equivalent to the sum of distributions of the Moho-depth underplating and mid/upper crustal intrusives.

for details) with deep crustal ponding and fractionation of ultramafic primary melts (Farnetani et al., 1996).

We note that the common presence of a thick ($\sim$ 5-15 km) underplated layer does not necessarily equate to a single magma body of equivalent size. Instead, frequent mafic intrusions(sills) at lower crustal depths along with visco-elastic deformation of the cumulate bodies can also lead to the formation of a large seismic underplate layer (J. D. White et al., 2009; Roman & Jaupart, 2016, 2017; Gorczyk & Vogt, 2018; Galland et al., 2018). We have observational support for this hypothesis from an exhumed lower crustal LIP section - the Seiland Igneous Province (SIP, R. B. Larsen et al., 2018, and references therein). The $\sim$ 5000 km^2 SIP is a dominantly mafic and ultramafic intrusive complex that was emplaced at the 25-35 km depths and represents the deep magmatic plumbing system of the Ediacaran age Central Iapetus Magmatic Province (e.g., Higgins & Breemen, 1998). With a total preserved volume of 17000 km^3 (Pastore et al., 2018), the SIP is made up of a number of multiple layered mafic plutons (85 % area, each $\sim$ 10-50 km^2), deep-rooted four ultramafic complexes (8-10 % area, each $\sim$ 20-100 km^2 and roots up to 9 km), as well as 2-5% carbonatitic rocks and alkaline and dioritic plutons. Based on field relationships, especially various chill margins between the mafic-ultramafic units and mafic-country rock metasediments (See R. B. Larsen et al., 2018, and references therein), SIP was clearly emplaced sequentially. The first mafic (and alkalic) magmas were intruded into lower crustal metasediments. Subsequent parental melts were emplaced into mafic gabbros, which were still close to solidus temperature. This is clearly evidenced in the field by extensive wall rock melting and assimilation between the gabbros and ultramafic intrusions (Griffin et al., 2013). The thermo-chemical insulation of emplacement into hot mafic rocks likely enabled the ultramafic melts to retain their parental composition with the deep ultra-mafic complexes acting as de facto LIP conduits for the shallow system (Grant et al., 2016; Degli Alessandrini et al., 2017).

In conclusion, observations clearly illustrate that the SIP magmatic system was never molten in total at the same time as a large lower crustal magma chamber but was rather assembled from multiple bodies. Additional support for this interpretation is provided by the seismic detection of a large (97 x 62 km) but thin (180 $\pm$ 40 m) igneous sill in the North Sea lower crust (17.5-22 km depths, Wrona et al., 2019) associated with the NAMP. As illustrated by a large number of intrusive steps and seismic reflection amplitude anomalies, the sill was formed sequentially with a complex pattern of lateral flow within the sill (Wrona et al. (2019), See Magee, Ernst, et al. (2019) for aerial examples of these features).

6.2 Upper Crustal Intrusive Bodies

With regards to upper crustal magma bodies, we do not find any evidence in the compiled sections for a large, continuous, upper crustal magma reservoir as hypothesized (See Section 2). Instead, the individual magma bodies, when detected, are typically small (5-15 km across and a few km thick, e.g., Patro & Sarma, 2016a; Prasad et al., 2018), are prismatic in shape, and are distributed in complex patterns depending on the pre-existing crustal structure. Since smaller magma bodies of this size are close to the resolution limit for many studies, our estimated Intrusive/Extrusive ratio may be biased to smaller values. We posit that, in reality, the upper crust may have more small magma bodies as petrologically required based on ubiquitous shallow fractionation (See Section 4 for details). A common feature across many studies, especially in the Narmada-Tapi rift zone region, is that the intrusive bodies are typically associated with pre-existing Precambrian age crustal and lithospheric fault zones (and other weak zones) (Kale et al., 2017, 2020). This suggests that Deccan Traps parental magma and magmatic volatiles utilized these pathways for melt transport to and through the crust (e.g., Bhattacharji et al., 1996; Naganjaneyulu & Santosh, 2010; Azeez et al., 2013;

Patro & Sarma, 2016a; Azeez et al., 2017a; G. P. Kumar et al., 2017; Patro et al., 2018). This is further reflected in the vertical magmatic features associated with fault zones (Chowdari et al., 2017). These magma bodies may have acted as conduits for upward transportation of magmatic material to other intrusive bodies (Patro & Sarma, 2016a; Naganjaneyulu & Santosh, 2011).

A number of other studies in LIPs and other magmatic systems have illustrated that pre-existing zones of lithospheric and crustal weakness play a critical role in magma transport (e.g., Begg et al., 2018; Peace et al., 2018; Alghamdi et al., 2018; Latyshev et al., 2019; Magee, Muirhead, et al., 2019). We note that the conclusions of our compilation with respect to the size of individual upper crustal magma bodies differs strongly from the results in Bhattacharji et al. (2004) (based on 2d and 3D gravity analysis). They inferred the presence of an extremely large (12 km thick, 300 x 30 km) magma upper crustal (6 km depth) body. However, G. S. Rao et al. (2018) used gravity datasets in combination with constraints from seismic observations, as well as magnetic datasets, and found that the observation can be better explained with much smaller crustal magma bodies along with a Moho depth underplate. Analogously, Patro and Sarma (2016a); Prasad et al. (2018) find that using higher-resolution datasets, the magma bodies in Narmada-Tapi Rift Zone are smaller and connected (if at all) thorough narrow zones instead of a larger, thicker, single magma body proposed originally by Bhattacharji et al. (2004).

Within our data compilation, the Phenai-mata and Pavagadh intrusive complexes in the Narmada-Tapti Rift Zone region are clear outliers (with very high intrusive/extrusive ratio, Figure 9). The Phenai-Mata complex consists of dominantly basaltic flows (2/3 by volume) along with alkaline plutonic rocks (1/3 by volume) and some orthopyroxene layered gabbro (Hari et al., 2011; Hari, Prasanth, et al., 2018). B. Singh et al. (2014a) used a combination of gravity and magnetic datasets to infer the presence of a large (11 km x 52 km) mafic body extending all the way from the surface to lower crustal depths ($\sim$ 20 km). The strong orientation of the intrusive body along the rift zone axis indicates the importance of a pre-existing tectonic structure for facilitating magma transport to the surface. The Pavagadh intrusive complex comprises twelve flows with a wide compositional range from olivine basalts and andesites to rhyolites (H. C. Sheth & Melluso, 2008; Hari et al., 2011). With similar gravity-magnetic analysis, B. Singh et al. (2014a) found a low-density rhyolitic body (3x 5 km) extending to about 10 km from the surface. This rhyolitic plug is, in turn, emplaced within a larger mafic intrusive body (20 km x 13 km x 10 km depth). Finally, both the rhyolite and the mafic rocks are underlain by an ultra-mafic body (20 km x 16 km) up to a depth of 20 km (and potentially larger). Thus, both the Phenai-Mata and Pavagadh intrusive complexes exhibit a trans-crustal DT magmatic system. Based on the different magnetization direction of the ultra-mafic and the rhyolitic magma bodies, B. Singh et al. (2014b) proposed that the Pavagadh complex may have been active between Chron 30N to Chron 29N/28N and was hence a long-lived system. Since most of the large WG flows are inferred to have been fed by dike swarms, we do not think that these igneous complexes are representative of the majority of DT magmatic architecture.

6.3 Relationship with Layered Mafic Intrusions

Another interesting conclusion of our data compilation is the lack of any intrusive bodies akin to large layered mafic intrusions such as the Rustenburg Layered Suite (RLS) of the Bushveld Igneous Complex. The RLS is the world's largest layered mafic intrusion that was emplaced about 2.06 Billion years ago. With an area of $\sim$ 65,000 km^2, a thickness of 7-9 km (Eales & Cawthorn, 1996; Cawthorn, 2015), and a shallow emplacement depth (0.15-0.25 GPa: Pitra & De Waal, 2001), R. E. Ernst et al. (2019) (and references therein) have suggested that RLS may be archetype for a

typical CFB upper crustal magma reservoir. It has been typically assumed that the RLS represents a single, long-lived magma reservoir of the same size as its present-day extent with rapid assembly through multiple magma injections followed by a long period of closed system fractionation (Wager & Brown, 1968; Cawthorn & Walraven, 1998; Kruger, 2005). Such an interpretation serves as one of the original motivations for the large magma reservoir models discussed in Section 2. However, Robb and Mungall (2020) used a combination of high-precision U-Pb dates, plagioclase zoning observations, and thermal models to illustrate that RLS was instead accreted as an out-of-sequence stack of sills corresponding to individual magma intrusions over a 1.2 Ma time-period (C. Lee & Butcher, 1990; A. A. Mitchell & Scoon, 2007; Mungall et al., 2016; Scoon et al., 2020; Scoon & Costin, 2018; Hayes et al., 2018; Scoon & Costin, 2018; A. Mitchell et al., 2019). Thus, instead of a single magma reservoir, RLS more likely represents a region of extensive sill emplacement and subsequent thermo-chemical insulation of individual magma bodies akin to Seiland Igneous Province (as described in the previous sections). Thus, the presence of a large Bushveld sized intrusive body does not necessarily correspond to a large, well-mixed crustal magma reservoir. In fact, based on field observations, RLS was emplaced after the surface eruptions of the basaltic-rhyolitic Rooiberg Group (Lenhardt & Eriksson, 2012). Thus, the RLS was not an upper crustal magma body feeding the surface lavas, but was instead accreted as a set of sills under a lithostatic load.

For the CFBs in the past 200 Ma, we are not aware of any large upper crustal magnetic or gravity anomalies of the spatial scale and amplitude expected for a Bushveld sized large magma reservoir (or crustal deformation features suggesting their presence and subsequent delamination) (e.g., Mammo, 2013; Sharma et al., 2018). For instance, the Marzen et al. (2020) and Gao et al. (2020) found no seismic evidence for a large magma body in the upper crust in the Triassic South Georgia Rift associated with the CAMP volcanism in North America. Instead, both of these studies only found a thick (> 5 km) magmatic underplating layer at Moho depths. Although there are layered mafic intrusions associated with recent CFBs such as the Doros Complex (~ 20 km^3, Parana–Etendeka CFB, T. Owen-Smith & Ashwal, 2015), NAMP associated central complexes such as Rum, Mull, Skye (< 100 km^3, O'Driscoll et al., 2006; O'driscoll, 2007; Namur et al., 2010), the Skaergaard intrusion (~ 280 km^3, NAMP, Nielsen, 2004), La Balma-Monte Capio intrusion (CAMP, Denyszyn et al., 2018), and the Graveyard Point Intrusion (Snake River Plain Basalt, C. M. White, 2007), they are much much smaller than RLS. In conclusion, we posit that a Bushveld layered mafic intrusion does not represent a typical upper crustal magma reservoir for Deccan Traps definitely, and potentially for many other CFBs in the last 200 Ma.

6.4 Implications for Magmatic Architecture

The main conclusion from the Deccan geophysical compilation of the Intrusive/Extrusive (I/E) ratio is that there is a significant volume of intrusives: I/E = 5-15 with a few outliers. Additionally, the majority of the intrusive magmatic volume is in the lower crust with no clear evidence for a large spatially homogeneous upper crustal magma body. To first order, the lack of an upper crustal large magma reservoir is inconsistent with the buoyancy-driven magmatic eruption model (See section 2.2.2, 2.2.3), whereas the large underplated layer is consistent. Nevertheless, the observations from Seiland Igneous Province, as well as observations from various Layered Mafic Intrusions, show that the presence of a large magmatic intrusive body does not imply that it was necessarily molten at the same time as a well-mixed magma reservoir.

Another added complication with the geophysical observations is that we see only the end-result of the system. Since there are no geochronological constraints for most of the intrusive bodies, it is not clear if they were emplaced prior to or post the main phase of volcanism. A particularly illustrative example is the McMurdo Dry Valleys

sill complex (B. D. Marsh, 2004) with four large sills (from top to bottom): the Mt. Fleming Sill, the Asgard Sill, the Peneplain Sill, and the Basement Sill. The sill system is capped by the Kirkpatrick flood basalts on top. Although the bottom-up sequence of intrusions for the system makes logical sense, at least as a first guess, B. D. Marsh (2004) used a variety of field, petrological, and textural observations to demonstrate that the system was instead formed top-down. The sills were emplaced after the eruption of the flood basalt lava flows instead of feeding the lava flows through sill-edge dikes (B. D. Marsh (2004); Jerram et al. (2010), see D. H. Elliot and Fleming (2018) for a detailed comparison with alternative scenarios). With an increasing lithostatic weight of the flood basalt sequence, the magma was emplaced in a progressively stepped down sills first through the Karoo sedimentary sequence (Mt. Fleming, Asgard, Peneplain Sill), and finally in the granitic basement (Basement Sill). This relationship is not unique for the McMurdo Dry Valleys and has been in multiple CFBs (e.g., Hansen et al., 2011; S. Burgess et al., 2017; Jerram et al., 2018) and has also been proposed for some CFB associate layered mafic intrusions (e.g., Higgins, 2005, Sept Iles intrusive Suite). Thus the intrusive structures and Intrusive/Extrusive Ratio calculated above should be considered as an upper limit (neglecting the methodological uncertainties) integrating over the whole CFB sequence.

7 Conclusions

In summary, the primary observations that strongly argue against the single, large magma reservoir model are as follows :

- Deccan Geochemistry (Section 3.1, 4) : In the Western Ghats sections for Deccan Traps, the crustal and lithospheric assimilates can vary rapidly between geochemical formations. Even within individual flows of a geochemical formation, there are quasi-oscillatory geochemical and petrological variations. Thus, the magmatic system has a relatively short geochemical memory. This is difficult to explain within a magmatic plumbing system is composed of only a few large magma chambers which integrate magma compositions over multiple 100s of kyr (Black & Manga, 2017). Additionally, the model result for a REAFC/RTF type shows that the intra-flow variations require a continuous recharge of at least a few percent of the reservoir mass which is inconsistent with a large reservoir model (Section 2.2.3). We find evidence for similar geochemical features in other CFBs including CAMP, Siberian Traps, Columbia River Basalts, and Karoo-Ferrar flood baslts. Finally, the Black and Manga (2017) style model predicts an increasing contribution from crustal assimilation with increasing thermal maturity of the upper crust. In contrast, the least contaminated DT lava flows constitute the Ambenali formation, which erupts towards the end of the sequence.
- Geochronology, Paleomagnetic, Mercury, Lava flow morphology (Section 3.2, 3.3, 3.4, 3.5) : The eruptive tempo of the Western Ghats sequence does not show any evidence for multiple 100 kyr hiatuses between eruptive time-periods contrary to the expectations of a large magma reservoir model. For a single WG composite section (spanning Kalsubai, Lonavala, and Wai subgroups), the typical time-period between eruptions is every 4000-6000 years (Section 3.3). Using Hg results, which integrate over the whole DT province, we find that individual eruptive episodes lasted approximately 100 to 1000 years and erupted around $\sim$ tens to hundred cubic kilometers of basalt per year. This conclusion is supported by eruptive estimates from lava flow morphology from Columbia River Basalt. These observational constraints on eruptive tempo do not match the large magma chamber model predictions. Furthermore, there is no clear eruptive/shallow sill emplacement hiatus for other CFBs with sufficiently high resolution datasets (Siberian Traps, Columbia River Basalts).

- Intra-Flow variation (Section 4.4) : Based on a few studies, there is evidence for isotopic, geochemical, and petrological variations within a single flow as well as composite dikes in the Deccan Traps and the Columbia River Basalts. These observations clearly suggest that a single eruptive episode was not necessarily fed by a homogeneous, well-mixed magma reservoir.
- Dike swarm distribution (Section 5) : No evidence for a single/few large magma reservoir sourcing the Deccan dike swarms since the spatial pattern of dikes is inconsistent with the crustal stress field from such a magmatic architecture. Instead, the spread in dike orientations and dike-dike intersection pattern, especially for the Deccan Central dike swarm, suggests a heterogenous (and likely time-dependent) crustal stress field from multiple magma reservoirs.
- Geophysical datasets (Section 6) : No geophysical evidence for a large, connected, upper crustal magma reservoir. We do find evidence for a large Moho-depth mafic underplating layer consistent with the presence of a large Moho-depth magma reservoir. However, based on the exposed section of analogous systems (e.g., Seiland Igneous Province), we conclude that a thick mafic layer inferred using geophysical methods does not necessarily imply a single magma body of equivalent size.

We posit that the most plausible magmatic structure that may be able to explain these (and other) observations is a multiply-connected magma reservoir model, with each reservoir undergoing REAFC-type processes. Driven by a large and spatially extensive mantle melt flux, the CFB magmatic system likely consists a number of small - medium ($<$ few thousand km^3) sized magma bodies instead of one/couple of large magma chambers. This new model of CFB magmatic architecture also likely has signficant implications for the impact triggering hypothesis for the most voluminous Deccan eruptions (M. A. Richards et al., 2015) since the stability of a multiply-connected magmatic system to seismic perturbations will be very different (likely higher) than the previous CFB architectures (Black & Manga, 2017) (low sensitivity to mantle flux variations). However we note that with existing studies, it is unclear if this proposed architecture can quantitatively explain the eruptive tempo associated with CFBs. In the Part II of this study, we use theoretical magma reservoir models to illustrate that this magmatic architecture can indeed describe the observations from Deccan Traps and other CFBs.

8 Tables

Table 1: Geophysical Estimates of Intrusive/Extrusive Ratio for Deccan Traps

Count	Paper reference	Deccan Traps Region	Category	I/E ratio
1	O. Pandey et al. (2009)	Western Ghats	Moho-Depth Intrusives	4.34
2	O. Pandey et al. (2009)	Central Deccan	Moho-Depth Intrusives	0.83
3	Vedanti et al. (2018)	Central Deccan	Moho-Depth Intrusives	3.33
4	Vedanti et al. (2018)	Central Deccan	Mid-Crustal Intrusives	10.00
5	G. S. Rao et al. (2018)	Western Ghats	Moho-Depth Intrusives	3.49
6	G. S. Rao et al. (2018)	Western Ghats	Moho-Depth Intrusives	2.12

7	G. S. Rao et al. (2018)	Saurashtra	Moho-Depth Intrusives	6.07
8	P. V. Kumar et al. (2018)	Saurashtra	Total Crustal Section	2.78
9	Tewari et al. (2018a)	Narmada Son Lineament-Central India	Mid-Crustal Intrusives	7.48
10	Tewari et al. (2018a)	Narmada Son Lineament-Central India	Total Crustal Section	14.56
11	Tewari et al. (2018a)	Narmada Son Lineament-Central India	Total Crustal Section	14.32
12	Tewari et al. (2018a)	Narmada Son Lineament-Central India	Moho-Depth Intrusives	15.00
13	Tewari et al. (2018b)	Western Ghats	Total Crustal Section	3.06
14	Tewari et al. (2018b)	Western Ghats	Moho-Depth Intrusives	1.64
15	Seshu et al. (2016)	Kutchh	Mid-Crustal Intrusives	0.65
16	Seshu et al. (2016)	Kutchh	Mid-Crustal Intrusives	0.30
17	Seshu et al. (2016)	Kutchh	Mid-Crustal Intrusives	0.54
18	Seshu et al. (2016)	Kutchh	Mid-Crustal Intrusives	0.30
19	A. Singh et al. (2015)	Narmada Son Lineament Central India	Total Crustal Section	27.41
20	Rajaram et al. (2017)	Koyna Central India	Moho-Depth Intrusives	1.86
21	Tewari et al. (2018b)	Saurashtra	Total Crustal Section	9.27
22	Tewari et al. (2018b)	Cambay Rift Zone	Moho-Depth Intrusives	6.92
23	Tewari et al. (2018b)	Cambay Rift Zone	Moho-Depth Intrusives	6.55
24	Tewari et al. (2018b)	Cambay Rift Zone	Moho-Depth Intrusives	4.61
25	Naganjaneyulu and Santosh (2010)	Cambay Rift Zone	Total Crustal Section	5.15
26	Naganjaneyulu and Santosh (2010)	Narmada Son Lineament Central india	Total Crustal Section	4.97
27	Azeez et al. (2017b)	Narmada Son Lineament Central india	Total Crustal Section	9.71
28	Naidu and Harinarayana (2009)	Narmada Son Lineament Central india	Moho-Depth Intrusives	7.83

29	Patro and Sarma (2016b)	Narmada Son Lineament Central india	Total Crustal Section	5.06
30	Patro and Sarma (2016b)	Narmada Son Lineament Central india	Total Crustal Section	8.05
31	Patro and Sarma (2016b)	Narmada Son Lineament Central india	Total Crustal Section	6.03
32	Prasad et al. (2018)	Narmada Son Lineament Central india	Mid-Crustal Intrusives	2.50
33	Prasad et al. (2018)	Narmada Son Lineament Central india	Mid-Crustal Intrusives	0.85
34	Prasad et al. (2018)	Narmada Son Lineament Central india	Mid-Crustal Intrusives	1.69
35	Prasad et al. (2018)	Narmada Son Lineament Central india	Mid-Crustal Intrusives	1.72
36	Prasad et al. (2018)	Narmada Son Lineament Central india	Mid-Crustal Intrusives	2.10
37	Prasad et al. (2018)	Narmada Son Lineament Central india	Mid-Crustal Intrusives	1.33
38	Prasad et al. (2018)	Narmada Son Lineament Central india	Mid-Crustal Intrusives	1.23
39	Prasad et al. (2018)	Narmada Son Lineament Central india	Mid-Crustal Intrusives	0.65
40	Prasad et al. (2018)	Narmada Son Lineament Central india	Mid-Crustal Intrusives	1.10
41	Prasad et al. (2018)	Narmada Son Lineament Central india	Mid-Crustal Intrusives	3.86
42	Prasad et al. (2018)	Narmada Son Lineament Central india	Mid-Crustal Intrusives	1.68
43	Krishna et al. (2002)	Western Ghats	Moho-Depth Intrusives	2.90
44	Krishna et al. (2002)	Saurashtra	Moho-Depth Intrusives	8.54
45	B. Singh et al. (2014b)	Saurashtra	Total Crustal Section	15.14
46	B. Singh et al. (2014b)	Saurashtra	Total Crustal Section	34.45
47	B. Singh et al. (2014b)	Saurashtra	Mid-Crustal Intrusives	5.94
48	B. Singh et al. (2014b)	Saurashtra	Total Crustal Section	30.33

49	Blanchard et al. (2017)	Saurashtra	Total Crustal Section	5.51
50	Chouhan et al. (2020)	Cambay Rift Zone	Moho-Depth Intrusives	10.22
51	Chouhan et al. (2020)	Cambay Rift Zone	Moho-Depth Intrusives	10.05
52	Chouhan et al. (2020)	Cambay Rift Zone	Moho-Depth Intrusives	11.18

Table 1: Geophysical Estimates of Intrusive/Extrusive Ratio for Deccan Traps

Acknowledgments

T. Mittal acknowledges graduate funding support from the NSF grant EAR #1615203 and the Crosby Postdoc Fellowship at MIT. I. Fendley was supported by an NSF Graduate Research Fellowship. We thank Paul Renne, Steve Self, Courtney Sprain, Benjamin Black, Michael Manga, Leif Karlstrom, and Loyc Vanderkluysen for useful discussions and suggestions for the manuscript text. We thank (reviewers and editor) for their valuable comments and suggestions. The authors declare that the research was conducted in the absence of any commercial or financial relationships that could be construed as a potential conflict of interest. The dataset for the MCMC analysis, the Deccan dike dataset & analysis code, as well as the code for the REAFC modeling is available from `https://figshare.com/s/aad2f0311d1c596b0d8e`. The other experimental and observational data associated to this study are from previous work.

References

Acid ring dykes and lava flows in deccan trap basalt, alech hills, saurashtra, gujarat. (1984). *Spec. Publ. Ser.-Geol. Surv. India*.

Albarede, F. (1992). How deep do common basaltic magmas form and differentiate? *Journal of Geophysical Research: Solid Earth*, *97*(B7), 10997–11009.

Alexander, P. O., & Purohit, M. (2019). Giant plagioclase basalt from the deccan volcanic province (dvp), sagar district, madhya pradesh, india: First report and implications. *Journal of the Geological Society of India*, *94*(2), 139–141.

Alghamdi, A. H., Aitken, A. R., & Dentith, M. C. (2018, apr). The deep crustal structure of the warakurna LIP, and insights on proterozoic LIP processes and mineralisation. *Gondwana Research*, *56*, 1–11. doi: 10.1016/j.gr.2017.12.001

Allegre, C., Birck, J., Capmas, F., & Courtillot, V. (1999). Age of the deccan traps using 187re–187os systematics. *Earth and Planetary Science Letters*, *170*(3), 197–204.

Amos, H. M., Jacob, D. J., Streets, D. G., & Sunderland, E. M. (2013). Legacy impacts of all-time anthropogenic emissions on the global mercury cycle. *Global Biogeochemical Cycles*, *27*(2), 410–421.

Anderson, S., Stofan, E., Smrekar, S., Guest, J., & Wood, B. (1999). Pulsed inflation of pahoehoe lava flows: implications for flood basalt emplacement. *Earth and Planetary Science Letters*, *168*(1-2), 7–18.

Andreasen, R., Peate, D. W., & Brooks, C. K. (2004). Magma plumbing systems in large igneous provinces: inferences from cyclical variations in palaeogene east greenland basalts. *Contributions to Mineralogy and Petrology*, *147*(4), 438–452.

Arndt, N. T. (1989). An open boundary between lower continental crust and mantle : its role in crust formation and crustal recycling. *Tectonophysics*, *161*, 201–212.

Arndt, N. T., & Christensen, U. (1992). The role of lithospheric mantle in continental flood volcanism: thermal and geochemical constraints. *Journal of Geophysical Research: Solid Earth*, *97*(B7), 10967–10981.

Arndt, N. T., Czamanske, G. K., Wooden, J. L., & Fedorenko, V. A. (1993). Mantle and crustal contributions to continental flood volcanism. *Tectonophysics*, *223*(1-2), 39–52.

Auden, J. (1949). Dykes in western india-a discussion on their relationships with the deccan traps. *Trans. Nat. Inst. Sci. India*, *3*, 123–157.

Augland, L., Ryabov, V., Vernikovsky, V., Planke, S., Polozov, A., Callegaro, S., ... Svensen, H. (2019). The main pulse of the siberian traps expanded in size and composition. *Scientific Reports*, *9*(1), 1–12.

Azeez, K. A., Patro, P. K., Harinarayana, T., & Sarma, S. (2017a, sep). Magnetotelluric imaging across the tectonic structures in the eastern segment of the central indian tectonic zone: Preserved imprints of polyphase tectonics and evidence for suture status of the tan shear. *Precambrian Research*, *298*, 325–340. doi: 10.1016/j.precamres.2017.06.018

Azeez, K. A., Patro, P. K., Harinarayana, T., & Sarma, S. (2017b, sep). Magnetotelluric imaging across the tectonic structures in the eastern segment of the central indian tectonic zone: Preserved imprints of polyphase tectonics and evidence for suture status of the tan shear. *Precambrian Research*, *298*, 325–340. doi: 10.1016/j.precamres.2017.06.018

Azeez, K. A., Unsworth, M. J., Patro, P. K., Harinarayana, T., & Sastry, R. (2013). Resistivity structure of the central indian tectonic zone (citz) from multiple magnetotelluric (mt) profiles and tectonic implications. *Pure and Applied Geophysics*, *170*(12), 2231–2256.

Baksi, A. K. (2001). The rajahmundry traps, andhra pradesh: evaluation of their petrogenesis relative to the deccan traps. *Journal of Earth System Science*, *110*(4), 397–407.

Barry, T., Kelley, S. P., Reidel, S. P., Camp, V. E., Self, S., Jarboe, N., ... Wolff, J. (2013). Eruption chronology of the columbia river basalt group. *The Columbia River Flood Basalt Province: Geological Society of America Special Paper*, *497*, 45–66.

Basu, A. R., Chakrabarty, P., Szymanowski, D., Ibañez-Mejia, M., Schoene, B., Ghosh, N., & Georg, R. B. (2020). Widespread silicic and alkaline magmatism synchronous with the deccan traps flood basalts, india. *Earth and Planetary Science Letters*, *552*, 116616.

Basu, A. R., Renne, P. R., DasGupta, D. K., Teichmann, F., & Poreda, R. J. (1993). Early and late alkali igneous pulses and a high-3he plume origin for the deccan flood basalts. *Science*, *261*(5123), 902–906.

Basu, A. R., Saha-Yannopoulos, A., & Chakrabarty, P. (2020). A precise geochemical volcano-stratigraphy of the deccan traps. *Lithos*, *376*, 105754.

Beane, J., & Hooper, P. (1988). A note on the picrite basalts of the western ghats, deccan trap, india. *Memoir-Geological Society of India*(10), 117–133.

Beane, J., Turner, C., Hooper, P., Subbarao, K., & Walsh, J. (1986). Stratigraphy, composition and form of the deccan basalts, western ghats, india. *Bulletin of Volcanology*, *48*(1), 61–83.

Bédard, J. H., Marsh, B. D., Hersum, T. G., Naslund, H. R., & Mukasa, S. B. (2007). Large-scale mechanical redistribution of orthopyroxene and plagioclase in the basement sill, ferrar dolerites, mcmurdo dry valleys, antarctica: petrological, mineral-chemical and field evidence for channelized movement of crystals and melt. *Journal of Petrology*, *48*(12), 2289–2326.

Begg, G. C., Hronsky, J. M., Griffin, W. L., & O'Reilly, S. Y. (2018). Global-to deposit-scale controls on orthomagmatic ni-cu (-pge) and pge reef ore formation. In *Processes and ore deposits of ultramafic-mafic magmas through space and time* (pp. 1–46). Elsevier.

Bhattacharji, S., Chatterjee, N., Wampler, J., Nayak, P., & Deshmukh, S. (1996). Indian intraplate and continental margin rifting, lithospheric extension, and mantle upwelling in deccan flood basalt volcanism near the k/t boundary: evidence from mafic dike swarms. *The Journal of Geology*, *104*(4), 379–398.

Bhattacharji, S., Sharma, R., & Chatterjee, N. (2004). Two-and three-dimensional gravity modeling along western continental margin and intraplate narmada-tapti rifts: Its relevance to deccan flood basalt volcanism. *Journal of Earth System Science*, *113*(4), 771–784.

Bhattacharya, G., & Yatheesh, V. (2015). Plate-tectonic evolution of the deep ocean basins adjoining the western continental margin of india—a proposed model for the early opening scenario. In *Petroleum geosciences: Indian contexts* (pp. 1–61). Springer.

Bhattacharya, S. K., Ma, G. S.-K., & Matsuhisa, Y. (2013, mar). Oxygen isotope evidence for crustal contamination in deccan basalts. *Geochemistry*, *73*(1), 105–112. doi: 10.1016/j.chemer.2012.11.007

Bistacchi, A., Tibaldi, A., Pasquarè, F. A., & Rust, D. (2012). The association of cone–sheets and radial dykes: data from the isle of skye (uk), numerical modelling, and implications for shallow magma chambers. *Earth and Planetary Science Letters*, *339*, 46–56.

Biswas, S. (1982). Rift basins in western margin of india and their hydrocarbon prospects with special reference to kutch basin. *AAPG Bulletin*, *66*(10), 1497–1513.

Biswas, S. (1987). Regional tectonic framework, structure and evolution of the western marginal basins of india. *Tectonophysics*, *135*(4), 307–327.

Black, B. A., & Gibson, S. A. (2019). Deep carbon and the life cycle of large igneous provinces. *Elements: An International Magazine of Mineralogy, Geochemistry, and Petrology*, *15*(5), 319–324.

Black, B. A., & Manga, M. (2017). Volatiles and the tempo of flood basalt magmatism. *Earth and Planetary Science Letters*, *458*, 130–140.

Blanchard, J., Ernst, R., & Samson, C. (2017, mar). Gravity and magnetic modelling of layered mafic–ultramafic intrusions in large igneous province plume centre regions: case studies from the 1.27 ga mackenzie, 1.38 ga kunene–kibaran, 0.06 ga deccan, and 0.13–0.08 ga high arctic events. *Canadian Journal of Earth Sciences*, *54*(3), 290–310. doi: 10.1139/cjes-2016-0132

Bodas, M., Khadri, S., & Subbarao, K. (1988). Stratigraphy of the jawhar and igatpuri formations, western ghat lava pile, india. *Memoir-Geological Society of India*(10).

Bohrson, W. A., & Spera, F. J. (2001). Energy-constrained open-system magmatic processes ii: application of energy-constrained assimilation–fractional crystallization (ec-afc) model to magmatic systems. *Journal of Petrology*, *42*(5), 1019–1041.

Bohrson, W. A., & Spera, F. J. (2007). Energy-constrained recharge, assimilation, and fractional crystallization (ec-raχfc): A visual basic computer code for calculating trace element and isotope variations of open-system magmatic systems. *Geochemistry, Geophysics, Geosystems*, *8*(11).

Bondre, N., Hart, W., & Sheth, H. (2006). Geology and geochemistry of the sangamner mafic dike swarm, western deccan volcanic province, india: implications for regional stratigraphy. *The Journal of geology*, *114*(2), 155–170.

Bondre, N. R., Duraiswami, R. A., & Dole, G. (2004). Morphology and emplacement of flows from the deccan volcanic province, india. *Bulletin of Volcanology*, *66*(1), 29–45.

Bondre, N. R., & Hart, W. K. (2008). Morphological and textural diversity of the steens basalt lava flows, southeastern oregon, usa: implications for emplacement style and nature of eruptive episodes. *Bulletin of Volcanology*, *70*(8), 999–1019.

Borges, M. R., Sen, G., Hart, G. L., Wolff, J. A., & Chandrasekharam, D. (2014). Plagioclase as recorder of magma chamber processes in the deccan traps: Sr-isotope zoning and implications for deccan eruptive event. *Journal of Asian Earth Sciences*, *84*, 95–101.

Braz Machado, F., Reis Viana Rocha-Júnior, E., Soares Marques, L., & Ranalli Nardy, A. (2015). Volcanological aspects of the northwest region of paraná continental flood basalts (brazil). *Solid Earth*, 227–241.

Brown, R. J., Blake, S., Bondre, N., Phadnis, V., & Self, S. (2011). ´ a´ ā lava flows in the deccan volcanic province, india, and their significance for the nature of continental flood basalt eruptions. *Bulletin of Volcanology*, *73*(6), 737–752.

Brueseke, M. E., Heizler, M. T., Hart, W. K., & Mertzman, S. A. (2007). Distribution and geochronology of oregon plateau (usa) flood basalt volcanism: The steens basalt revisited. *Journal of Volcanology and Geothermal Research*, *161*(3), 187–214.

Bryan, S. E., & Ferrari, L. (2013). Large igneous provinces and silicic large igneous provinces: Progress in our understanding over the last 25 years. *GSA Bulletin*, *125*(7-8), 1053–1078.

Bryan, S. E., Peate, I. U., Peate, D. W., Self, S., Jerram, D. A., Mawby, M. R., ... Miller, J. A. (2010). The largest volcanic eruptions on earth. *Earth-Science Reviews*, *102*(3-4), 207–229.

Buchan, K. L., & Ernst, R. E. (2019). Giant circumferential dyke swarms: catalogue and characteristics. In *Dyke swarms of the world: A modern perspective* (pp. 1–44). Springer.

Buntin, S., Malehmir, A., Koyi, H., Högdahl, K., Malinowski, M., Larsson, S. Å., ... Górszczyk, A. (2019). Emplacement and 3d geometry of crustal-scale saucer-shaped intrusions in the fennoscandian shield. *Scientific reports*, *9*(1), 1–11.

Burgess, S., Muirhead, J., & Bowring, S. (2017). Initial pulse of siberian traps sills as the trigger of the end-permian mass extinction. *Nature Communications*, *8*(1), 1–6.

Burgess, S. D., & Bowring, S. A. (2015). High-precision geochronology confirms voluminous magmatism before, during, and after earth's most severe extinction. *Science Advances*, *1*(7), e1500470.

Bürgmann, R., & Dresen, G. (2008). Rheology of the lower crust and upper mantle: Evidence from rock mechanics, geodesy, and field observations. *Annu. Rev. Earth Planet. Sci.*, *36*, 531–567.

Calvès, G., Schwab, A. M., Huuse, M., Clift, P. D., Gaina, C., Jolley, D., ... Inam, A. (2011). Seismic volcanostratigraphy of the western indian rifted margin: The pre-deccan igneous province. *Journal of Geophysical Research: Solid Earth*, *116*(B1).

Campbell, I. H., & Griffiths, R. W. (1990). Implications of mantle plume structure for the evolution of flood basalts. *Earth and Planetary Science Letters*, *99*(1-2), 79–93.

Cande, S. C., & Patriat, P. (2015). The anticorrelated velocities of africa and india in the late cretaceous and early cenozoic. *Geophysical Journal International*, *200*(1), 227–243.

Caricchi, L., Annen, C., Blundy, J., Simpson, G., & Pinel, V. (2014). Frequency and magnitude of volcanic eruptions controlled by magma injection and buoyancy. *Nature Geoscience*, *7*(2), 126–130. doi: 10.1038/ngeo2041

Cashman, K. V., & Kauahikaua, J. P. (1997). Reevaluation of vesicle distributions in basaltic lava flows. *Geology*, *25*(5), 419–422.

Cawthorn, R. G. (2015). The bushveld complex, south africa. In *Layered intrusions* (pp. 517–587). Springer.

Cawthorn, R. G., & Walraven, F. (1998). Emplacement and crystallization time for the bushveld complex. *Journal of Petrology*, *39*(9), 1669–1687.

Chandra, J., Paul, D., Stracke, A., Chabaux, F., & Granet, M. (2019, may). The origin of carbonatites from amba dongar within the deccan large igneous province. *Journal of Petrology*, *60*(6), 1119–1134. doi: 10.1093/petrology/egz026

Chandrasekharam, D., Vaselli, O., Sheth, H., & Keshav, S. (2000). Petrogenetic significance of ferro-enstatite orthopyroxene in basaltic dikes from the tapi rift, deccan flood basalt province, india. *Earth and Planetary Science Letters*, *179*(3-4), 469–476.

Chatterjee, N., & Bhattacharji, S. (2001). Origin of the felsic and basaltic dikes and flows in the rajula-palitana-sihor area of the deccan traps, saurashtra, india: A geochemical and geochronological study. *International Geology Review*, *43*(12), 1094–1116.

Chatterjee, N., & Bhattacharji, S. (2008). Trace element variations in deccan basalts: roles of mantle melting, fractional crystallization and crustal assimilation. *Journal of the Geological Society of India*, *71*(2), 171.

Chenet, A.-L., Courtillot, V., Fluteau, F., Gérard, M., Quidelleur, X., Khadri, S., ... Thordarson, T. (2009). Determination of rapid deccan eruptions across the cretaceous-tertiary boundary using paleomagnetic secular variation: 2. constraints from analysis of eight new sections and synthesis for a 3500-m-thick composite section. *Journal of Geophysical Research: Solid Earth*, *114*(B6).

Chenet, A.-L., Fluteau, F., Courtillot, V., Gérard, M., & Subbarao, K. (2008). Determination of rapid deccan eruptions across the cretaceous-tertiary boundary using paleomagnetic secular variation: Results from a 1200-m-thick section in the mahabaleshwar escarpment. *Journal of Geophysical Research: Solid Earth*, *113*(B4).

Choudhary, B. R., & Jadhav, G. N. (2014). Petrogenesis of fractionated basaltic lava flows of poladpur-mahabaleshwar formation around mahabaleshwar, western ghats, india. *Journal of the Geological Society of India*, *84*(2), 197–208.

Chouhan, A. K., Choudhury, P., & Pal, S. K. (2020, feb). New evidence for a thin crust and magmatic underplating beneath the cambay rift basin, western india through modelling of EIGEN-6c4 gravity data. *Journal of Earth System Science*, *129*(1). doi: 10.1007/s12040-019-1335-y

Chowdari, S., Singh, B., Rao, B. N., Kumar, N., Singh, A., & Chandrasekhar, D. (2017). Structural mapping based on potential field and remote sensing data, south rewa gondwana basin, india. *Journal of Earth System Science*, *126*(6), 84.

Clapham, M. E., & Renne, P. R. (2019). Flood basalts and mass extinctions. *Annual Review of Earth and Planetary Sciences*, *47*, 275–303.

Coetzee, A., & Kisters, A. F. (2018). The elusive feeders of the karoo large igneous province and their structural controls. *Tectonophysics*, *747*, 146–162.

Coffin, M. F., & Eldholm, O. (1994). Large igneous provinces: crustal structure, dimensions, and external consequences. *Reviews of Geophysics*, *32*(1), 1–36.

Courtillot, V., & Fluteau, F. (2014). A review of the embedded time scales of flood basalt volcanism with special emphasis on dramatically short magmatic pulses. *Geological Society of America Special Papers*, *505*, SPE505–15.

Courtillot, V., Gallet, Y., Rocchia, R., Féraud, G., Robin, E., Hofmann, C., ... Ghevariya, Z. (2000). Cosmic markers, 40ar/39ar dating and paleomagnetism of the kt sections in the anjar area of the deccan large igneous province. *Earth and Planetary Science Letters*, *182*(2), 137–156.

Courtillot, V. E., & Renne, P. R. (2003). On the ages of flood basalt events. *Comptes Rendus Geoscience*, *335*(1), 113–140.

Cox, K. (1988). Numerical modelling of a randomized rtf magma chamber: a comparison with continental flood basalt sequences. *Journal of Petrology*, *29*(3), 681–697.

Cox, K., & Devey, C. W. (1987). Fractionation processes in deccan traps magmas: Comments on the paper by g. sen? mineralogy and petrogenesis of the deccan trap lava flows around mahabaleshwar, india. *Journal of Petrology*, *28*(1), 235–238.

Cox, K., & Hawkesworth, C. (1985). Geochemical stratigraphy of the deccan traps at mahabaleshwar, western ghats, india, with implications for open system magmatic processes. *Journal of Petrology*, *26*(2), 355–377.

Cox, K. G. (1980). A model for flood basalt volcanism. *Journal of Petrology*, *21*(4), 629–650. doi: 10.1093/petrology/21.4.629

Cox, K. G. (1993). Continental magmatic underplating. *Philosophical Transactions of the Royal Society of London. Series A: Physical and Engineering Sciences*, *342*(1663), 155–166.

Cox, K. G., & Hawkesworth, C. J. (1984). Relative contribution of crust and mantle to flood basalt magmatism, mahabaleshwar area, deccan traps. *Philosophical Transactions of the Royal Society of London. Series A, Mathematical and Physical Sciences*, *310*(1514), 627–641.

Cox, K. G., & Mitchell, C. (1988). Importance of crystal settling in the differentiation of deccan trap basaltic magmas. *Nature*, *333*(6172), 447–449.

Crookshank, H. (1936). Geology of the northern slopes of the satpuras between morand and sher rivers-mem. *Geol. Sur. of India*, *66*(Pt 2).

Cruden, A. R., & Weinberg, R. F. (2018). Mechanisms of magma transport and storage in the lower and middle crust—magma segregation, ascent and emplacement. In *Volcanic and igneous plumbing systems* (pp. 13–53). Elsevier.

Cucciniello, C., Choudhary, A. K., Pande, K., & Sheth, H. (2019). Mineralogy, geochemistry and 40 ar–39 ar geochronology of the barda and alech complexes, saurashtra, northwestern deccan traps: early silicic magmas derived by flood basalt fractionation. *Geological Magazine*, *156*(10), 1668–1690.

Cucciniello, C., Choudhary, A. K., Zanetti, A., Sheth, H. C., Vichare, S., & Pereira, R. (2014). Mineralogy, geochemistry and petrogenesis of the khopoli mafic intrusion, deccan traps, india. *Mineralogy and Petrology*, *108*(3), 333–351.

Cucciniello, C., Demonterova, E. I., Sheth, H., Pande, K., & Vijayan, A. (2015). 40ar/39ar geochronology and geochemistry of the central saurashtra mafic dyke swarm: insights into magmatic evolution, magma transport, and dyke-flow relationships in the northwestern deccan traps. *Bulletin of Volcanology*, *77*(5), 45.

Cucciniello, C., Sheth, H., Duraiswami, R. A., Wegner, W., Koeberl, C., Das, T., & Ghule, V. (2020). The southeastern saurashtra dyke swarm, deccan traps: Magmatic evolution of a tholeiitic basalt–basaltic andesite–andesite–rhyolite suite. *Lithos*, *376*, 105759.

Das, A., & Mallik, J. (2020). Applicability of ams technique as a flow fabric indicator in dykes: insight from nandurbar–dhule deccan dyke swarm. *International Journal of Earth Sciences*, 1–12.

Dave, S. (1971). The geology of the igneous complex of the barda hills, saurashtra, gujarat state (india). *Bulletin Volcanologique*, *35*(3), 619–632.

Degli Alessandrini, G., Menegon, L., Malaspina, N., Dijkstra, A., & Anderson, M. (2017). Creep of mafic dykes infiltrated by melt in the lower continental crust (seiland igneous province, norway). *Lithos*, *274*, 169–187.

Deng, Y., Chen, Y., Wang, P., Essa, K. S., Xu, T., Liang, X., & Badal, J. (2016). Magmatic underplating beneath the emeishan large igneous province (south china) revealed by the comgra-elip experiment. *Tectonophysics*, *672*, 16–23.

Denyszyn, S. W., Fiorentini, M. L., Maas, R., & Dering, G. (2018). A bigger tent for camp. *Geology*, *46*(9), 823–826.

DePaolo, D. J. (1981). Trace element and isotopic effects of combined wallrock assimilation and fractional crystallization. *Earth and planetary science letters*, *53*(2), 189–202.

Deshmukh, S. (1977). *A critical petrological study of the deccan basalts and associated high level laterites in parts of the western ghats, maharashtra state* (Unpublished doctoral dissertation). PhD thesis, Nagpur University, p 306.

de Silva, S. L., & Gregg, P. M. (2014). Thermomechanical feedbacks in magmatic systems: Implications for growth, longevity, and evolution of large caldera-forming magma reservoirs and their supereruptions. *Journal of Volcanology and Geothermal Research*, *282*, 77–91.

Dessai, A., Downes, H., López-Moro, F.-J., & López-Plaza, M. (2008). Lower crustal contamination of deccan traps magmas: evidence from tholeiitic dykes and granulite xenoliths from western india. *Mineralogy and Petrology*, *93*(3-4), 243–272.

Dessai, A., & Vaselli, O. (1999). Petrology and geochemistry of xenoliths in lamprophyres from the deccan traps: implications for the nature of the deep crust boundary in western india. *Mineralogical Magazine*, *63*(5), 703–722.

Dessert, C., Dupré, B., Gaillardet, J., François, L. M., & Allegre, C. J. (2003). Basalt weathering laws and the impact of basalt weathering on the global carbon cycle. *Chemical Geology*, *202*(3-4), 257–273.

Devey, C. W., & Cox, K. (1987). Relationships between crustal contamination and crystallisation in continental flood basalt magmas with special reference to the deccan traps of the western ghats, india. *Earth and Planetary Science Letters*, *84*(1), 59–68.

Devey, C. W., & Lightfoot, P. (1986). Volcanological and tectonic control of stratigraphy and structure in the western deccan traps. *Bulletin of Volcanology*, *48*(4), 195–207.

Devey, C. W., & Stephens, W. (1991). Tholeiitic dykes in the seychelles and the original spatial extent of the deccan. *Journal of the Geological Society*, *148*(6), 979–983.

Dole, G., Patil-Pillai, S., & Kale, V. S. (2020). Multi-tiered, disrupted crust of a sheet lava flow from the diveghat formation of deccan traps: Implications on emplacement mechanisms. *Journal of Earth System Science*, *129*(1), 1–9.

Dolson, J., Burley, S. D., Sunder, V., Kothari, V., Naidu, B., Whiteley, N. P., ... Ananthakrishnan, B. (2015). The discovery of the barmer basin, rajasthan, india, and its petroleum geology. *AAPG Bulletin*, *99*(3), 433–465.

Duraiswami, R. A., Bondre, N. R., & Dole, G. (2004). Possible lava tube system in a hummocky lava flow at daund, western deccan volcanic province, india. *Journal of Earth System Science*, *113*(4), 819–829.

Duraiswami, R. A., Bondre, N. R., & Managave, S. (2008). Morphology of rubbly pahoehoe (simple) flows from the deccan volcanic province: Implications for style of emplacement. *Journal of Volcanology and Geothermal Research*, *177*(4), 822–836.

Duraiswami, R. A., Jutzeler, M., Karve, A. V., Gadpallu, P., & Kale, M. G. (2019). Subaqueous effusive and explosive phases of late deccan volcanism: evidence from mumbai islands, india. *Arabian Journal of Geosciences*, *12*(23), 703.

Duraiswami, R. A., & Shaikh, T. N. (2013, jun). Geology of the saucer-shaped sill near mahad, western deccan traps, india, and its significance to the flood basalt model. *Bulletin of Volcanology*, *75*(7). doi: 10.1007/s00445-013-0731-4

Eales, H., & Cawthorn, R. (1996). The bushveld complex. In *Developments in petrology* (Vol. 15, pp. 181–229). Elsevier.

El Hachimi, H., Youbi, N., Madeira, J., Bensalah, M. K., Martins, L., Mata, J., ... others (2011). Morphology, internal architecture and emplacement mechanisms of lava flows from the central atlantic magmatic province (camp) of argana basin (morocco). *Geological Society, London, Special Publications*, *357*(1),

167–193.

Elliot, D., Fleming, T., Haban, M., & Siders, M. (1995). Petrology and mineralogy of the kirkpatrick basalt and ferrar dolerite, mesa range region, north victoria land, antarctica. *Contributions to Antarctic Research IV*, *67*, 103–141.

Elliot, D. H., & Fleming, T. H. (2018). The ferrar large igneous province: field and geochemical constraints on supra-crustal (high-level) emplacement of the magmatic system. *Geological Society, London, Special Publications*, *463*(1), 41–58.

Ernst, R., Grosfils, E., & Mège, D. (2001, may). Giant Dike Swarms : Earth, Venus, and Mars. *Annual Review of Earth and Planetary Sciences*, *29*(1), 489–534. doi: 10.1146/annurev.earth.29.1.489

Ernst, R., Liikane, D., Jowitt, S., Buchan, K., & Blanchard, J. (2019, oct). A new plumbing system framework for mantle plume-related continental large igneous provinces and their mafic-ultramafic intrusions. *Journal of Volcanology and Geothermal Research*, *384*, 75–84. doi: 10.1016/j.jvolgeores.2019.07.007

Ernst, R., Srivastava, R., Bleeker, W., & Hamilton, M. (2010). Precambrian large igneous provinces (lips) and their dyke swarms: new insights from high-precision geochronology integrated with paleomagnetism and geochemistry. *Precambrian Research*, *3*(183), vii–xi.

Ernst, R. E. (2014). *Large igneous provinces*. Cambridge University Press.

Ernst, R. E., & Bell, K. (2010). Large igneous provinces (lips) and carbonatites. *Mineralogy and Petrology*, *98*(1-4), 55–76.

Ernst, R. E., Liikane, D. A., Jowitt, S. M., Buchan, K., & Blanchard, J. (2019). A new plumbing system framework for mantle plume-related continental large igneous provinces and their mafic-ultramafic intrusions. *Journal of Volcanology and Geothermal Research*, *384*, 75–84.

Ernst, R. E., & Youbi, N. (2017). How large igneous provinces affect global climate, sometimes cause mass extinctions, and represent natural markers in the geological record. *Palaeogeography, Palaeoclimatology, Palaeoecology*, *478*, 30–52.

Evelyne, T., Annelore, B., François, B., & Sébastien, P. (2018, dec). Thermal model of successive dike injections and implications for the development of intraplate volcanoes. *Lithos*, *322*, 129–147. doi: 10.1016/j.lithos.2018.10.007

Fainstein, R., Richards, M., & Kalra, R. (2019). Seismic imaging of deccan-related lava flows at the kt boundary, deepwater west india. *The Leading Edge*, *38*(4), 286–290.

Farnetani, C. G., & Richards, M. A. (1994). Numerical investigations of the mantle plume initiation model for flood basalt events. *Journal of Geophysical Research: Solid Earth*, *99*(B7), 13813–13833.

Farnetani, C. G., Richards, M. A., & Ghiorso, M. S. (1996). Petrological models of magma evolution and deep crustal structure beneath hotspots and flood basalt provinces. *Earth and Planetary Science Letters*, *143*(1-4), 81–94.

Fedorenko, V. A., Lightfoot, P. C., Naldrett, A. J., Czamanske, G. K., Hawkesworth, C. J., Wooden, J. L., & Ebel, D. S. (1996). Petrogenesis of the flood-basalt sequence at noril'sk, north central siberia. *International Geology Review*, *38*(2), 99–135.

Fendley, I., Mittal, T., Schmidt, A., & Hull, P. M. (2019). Environmental effects and eruptive dynamics of large igneous provinces: A multidisciplinary perspective ii posters. In *Agu fall meeting 2019.*

Fendley, I. M., Mittal, T., Renne, P. R., & Marvin-DiPasquale, M. (2019). Mercury chemostratigraphy and geochemical box model constraints on large igneous province eruption rates: Case studies from the deccan and siberian traps. In *Agu fall meeting 2019.*

Fendley, I. M., Mittal, T., Sprain, C. J., Marvin-DiPasquale, M., Tobin, T. S., & Renne, P. R. (2019). Constraints on the volume and rate of deccan traps flood

basalt eruptions using a combination of high-resolution terrestrial mercury records and geochemical box models. *Earth and Planetary Science Letters*, *524*, 115721.

Fendley, I. M., Sprain, C. J., Renne, P. R., Arenillas, I., Arz, J. A., Gilabert, V., ... others (2020). No cretaceous-paleogene boundary in exposed rajahmundry traps: A refined chronology of the longest deccan lava flows from 40ar/39ar dates, magnetostratigraphy, and biostratigraphy. *Geochemistry, Geophysics, Geosystems*, *21*(9), e2020GC009149.

Ferris, J., Johnson, A., & Storey, B. (1998). Form and extent of the dufek intrusion, antarctica, from newly compiled aeromagnetic data. *Earth and Planetary Science Letters*, *154*(1-4), 185–202.

Finch, R., & Macdonald, G. A. (1953). *Hawaiian volcanoes during 1950* (Tech. Rep.). US Govt. Print. Off.,.

Fleming, T. H. (1995). *Isotopic and chemical evolution of the ferrar group, beardmore glacier region, antarctica* (Unpublished doctoral dissertation). The Ohio State University.

Fleming, T. H., Elliot, D. H., Jones, L. M., Bowman, J. R., & Siders, M. A. (1992). Chemical and isotopic variations in an iron-rich lava flow from the kirkpatrick basalt, north victoria land, antarctica: implications for low-temperature alteration. *Contrib Mineral Petrol*, *1111440*, 45.

Font, E., Adatte, T., Sial, A. N., Drude de Lacerda, L., Keller, G., & Punekar, J. (2016). Mercury anomaly, deccan volcanism, and the end-cretaceous mass extinction. *Geology*, *44*(2), 171–174.

Font, E., Youbi, N., Fernandes, S., El Hachimi, H., Kratinova, Z., & Hamim, Y. (2011). Revisiting the magnetostratigraphy of the central atlantic magmatic province (camp) in morocco. *Earth and Planetary Science Letters*, *309*(3-4), 302–317.

Fowler, a. C. (2011). *Mathematical Geoscience* (Vol. 36). doi: 10.1007/978-0-85729-721-1

Furlong, K. P., & Fountain, D. M. (1986). Continental crustal underplating: Thermal considerations and seismic-petrologic consequences. *Journal of Geophysical Research: Solid Earth*, *91*(B8), 8285–8294.

Fyfe, W. (1992). Magma underplating of continental crust. *Journal of Volcanology and Geothermal Research*, *50*(1-2), 33–40.

Gadgil, R., Viegas, A., & Iyer, S. D. (2019). Structure and emplacement of the coastal deccan tholeiitic dyke swarm in goa, on the western indian rifted margin. *Bulletin of Volcanology*, *81*(6), 35.

Galerne, C. Y., Galland, O., Neumann, E.-R., & Planke, S. (2011). 3d relationships between sills and their feeders: evidence from the golden valley sill complex (karoo basin) and experimental modelling. *Journal of Volcanology and Geothermal Research*, *202*(3-4), 189–199.

Galerne, C. Y., Neumann, E.-R., & Planke, S. (2008, oct). Emplacement mechanisms of sill complexes: Information from the geochemical architecture of the golden valley sill complex, south africa. *Journal of Volcanology and Geothermal Research*, *177*(2), 425–440. doi: 10.1016/j.jvolgeores.2008.06.004

Galindo, I., & Gudmundsson, A. (2012). Basaltic feeder dykes in rift zones: geometry, emplacement, and effusion rates. *Natural Hazards and Earth System Sciences*, *12*(12), 3683.

Gallagher, K., & Hawkesworth, C. (1992). Dehydration melting and the generation of continental flood basalts. *Nature*, *358*(6381), 57–59.

Galland, O., Bertelsen, H., Eide, C., Guldstrand, F., Haug, Ø., Leanza, H. A., ... others (2018). Storage and transport of magma in the layered crust—formation of sills and related flat-lying intrusions. In *Volcanic and igneous plumbing systems* (pp. 113–138). Elsevier.

Galland, O., Planke, S., Neumann, E.-R., & Malthe-Sørenssen, A. (2009). Experimental modelling of shallow magma emplacement: Application to saucer-shaped intrusions. *Earth and Planetary Science Letters*, *277*(3-4), 373–383.

Galland, O., Spacapan, J. B., Rabbel, O., Mair, K., Soto, F. G., Eiken, T., ... Leanza, H. A. (2019). Structure, emplacement mechanism and magma-flow significance of igneous fingers–implications for sill emplacement in sedimentary basins. *Journal of Structural Geology*, *124*, 120–135.

Ganerød, M., Torsvik, T. H., van Hinsbergen, D. J. J., Gaina, C., Corfu, F., Werner, S., ... Hendriks, B. W. H. (2011). Palaeoposition of the seychelles microcontinent in relation to the deccan traps and the plume generation zone in late cretaceous-early palaeogene time. *Geological Society, London, Special Publications*, *357*(1), 229–252. doi: 10.1144/sp357.12

Gangopadhyay, A., Sen, G., & Keshav, S. (2003). Experimental crystallization of deccan basalts at low pressure: effect of contamination on phase equilibrium. *Indian Journal of Geology*, *75*(1/4), 54.

Ganguly, S., Ray, J., Koeberl, C., Saha, A., Thöni, M., & Balaram, V. (2014). Geochemistry and petrogenesis of lava flows around linga, chhindwara area in the eastern deccan volcanic province (edvp), india. *Journal of Asian Earth Sciences*, *91*, 174–193.

Gao, H., Yang, X., Long, M. D., & Aragon, J. C. (2020). Seismic evidence for crustal modification beneath the hartford rift basin in the northeastern united states. *Geophysical Research Letters*, *47*(17), e2020GL089316.

Gibson, S., & Geist, D. (2010). Geochemical and geophysical estimates of lithospheric thickness variation beneath galápagos. *Earth and Planetary Science Letters*, *300*(3-4), 275–286.

Gibson, S., Thompson, R., & Day, J. (2006). Timescales and mechanisms of plume–lithosphere interactions: 40ar/39ar geochronology and geochemistry of alkaline igneous rocks from the paraná–etendeka large igneous province. *Earth and Planetary Science Letters*, *251*(1-2), 1–17.

Gibson, S. A. (2002). Major element heterogeneity in archean to recent mantle plume starting-heads. *Earth and Planetary Science Letters*, *195*(1-2), 59–74.

Gibson, S. A., Rooks, E. E., Day, J. A., Petrone, C. M., & Leat, P. T. (2020). The role of sub-continental mantle as both "sink" and "source" in deep earth volatile cycles. *Geochimica et Cosmochimica Acta*. doi: https://doi.org/10.1016/j.gca.2020.02.018

Gombos Jr, A. M., Powell, W. G., & Norton, I. O. (1995). The tectonic evolution of western india and its impact on hydrocarbon occurrences: an overview. *Sedimentary Geology*, *96*(1-2), 119–129.

Gorczyk, W., & Vogt, K. (2018). Intrusion of magmatic bodies into the continental crust: 3-d numerical models. *Tectonics*, *37*(3), 705–723.

Gorring, M. L., & Naslund, H. (1995). Geochemical reversals within the lower 100 m of the palisades sill, new jersey. *Contributions to Mineralogy and Petrology*, *119*(2-3), 263–276.

Grant, T. B., Larsen, R. B., Anker-Rasch, L., Grannes, K. R., Iljina, M., McEnroe, S., ... Øen, E. (2016). Anatomy of a deep crustal volcanic conduit system; the reinfjord ultramafic complex, seiland igneous province, northern norway. *Lithos*, *252*, 200–215.

Greenough, J. D., Hari, K., Chatterjee, A., & Santosh, M. (1998). Mildly alkaline basalts from pavagadh hill, india: Deccan flood basalts with an asthenospheric origin. *Mineralogy and Petrology*, *62*(3-4), 223–245.

Griffin, W., Sturt, B., O'Neill, C., Kirkland, C., & O'Reilly, S. Y. (2013). Intrusion and contamination of high-temperature dunitic magma: the nordre bumandsfjord pluton, seiland, arctic norway. *Contributions to Mineralogy and Petrology*, *165*(5), 903–930.

Grunder, A., & Taubeneck, W. (1997). Partial melting of tonalite at the margins of columbia river basalt group dikes, wallowa mountains, oregon. In *Geol. soc. am. abstr. prog* (Vol. 29, p. 18).

GSI Bhukosh. (2020 (accessed December 1, 2020)). Bhukosh [Computer software manual]. Retrieved from \url{http://bhukosh.gsi.gov.in/}

GSI District Resource Map. (2001). *District resource maps - india* (Tech. Rep.).

Gudmundsson, A. (2016). The mechanics of large volcanic eruptions. *Earth-science reviews*, *163*, 72–93.

Guilbaud, M.-N., Self, S., Thordarson, T., & Blake, S. (2005). Morphology, surface structures, and emplacement of lavas produced by laki, ad 1783–1784. *Geological Society of America Special Papers*, *396*, 81–102.

Gunn, B. M., & Warren, G. (1962). *Geology of victoria land between the mawson and mulock glaciers, antarctica* (No. 70-71). Trans-Antarctic Expedition Committee.

Haase, K., Regelous, M., Schöbel, S., Günther, T., & de Wall, H. (2019). Variation of melting processes and magma sources of the early deccan flood basalts, malwa plateau, india. *Earth and Planetary Science Letters*, *524*, 115711.

Hansen, J., Jerram, D., McCaffrey, K., & Passey, S. (2011). Early cenozoic saucer-shaped sills of the faroe islands: an example of intrusive styles in basaltic lava piles. *Journal of the Geological Society*, *168*(1), 159–178.

Hari, K., Prasanth, M. M., Swarnkar, V., Kumar, J. V., & Randive, K. R. (2018). Evidence for the contrasting magmatic conditions in the petrogenesis of a-type granites of phenai mata igneous complex: implications for felsic magmatism in the deccan large igneous province. *Journal of the Indian Institute of Science*, *98*(4), 379–399.

Hari, K., Rao, N. C., & Swarnkar, V. (2011). Petrogenesis of gabbro and orthopyroxene gabbro from the phenai mata igneous complex, deccan volcanic province: Products of concurrent assimilation and fractional crystallization. *Journal of the Geological Society of India*, *78*(6), 501–509.

Hari, K., Swarnkar, V., & Prasanth, M. M. (2018). Significance of assimilation and fractional crystallization (afc) process in the generation of basaltic lava flows from chhotaudepur area, deccan large igneous province, nw india. *Journal of Earth System Science*, *127*(6), 85.

Hawkesworth, C., & Gallagher, K. (1993). Mantle hotspots, plumes and regional tectonics as causes of intraplate magmatism. *Terra Nova*, *5*(6), 552–559.

Hawkesworth, C., Kempton, P., Rogers, N., Ellam, R., & Van Calsteren, P. (1990). Continental mantle lithosphere, and shallow level enrichment processes. *Earth and Planetary Science Letters*, *96*, 256–268.

Hayes, B., Bybee, G. M., Mawela, M., Nex, P. A., & van Niekerk, D. (2018). Residual melt extraction and out-of-sequence differentiation in the bushveld complex, south africa. *Journal of Petrology*, *59*(12), 2413–2434.

Hegde, V., Koti, B., & Kruger, S. (2014). Geochemistry of the desur lavas, deccan traps: Case study from the vicinity of belgaum, karnataka and their petrogenetic inferences. *Journal of the Geological Society of India*, *83*(4), 363–375.

Heinonen, J. S., Iles, K. A., Heinonen, A., Fred, R., Virtanen, V. J., Bohrson, W. A., & Spera, F. J. (2020). From binary mixing to magma chamber simulator–geochemical modeling of assimilation in magmatic systems. In *Crustal magmatic system evolution.* American Geophysical Union.

Heinonen, J. S., Luttinen, A. V., Spera, F. J., & Bohrson, W. A. (2019a). Deep open storage and shallow closed transport system for a continental flood basalt sequence revealed with magma chamber simulator. *Contributions to Mineralogy and Petrology*, *174*(11), 87.

Heinonen, J. S., Luttinen, A. V., Spera, F. J., & Bohrson, W. A. (2019b, oct). Deep open storage and shallow closed transport system for a continental flood basalt sequence revealed with magma chamber simulator. *Contributions to*

Mineralogy and Petrology, *174*(11). doi: 10.1007/s00410-019-1624-0

Herzberg, C., & Gazel, E. (2009). Petrological evidence for secular cooling in mantle plumes. *Nature*, *458*(7238), 619–622.

Higgins, M. D. (2005). A new interpretation of the structure of the sept iles intrusive suite, canada. *Lithos*, *83*(3-4), 199–213.

Higgins, M. D., & Breemen, O. V. (1998). The age of the sept iles layered mafic intrusion, canada: implications for the late neoproterozoic/cambrian history of southeastern canada. *The Journal of Geology*, *106*(4), 421–432.

Higgins, M. D., & Chandrasekharam, D. (2007, mar). Nature of sub-volcanic magma chambers, deccan province, india: Evidence from quantitative textural analysis of plagioclase megacrysts in the giant plagioclase basalts. *Journal of Petrology*, *48*(5), 885–900. doi: 10.1093/petrology/egm005

Ho, A. M., & Cashman, K. V. (1997). Temperature constraints on the ginkgo flow of the columbia river basalt group. *Geology*, *25*(5), 403–406.

Hoggett, M. (2019). *A global analysis of igneous sill dimensions and their effect on sedimentary basins and petroleum system-statistics and modelling of seismic observations* (Unpublished doctoral dissertation). University of Birmingham.

Hon, K., Kauahikaua, J., Denlinger, R., & Mackay, K. (1994). Emplacement and inflation of pahoehoe sheet flows: Observations and measurements of active lava flows on kilauea volcano, hawaii. *Geological Society of America Bulletin*, *106*(3), 351–370.

Hooper, P. (1988a). The columbia river basalt. In *Continental flood basalts* (pp. 1–33). Springer.

Hooper, P. (1988b). Crystal fractionation and recharge (rfc) in the american bar flows of the imnaha basalt, columbia river basalt group. *Journal of Petrology*, *29*(5), 1097–1118.

Hooper, P., & Hawkesworth, C. (1993). Isotopic and geochemical constraints on the origin and evolution of the columbia river basalt. *Journal of Petrology*, *34*(6), 1203–1246.

Hooper, P., & Subbarao, K. (1999). The deccan traps. *Deccan Volcanic Province: Geological Society of India Memoir*, *43*, 153–165.

Hooper, P., Widdowson, M., & Kelley, S. (2010). Tectonic setting and timing of the final deccan flood basalt eruptions. *Geology*, *38*(9), 839–842.

Hooper, P. R. (2000). Chemical discrimination of columbia river basalt flows. *Geochemistry, Geophysics, Geosystems*, *1*(6).

Horowitz, H. M., Jacob, D. J., Zhang, Y., Dibble, T. S., Slemr, F., Amos, H. M., ... Sunderland, E. M. (2017). A new mechanism for atmospheric mercury redox chemistry: implications for the global mercury budget. *Atmospheric Chemistry and Physics*, *17*(10).

Husch, J. M. (1990). Palisades sill: origin of the olivine zone by separate magmatic injection rather than gravity settling. *Geology*, *18*(8), 699–702.

Ingebritsen, S., & Manning, C. E. (2010). Permeability of the continental crust: dynamic variations inferred from seismicity and metamorphism. *Geofluids*, *10*(1-2), 193–205.

Jagannathan, K., & members, a. (2010, 02). *Manual for national geomorphological and lineament mapping on 1:50,000 scale, document control number: Nrsc-rs gisaa-erg-g-gd-feb 10-tr149. hyderabad, national remote sensing centre.* (Tech. Rep.).

Jay, A. E. (2005). *Volcanic architecture of the deccan traps, western maharashtra, india: an integrated chemostratigraphic and paleomagnetic study* (Unpublished doctoral dissertation). The Open University.

Jay, A. E., Mac Niocaill, C., Widdowson, M., Self, S., & Turner, W. (2009). New palaeomagnetic data from the mahabaleshwar plateau, deccan flood basalt province, india: implications for the volcanostratigraphic architecture of continental flood basalt provinces. *Journal of the Geological Society*, *166*(1),

13–24.

Jay, A. E., & Widdowson, M. (2008). Stratigraphy, structure and volcanology of the se deccan continental flood basalt province: implications for eruptive extent and volumes. *Journal of the Geological Society*, *165*(1), 177–188.

Jellinek, A. M., & DePaolo, D. J. (2003). A model for the origin of large silicic magma chambers: precursors of caldera-forming eruptions. *Bulletin of Volcanology*, *65*(5), 363–381.

Jennings, E. S., Gibson, S. A., & Maclennan, J. (2019). Hot primary melts and mantle source for the paraná-etendeka flood basalt province: New constraints from al-in-olivine thermometry. *Chemical Geology*, *529*, 119287.

Jennings, E. S., Gibson, S. A., Maclennan, J., & Heinonen, J. S. (2017). Deep mixing of mantle melts beneath continental flood basalt provinces: Constraints from olivine-hosted melt inclusions in primitive magmas. *Geochimica et Cosmochimica Acta*, *196*, 36–57.

Jerram, D. A., Davis, G. R., Mock, A., Charrier, A., & Marsh, B. D. (2010). Quantifying 3d crystal populations, packing and layering in shallow intrusions: a case study from the basement sill, dry valleys, antarctica. *Geosphere*, *6*(5), 537–548.

Jerram, D. A., Dobson, K. J., Morgan, D. J., & Pankhurst, M. J. (2018). The petrogenesis of magmatic systems: Using igneous textures to understand magmatic processes. In *Volcanic and igneous plumbing systems* (pp. 191–229). Elsevier.

Jerram, D. A., Svensen, H. H., Planke, S., Polozov, A. G., & Torsvik, T. H. (2016). The onset of flood volcanism in the north-western part of the siberian traps: Explosive volcanism versus effusive lava flows. *Palaeogeography, Palaeoclimatology, Palaeoecology*, *441*, 38–50.

Jerram, D. A., & Widdowson, M. (2005). The anatomy of continental flood basalt provinces: geological constraints on the processes and products of flood volcanism. *Lithos*, *79*(3-4), 385–405.

Johansson, L., Zahirovic, S., & Müller, R. D. (2018). The interplay between the eruption and weathering of large igneous provinces and the deep-time carbon cycle. *Geophysical Research Letters*, *45*(11), 5380–5389.

Johnson, R. B. (1961). Patterns and origin of radial dike swarms associated with west spanish peak and dike mountain, south-central colorado. *Geological Society of America Bulletin*, *72*(4), 579–589.

Jones, M. T., Jerram, D. A., Svensen, H. H., & Grove, C. (2016). The effects of large igneous provinces on the global carbon and sulphur cycles. *Palaeogeography, Palaeoclimatology, Palaeoecology*, *441*, 4–21.

Jones, S. M., Hoggett, M., Greene, S. E., & Jones, T. D. (2019). Large igneous province thermogenic greenhouse gas flux could have initiated paleocene-eocene thermal maximum climate change. *Nature Communications*, *10*(1), 1–16.

Kale, V. S., Dole, G., Shandilya, P., & Pande, K. (2020). Stratigraphy and correlations in deccan volcanic province, india: quo vadis? *GSA Bulletin*, *132*(3-4), 588–607.

Kale, V. S., Dole, G., Upasani, D., & Pillai, S. P. (2017). Deccan plateau uplift: insights from parts of western uplands, maharashtra, india. *Geological Society, London, Special Publications*, *445*(1), 11–46.

Kalsbeek, F., & Taylor, P. N. (1986). Chemical and isotopic homogeneity of a 400 km long basic dyke in central west greenland. *Contributions to Mineralogy and Petrology*, *93*(4), 439–448.

Kaotekwar, A. B., Meshram, R. R., Sathyanarayanan, M., Krishna, A. K., & Charan, S. (2014). Structures, petrography and geochemistry of deccan basalts at anantagiri hills, andhra pradesh. *Journal of the Geological Society of India*, *84*(6), 675–685.

Karkare, S., & Srivastava, R. K. (1990). Regional dyke swarms related to the deccan trap alkaline province, india. In *International dyke conference. 2* (pp. 335–347).

Karlstrom, L., Dufek, J., & Manga, M. (2009). Organization of volcanic plumbing through magmatic lensing by magma chambers and volcanic loads. *Journal of Geophysical Research: Solid Earth*, *114*(B10).

Karlstrom, L., Dufek, J., & Manga, M. (2010). Magma chamber stability in arc and continental crust. *Journal of Volcanology and Geothermal Research*, *190*(3-4), 249–270.

Karlstrom, L., Murray, K. E., & Reiners, P. W. (2019, apr). Bayesian markov-chain monte carlo inversion of low-temperature thermochronology around two 8 - 10 m wide columbia river flood basalt dikes. *Frontiers in Earth Science*, *7*. doi: 10.3389/feart.2019.00090

Karlstrom, L., Paterson, S. R., & Jellinek, A. M. (2017). A reverse energy cascade for crustal magma transport. *Nature Geoscience*, *10*(8), 604.

Karlstrom, L., & Richards, M. (2011). On the evolution of large ultramafic magma chambers and timescales for flood basalt eruptions. *Journal of Geophysical Research: Solid Earth*, *116*(B8).

Karlstrom, L., Wright, H. M., & Bacon, C. R. (2015). The effect of pressurized magma chamber growth on melt migration and pre-caldera vent locations through time at Mount Mazama, Crater Lake, Oregon. *Earth and Planetary Science Letters*, *412*, 209–219. doi: 10.1016/j.epsl.2014.12.001

Karmalkar, N., Duraiswami, R., Jonnalagadda, M., Griffin, W., Gregoire, M., Benoit, M., & Delpech, G. (2016). Magma types and source characterization of the early deccan magmatism, kutch region, nw india: Insights from geochemistry of igneous intrusions. *J Geol Soc India Spl Pub*, *6*, 193–208.

Kasbohm, J., & Schoene, B. (2018). Rapid eruption of the columbia river flood basalt and correlation with the mid-miocene climate optimum. *Science advances*, *4*(9), eaat8223.

Katz, M. G., & Cashman, K. V. (2003). Hawaiian lava flows in the third dimension: Identification and interpretation of pahoehoe and a'a distribution in the kp-1 and soh-4 cores. *Geochemistry, Geophysics, Geosystems*, *4*(2).

Kavanagh, J. L. (2018). Mechanisms of magma transport in the upper crust—dyking. In *Volcanic and igneous plumbing systems* (pp. 55–88). Elsevier.

Keller, G., Mateo, P., Punekar, J., Khozyem, H., Gertsch, B., Spangenberg, J., ... Adatte, T. (2018). Environmental changes during the cretaceous-paleogene mass extinction and paleocene-eocene thermal maximum: Implications for the anthropocene. *Gondwana Research*, *56*, 69–89.

Keller, T., May, D. A., & Kaus, B. J. P. (2013). Numerical modelling of magma dynamics coupled to tectonic deformation of lithosphere and crust. *Geophysical Journal International*, *195*(3), 1406–1442. doi: 10.1093/gji/ggt306

Kempton, P. D., & Harmon, R. S. (1992). Oxygen isotope evidence for large-scale hybridization of the lower crust during magmatic underplating. *Geochimica et Cosmochimica Acta*, *56*(3), 971–986.

Keszthelyi, L., & Self, S. (1998). Some physical requirements for the emplacement of long basaltic lava flows. *Journal of Geophysical Research: Solid Earth*, *103*(B11), 27447–27464.

Keszthelyi, L., Self, S., & Thordarson, T. (2006). Flood lavas on earth, io and mars. *Journal of the geological society*, *163*(2), 253–264.

Khadri, S., Subbarao, K., Hooper, P., & Walsh, J. (1988). Stratigraphy of thakurvadi formation, western deccan basalt province, india. *Memoir-Geological Society of India*(10), 281–304.

Khan, W., McCormick, G. R., & Reagan, M. K. (1999). Parh group basalts of northeastern balochistan, pakistan: precursors to the deccan traps. *Special*

Papers-Geological Society of America, 59–74.

Kieffer, B., Arndt, N., Lapierre, H., Bastien, F., Bosch, D., Pecher, A., ... others (2004). Flood and shield basalts from ethiopia: magmas from the african superswell. *Journal of Petrology*, *45*(4), 793–834.

Knight, K., Nomade, S., Renne, P., Marzoli, A., Bertrand, H., & Youbi, N. (2004). The central atlantic magmatic province at the triassic–jurassic boundary: paleomagnetic and 40ar/39ar evidence from morocco for brief, episodic volcanism. *Earth and Planetary Science Letters*, *228*(1-2), 143–160.

Krans, S., Rooney, T., Kappelman, J., Yirgu, G., & Ayalew, D. (2018). From initiation to termination: a petrostratigraphic tour of the ethiopian low-ti flood basalt province. *Contributions to Mineralogy and Petrology*, *173*(5), 37.

Krans, S. R., Rooney, T. O., Kappelman, J., Yirgu, G., & Ayalew, D. (2018, apr). From initiation to termination: a petrostratigraphic tour of the ethiopian low-ti flood basalt province. *Contributions to Mineralogy and Petrology*, *173*(5). doi: 10.1007/s00410-018-1460-7

Krishna, M. R., Verma, R., & Purushotham, A. K. (2002). Lithospheric structure below the eastern arabian sea and adjoining west coast of india based on integrated analysis of gravity and seismic data. *Marine Geophysical Researches*, *23*(1), 25–42.

Krishnamurthy, P. (2020). The deccan volcanic province (dvp), india: A review. *Journal of the Geological Society of India*, *96*(2), 111–147.

Krishnamurthy, P., & Cox, K. (1977). Picrite basalts and related lavas from the deccan traps of western india. *Contributions to Mineralogy and Petrology*, *62*(1), 53–75.

Krishnamurthy, P., & Cox, K. (1980). A potassium-rich alkalic suite from the deccan traps, rajpipla, india. *Contributions to Mineralogy and Petrology*, *73*(2), 179–189.

Krishnamurthy, P., Gopalan, K., & Macdougall, J. (2000). Olivine compositions in picrite basalts and the deccan volcanic cycle. *Journal of Petrology*, *41*(7), 1057–1069.

Krivolutskaya, N., & Kedrovskaya, T. (2020). Structure and composition of the nadayansky lava flow: an example of the homogeneity of lava flows of the siberian trap province. *Geochemistry International*, *58*, 363–376.

Krivolutskaya, N., Kuzmin, D., Gongalsky, B., Roshchina, I., Kononkova, N., Svirskaya, N., & Romashova, T. (2018). Stages of trap magmatism in the norilsk area: New data on the structure and geochemistry of the volcanic rocks. *Geochemistry International*, *56*(5), 419–437.

Krivolutskaya, N. A., Kuzmin, D. V., Gongalsky, B. I., Roshchina, I. A., Kononkova, N. N., Svirskaya, N. M., & Romashova, T. V. (2018, may). Stages of trap magmatism in the norilsk area: New data on the structure and geochemistry of the volcanic rocks. *Geochemistry International*, *56*(5), 419–437. doi: 10.1134/s0016702918050026

Krivolutskaya, N. A., & Sobolev, A. I. (2016). *Siberian traps and pt-cu-ni deposits in the noril'sk area*. Springer.

Kruger, F. J. (2005). Filling the bushveld complex magma chamber: lateral expansion, roof and floor interaction, magmatic unconformities, and the formation of giant chromitite, pge and ti-v-magnetitite deposits. *Mineralium Deposita*, *40*(5), 451–472.

Kumar, G. P., Mahesh, P., Nagar, M., Mahender, E., Kumar, V., Mohan, K., & Kumar, M. R. (2017, may). Role of deep crustal fluids in the genesis of intraplate earthquakes in the kachchh region, northwestern india. *Geophysical Research Letters*, *44*(9), 4054–4063. doi: 10.1002/2017gl072936

Kumar, K. V., Chavan, C., Sawant, S., Raju, K. N., Kanakdande, P., Patode, S., ... Balaram, V. (2010). Geochemical investigation of a semi-continuous extrusive basaltic section from the deccan volcanic province, india: implications for

the mantle and magma chamber processes. *Contributions to Mineralogy and Petrology*, *159*(6), 839–862.

Kumar, P., & Chaubey, A. (2019). Extension of flood basalt on the northwestern continental margin of india. *Journal of Earth System Science*, *128*(4), 81.

Kumar, P. V., Patro, P. K., Rao, P. S., Singh, A., Kumar, A., & Nagarjuna, D. (2018). Electrical resistivity cross-section across northern part of saurashtra region: An insight to crystallized magma and fluids. *Tectonophysics*, *744*, 205–214.

Larsen, L. M., & Pedersen, A. K. (2009). Petrology of the paleocene picrites and flood basalts on disko and nuussuaq, west greenland. *Journal of Petrology*, *50*(9), 1667–1711.

Larsen, R. B., Grant, T., Sørensen, B. E., Tegner, C., McEnroe, S., Pastore, Z., ... others (2018). Portrait of a giant deep-seated magmatic conduit system: The seiland igneous province. *Lithos*, *296*, 600–622.

Lassiter, J. C., & DePaolo, D. J. (1997). Plume/lithosphere interaction in the generation of continental and oceanic flood basalts: chemical and isotopic constraints. *Geophysical Monograph-American Geophysical Union*, *100*, 335–356.

Latyshev, A., Krivolutskaya, N., Ulyahina, P., Bychkova, Y. V., & Gongalsky, B. (2019). Intrusions of the kulumbe river valley, nw siberian traps province: Paleomagnetism, magnetic fabric and geochemistry. In *Recent advances in rock magnetism, environmental magnetism and paleomagnetism* (pp. 67–82). Springer.

Lee, C., & Butcher, A. (1990). Cyclicity in the sr isotope stratigraphy through the merensky and bastard reef units, atok section, eastern bushveld complex. *Economic Geology*, *85*(4), 877–883.

Lee, C.-T. A., Lee, T. C., & Wu, C.-T. (2014). Modeling the compositional evolution of recharging, evacuating, and fractionating (refc) magma chambers: Implications for differentiation of arc magmas. *Geochimica et Cosmochimica Acta*, *143*, 8–22.

Leeman, W., & Hawkesworth, C. (1986). Open magma systems: trace element and isotopic constraints. *Journal of Geophysical Research: Solid Earth*, *91*(B6), 5901–5912.

Lenhardt, N., & Eriksson, P. G. (2012). Volcanism of the palaeoproterozoic bushveld large igneous province: the rooiberg group, kaapvaal craton, south africa. *Precambrian Research*, *214*, 82–94.

Lightfoot, P., & Hawkesworth, C. (1988). Origin of deccan trap lavas: evidence from combined trace element and sr-, nd-and pb-isotope studies. *Earth and Planetary Science Letters*, *91*(1-2), 89–104.

Lightfoot, P., Hawkesworth, C., Devey, C. W., Rogers, N., & Calsteren, P. V. (1990). Source and differentiation of deccan trap lavas: implications of geochemical and mineral chemical variations. *Journal of Petrology*, *31*(5), 1165–1200.

Lightfoot, P., Hawkesworth, C., Hergt, J., Naldrett, A., Gorbachev, N., Fedorenko, V., & Doherty, W. (1993). Remobilisation of the continental lithosphere by a mantle plume: major-, trace-element, and sr-, nd-, and pb-isotope evidence from picritic and tholeiitic lavas of the noril'sk district, siberian trap, russia. *Contributions to Mineralogy and Petrology*, *114*(2), 171–188.

Lightfoot, P., Hawkesworth, C., & Sethna, S. (1987). Petrogenesis of rhyolites and trachytes from the deccan trap: Sr, nd and pb isotope and trace element evidence. *Contributions to Mineralogy and Petrology*, *95*(1), 44–54.

Lightfoot, P., Naldrett, A., Gorbachev, N., Doherty, W., & Fedorenko, V. (1990). Geochemistry of the siberian trap of the noril'sk area, ussr, with implications for the relative contributions of crust and mantle to flood basalt magmatism. *Contributions to Mineralogy and Petrology*, *104*(6), 631–644.

Lipman, P. W., & Banks, N. G. (1987). Aa flow dynamics, mauna loa 1984. *US Geol Surv Prof Pap*, *1350*, 1527–1567.

Lister, J. R., & Kerr, R. C. (1991). Fluid-mechanical models of crack propagation and their application to magma transport in dykes. *Journal of Geophysical Research: Solid Earth*, *96*(B6), 10049–10077.

Luttinen, A. V., & Furnes, H. (2000). Flood basalts of vestfjella: Jurassic magmatism across an archaean–proterozoic lithospheric boundary in dronning maud land, antarctica. *Journal of Petrology*, *41*(8), 1271–1305.

Maccaferri, F., Bonafede, M., & Rivalta, E. (2011). A quantitative study of the mechanisms governing dike propagation, dike arrest and sill formation. *Journal of Volcanology and Geothermal Research*, *208*(1-2), 39–50. doi: 10.1016/j.jvolgeores.2011.09.001

Machado, F. B., Rocha-Júnior, E. R. V., Marques, L. S., Nardy, A. J. R., Zezzo, L. V., & Marteleto, N. S. (2018). Geochemistry of the northern paraná continental flood basalt (pcfb) province: implications for regional chemostratigraphy. *Brazilian Journal of Geology*, *48*(2), 177–199.

Madrigal, P., Gazel, E., Denyer, P., Smith, I., Jicha, B., Flores, K. E., ... Snow, J. (2015). A melt-focusing zone in the lithospheric mantle preserved in the Santa Elena Ophiolite, Costa Rica. *Lithos*, *230*, 189–205. doi: 10.1016/j.lithos.2015.04.015

Magee, C., Ernst, R. E., Muirhead, J., Phillips, T., & Jackson, C. A.-L. (2019). Magma transport pathways in large igneous provinces: Lessons from combining field observations and seismic reflection data. In *Dyke swarms of the world: A modern perspective* (pp. 45–85). Springer.

Magee, C., Muirhead, J., Schofield, N., Walker, R. J., Galland, O., Holford, S., ... McCarthy, W. (2019). Structural signatures of igneous sheet intrusion propagation. *Journal of Structural Geology*, *125*, 148–154.

Magee, C., Stevenson, C. T., Ebmeier, S. K., Keir, D., Hammond, J. O., Gottsmann, J. H., ... others (2018). Magma plumbing systems: a geophysical perspective. *Journal of Petrology*, *59*(6), 1217–1251.

Mahoney, J., Duncan, R., Khan, W., Gnos, E., & McCormick, G. (2002). Cretaceous volcanic rocks of the south tethyan suture zone, pakistan: implications for the réunion hotspot and deccan traps. *Earth and Planetary Science Letters*, *203*(1), 295–310.

Mahoney, J., Macdougall, J., Lugmair, G., Murali, A., Das, M. S., & Gopalan, K. (1982). Origin of the deccan trap flows at mahabaleshwar inferred from nd and sr isotopic and chemical evidence. *Earth and Planetary Science Letters*, *60*(1), 47–60.

Mahoney, J., Sheth, H., Chandrasekharam, D., & Peng, Z. (2000). Geochemistry of flood basalts of the toranmal section, northern deccan traps, india: implications for regional deccan stratigraphy. *Journal of Petrology*, *41*(7), 1099–1120.

Mahoney, J. J. (1984). *Isotopic and chemical studies of the deccan and rajmahal traps, india: mantle sources and petrogenesis* (Unpublished doctoral dissertation).

Mahoney, J. J. (1988). Deccan traps. In *Continental flood basalts* (pp. 151–194). Springer.

Mahoney, J. J., & Coffin, M. F. (1997). *Large igneous provinces: continental, oceanic, and planetary flood volcanism* (Vol. 100). American Geophysical Union.

Malthe-Sørenssen, A., Planke, S., Svensen, H., Jamtveit, B., Breitkreuz, C., & Petford, N. (2004). Formation of saucer-shaped sills. *Physical geology of high-level magmatic systems. Geological Society, London, Special Publications*, *234*, 215–227.

Mammo, T. (2013). Crustal structure of the flood basalt province of ethiopia from constrained 3-d gravity inversion. *Pure and Applied Geophysics*, *170*(12),

2185–2206.

Manga, M., & Michaut, C. (2017). Formation of lenticulae on europa by saucer-shaped sills. *Icarus*, *286*, 261–269.

Mangan, M. T., Wright, T. L., Swanson, D. A., & Byerly, G. R. (1986). Regional correlation of grande ronde basalt flows, columbia river basalt group, washington, oregon, and idaho. *Geological Society of America Bulletin*, *97*(11), 1300–1318.

Manu Prasanth, M., Hari, K., & Santosh, M. (2019). Tholeiitic basalts of deccan large igneous province, india: An overview. *Geological Journal*, *54*(5), 2980–2993.

Marsh, B. (2004). A magmatic mush column rosetta stone: The McMurdo Dry Valleys of Antarctica. *Eos, Transactions American Geophysical Union*, *85*(47), 497. doi: 10.1029/2004EO470001

Marsh, B. D. (2004). A magmatic mush column rosetta stone: the mcmurdo dry valleys of antarctica. *Eos, Transactions American Geophysical Union*, *85*(47), 497–502.

Marsh, B. D. (2013, aug). On some fundamentals of igneous petrology. *Contributions to Mineralogy and Petrology*, *166*(3), 665–690. doi: 10.1007/s00410-013-0892-3

Marsh, J., Hooper, P., Rehacek, J., Duncan, R., & Duncan, A. (1997). Stratigraphy and age of karoo basalts of lesotho and implications for correlations within the karoo igneous province. *Geophysical Monograph-American Geophysical Union*, *100*, 247–272.

Marsh, J. S. (1987). Basalt geochemistry and tectonic discrimination within continental flood basalt provinces. *Journal of Volcanology and Geothermal Research*, *32*(1-3), 35–49.

Marsh, J. S. (1989). Geochemical constraints on coupled assimilation and fractional crystallization involving upper crustal compositions and continental tholeiitic magma. *Earth and Planetary Science Letters*, *92*(1), 70–80.

Marzen, R., Shillington, D., Lizarralde, D., Knapp, J., Heffner, D., Davis, J., & Harder, S. (2020). Limited and localized magmatism in the central atlantic magmatic province. *Nature communications*, *11*(1), 1–8.

Marzoli, A., Bertrand, H., Youbi, N., Callegaro, S., Merle, R., Reisberg, L., ... others (2019). The central atlantic magmatic province (camp) in morocco. *Journal of Petrology*, *60*(5), 945–996.

Maurya, S., Montagner, J.-P., Kumar, M. R., Stutzmann, E., Kiselev, S., Burgos, G., ... Srinagesh, D. (2016, oct). Imaging the lithospheric structure beneath the indian continent. *Journal of Geophysical Research: Solid Earth*, *121*(10), 7450–7468. doi: 10.1002/2016jb012948

Mckenzie, D., & Bickle, M. (1988). The volume and composition of melt generated by extension of the lithosphere. *Journal of petrology*, *29*(3), 625–679.

McKenzie, D., & O'nions, R. (1991). Partial melt distributions from inversion of rare earth element concentrations. *Journal of Petrology*, *32*(5), 1021–1091.

Melluso, L., Barbieri, M., & Beccaluva, L. (2004). Chemical evolution, petrogenesis, and regional chemical correlations of the flood basalt sequence in the central deccan traps, india. *Journal of Earth System Science*, *113*(4), 587–603.

Melluso, L., Beccaluva, L., Brotzu, P., Gregnanin, A., Gupta, A., Morbidelli, L., & Traversa, G. (1995). Constraints on the mantle sources of the deccan traps from the petrology and geochemistry of the basalts of gujarat state (western india). *Journal of Petrology*, *36*(5), 1393–1432.

Melluso, L., Mahoney, J. J., & Dallai, L. (2006). Mantle sources and crustal input as recorded in high-mg deccan traps basalts of gujarat (india). *Lithos*, *89*(3-4), 259–274.

Melluso, L., Sethna, S., d'Antonio, M., Javeri, P., & Bennio, L. (2002). Geochemistry and petrogenesis of sodic and potassic mafic alkaline rocks in the deccan

volcanic province, mumbai area (india). *Mineralogy and Petrology*, *74*(2-4), 323–342.

Melluso, L., Sethna, S., Morra, V., Khateeb, A., & Javeri, P. (1999). Petrology of mafic dyke swarm of the tapti river in the nandurbar area. *Deccan volcanic province*, *3*(1), 735–738.

Millett, J., Hole, M., Jolley, D., & Passey, S. (2017). Geochemical stratigraphy and correlation within large igneous provinces: the final preserved stages of the faroe islands basalt group. *Lithos*, *286*, 1–15.

Millett, J., Hole, M., Jolley, D., Schofield, N., & Campbell, E. (2016). Frontier exploration and the north atlantic igneous province: new insights from a 2.6 km offshore volcanic sequence in the ne faroe–shetland basin. *Journal of the Geological Society*, *173*(2), 320–336.

Mishra, S., Misra, S., Vyas, D., Nikalje, D., Warhade, A., & Roy, S. (2017). A 1251m-thick deccan flood basalt pile recovered by scientific drilling in the koyna region, western india. *Journal of the Geological Society of India*, *90*(6), 788–794.

Misra, A. A., Bhattacharya, G., Mukherjee, S., & Bose, N. (2014). Near n–s paleo-extension in the western deccan region, india: does it link strike-slip tectonics with india–seychelles rifting? *International Journal of Earth Sciences*, *103*(6), 1645–1680.

Misra, A. A., & Mukherjee, S. (2017). Dyke–brittle shear relationships in the western deccan strike-slip zone around mumbai (maharashtra, india). *Geological Society, London, Special Publications*, *445*(1), 269–295.

Mitchell, A., Scoon, R., & Sharpe, M. (2019). The upper critical zone in the swartklip sector, north-western bushveld complex, on the farm wilgerspruit 2jq: Ii. origin by intrusion of ultramafic sills with concomitant partial melting of host norite-anorthosite cumulates. *South African Journal of Geology 2019*, *122*(2), 143–162.

Mitchell, A. A., & Scoon, R. N. (2007). The merensky reef at winnaarshoek, eastern bushveld complex: a primary magmatic hypothesis based on a wide reef facies. *Economic Geology*, *102*(5), 971–1009.

Mitchell, C., & Widdowson, M. (1991). A geological map of the southern deccan traps, india and its structural implications. *Journal of the Geological Society*, *148*(3), 495–505.

Mittal, T., & Richards, M. A. (2019). Volatile degassing from magma chambers as a control on volcanic eruptions. *Journal of Geophysical Research: Solid Earth*.

Mittal, T., Sprain, C. J., Fendley, I., Self, S., Renne, P. R., & Richards, M. A. (2019). Constraining the eruptive tempo of the deccan traps to understand potential climate consequences. In *Agu fall meeting 2019*.

Moore, N., Grunder, A., & Bohrson, W. (2018). The three-stage petrochemical evolution of the steens basalt (southeast oregon, usa) compared to large igneous provinces and layered mafic intrusions. *Geosphere*, *14*(6), 2505–2532.

Morrison, M. A., Thompson, R., & Dickin, A. (1985). Geochemical evidence for complex magmatic plumbing during development of a continental volcanic center. *Geology*, *13*(8), 581–584.

Morriss, M. C., Karlstrom, L., Nasholds, M. W., & Wolff, J. A. (2020). The chief joseph dike swarm of the columbia river flood basalts, and the legacy data set of william h. taubeneck. *Geosphere*.

Morse, S. A. (1980). *Basalts and phase diagrams: an introduction to the quantitative use of phase diagrams in igneous petrology*. Springer-Verlag.

Moulin, M., Fluteau, F., Courtillot, V., Marsh, J., Delpech, G., Quidelleur, X., & Gérard, M. (2017, feb). Eruptive history of the karoo lava flows and their impact on early jurassic environmental change. *Journal of Geophysical Research: Solid Earth*, *122*(2), 738–772. doi: 10.1002/2016jb013354

Mungall, J. E., Kamo, S. L., & McQuade, S. (2016). U–pb geochronology documents out-of-sequence emplacement of ultramafic layers in the bushveld igneous complex of south africa. *Nature Communications*, *7*(1), 1–13.

Naganjaneyulu, K., & Santosh, M. (2010, nov). The central india tectonic zone: A geophysical perspective on continental amalgamation along a mesoproterozoic suture. *Gondwana Research*, *18*(4), 547–564. doi: 10.1016/j.gr.2010.02.017

Naganjaneyulu, K., & Santosh, M. (2011, jul). Geophysical signatures of fluids in a reactivated precambrian collisional suture in central india. *Geoscience Frontiers*, *2*(3), 289–301. doi: 10.1016/j.gsf.2011.06.001

Naidu, G. D., & Harinarayana, T. (2009, oct). Deep electrical imaging of the narmada–tapti region, central india from magnetotellurics. *Tectonophysics*, *476*(3-4), 538–549. doi: 10.1016/j.tecto.2009.07.010

Namur, O., Charlier, B., Toplis, M. J., Higgins, M. D., Liégeois, J.-P., & Vander Auwera, J. (2010). Crystallization sequence and magma chamber processes in the ferrobasaltic sept iles layered intrusion, canada. *Journal of Petrology*, *51*(6), 1203–1236.

Natali, C., Beccaluva, L., Bianchini, G., Siena, F., et al. (2017). Comparison among ethiopia-yemen, deccan, and karoo continental flood basalts of central gondwana: Insights on lithosphere versus asthenosphere contributions in compositionally zoned magmatic provinces. *The Crust-Mantle and lithosphere-asthenosphere boundaries: insights from xenoliths, orogenic deep sections, and geophysical studies*, *526*, 191–215.

Neal, C. A., Brantley, S., Antolik, L., Babb, J., Burgess, M., Calles, K., ... others (2019). The 2018 rift eruption and summit collapse of kilauea volcano. *Science*, *363*(6425), 367–374.

Neumann, E.-R., Svensen, H., Galerne, C. Y., & Planke, S. (2011). Multistage evolution of dolerites in the karoo large igneous province, central south africa. *Journal of Petrology*, *52*(5), 959–984.

Nielsen, T. F. (2004). The shape and volume of the skaergaard intrusion, greenland: implications for mass balance and bulk composition. *Journal of Petrology*, *45*(3), 507–530.

O'Driscoll, B., Troll, V. R., Reavy, R. J., & Turner, P. (2006). The great eucrite intrusion of ardnamurchan, scotland: Reevaluating the ring-dike concept. *Geology*, *34*(3), 189–192.

Ohneiser, C., Acton, G., Channell, J. E., Wilson, G. S., Yamamoto, Y., & Yamazaki, T. (2013). A middle miocene relative paleointensity record from the equatorial pacific. *Earth and Planetary Science Letters*, *374*, 227–238.

Oppenheimer, C., Orchard, A., Stoffel, M., Newfield, T. P., Guillet, S., Corona, C., ... Büntgen, U. (2018). The eldgjá eruption: timing, long-range impacts and influence on the christianisation of iceland. *Climatic change*, *147*(3-4), 369–381.

Óskarsson, B. V., & Riishuus, M. S. (2014, dec). The mode of emplacement of neogene flood basalts in eastern iceland: Facies architecture and structure of simple aphyric basalt groups. *Journal of Volcanology and Geothermal Research*, *289*, 170–192. doi: 10.1016/j.jvolgeores.2014.11.009

Owen-Smith, T., & Ashwal, L. (2015). Evidence for multiple pulses of crystal-bearing magma during emplacement of the doros layered intrusion, namibia. *Lithos*, *238*, 120–139.

Owen-Smith, T. M., Ashwal, L. D., Torsvik, T. H., Ganerød, M., Nebel, O., Webb, S. J., & Werner, S. C. (2013). Seychelles alkaline suite records the culmination of deccan traps continental flood volcanism. *Lithos*, *182*, 33–47.

O'driscoll, B. (2007). The centre 3 layered gabbro intrusion, ardnamurchan, nw scotland. *Geological Magazine*, *144*(6), 897–908.

O'Hara, M., & Herzberg, C. (2002). Interpretation of trace element and isotope features of basalts: relevance of field relations, petrology, major element

data, phase equilibria, and magma chamber modeling in basalt petrogenesis. *Geochimica et Cosmochimica Acta*, *66*(12), 2167–2191.

O'Hara, M., & Mathews, R. (1981). Geochemical evolution in an advancing, periodically replenished, periodically tapped, continuously fractionated magma chamber. *Journal of the Geological Society*, *138*(3), 237–277.

Pande, K., Cucciniello, C., Sheth, H., Vijayan, A., Sharma, K. K., Purohit, R., ... Shinde, S. (2017). Polychronous (early cretaceous to palaeogene) emplacement of the mundwara alkaline complex, rajasthan, india: 40 ar/39 ar geochronology, petrochemistry and geodynamics. *International Journal of Earth Sciences*, *106*(5), 1487–1504.

Pande, K., Yatheesh, V., & Sheth, H. (2017). 40ar/39ar dating of the mumbai tholeiites and panvel flexure: intense 62.5 ma onshore–offshore deccan magmatism during india-laxmi ridge–seychelles breakup. *Geophysical Journal International*, *210*(2), 1160–1170.

Pandey, A., Dasgupta, S., Yadav, R. K., Kuila, U., Mishra, P., & Mohapatra, P. (2017). Various characteristics of deccan lava flow sequences identified in core, wireline and seismic in barmer basin. *Society of Petroleum Geophysicists (SPG), Jaipur India*.

Pandey, D., Pandey, A., & Rajan, S. (2011). Offshore extension of deccan traps in kachchh, central western india: implications for geological sequestration studies. *Natural resources research*, *20*(1), 33–43.

Pandey, O., Chandrakala, K., Parthasarathy, G., Reddy, P., & Reddy, G. K. (2009). Upwarped high velocity mafic crust, subsurface tectonics and causes of intraplate latur-killari (m 6.2) and koyna (m 6.3) earthquakes, india–a comparative study. *Journal of Asian Earth Sciences*, *34*(6), 781–795.

Pandey, O. P. (2020). *Geodynamic evolution of the indian shield: Geophysical aspects*. Springer.

Panovska, S., Korte, M., & Constable, C. (2019). One hundred thousand years of geomagnetic field evolution. *Reviews of Geophysics*, *57*(4), 1289–1337.

Parisio, L., Jourdan, F., Marzoli, A., Melluso, L., Sethna, S. F., & Bellieni, G. (2016). 40ar/39ar ages of alkaline and tholeiitic rocks from the northern deccan traps: implications for magmatic processes and the k–pg boundary. *Journal of the Geological Society*, *173*(4), 679–688.

Passey, S. R., & Bell, B. R. (2007). Morphologies and emplacement mechanisms of the lava flows of the Faroe Islands Basalt Group, Faroe Islands, NE Atlantic Ocean. *Bulletin of Volcanology*, *70*(2), 139–156. doi: 10.1007/s00445-007-0125-6

Passmore, E., Maclennan, J., Fitton, G., & Thordarson, T. (2012, sep). Mush disaggregation in basaltic magma chambers: Evidence from the ad 1783 laki eruption. *Journal of Petrology*, *53*(12), 2593–2623. doi: 10.1093/petrology/egs061

Pastore, Z., Fichler, C., & McEnroe, S. A. (2018, apr). Magnetic anomalies of the mafic/ultramafic seiland igneous province. *Norwegian Journal of Geology*. doi: 10.17850/njg98-1-06

Patel, V., Sheth, H., Cucciniello, C., Joshi, G. W., Wegner, W., Samant, H., ... Koeberl, C. (2020). Geochemistry of deccan tholeiite flows and dykes of elephanta island: Insights into the stratigraphy and structure of the panvel flexure zone, western indian rifted margin. *Geosciences*, *10*(4), 118.

Pathak, V., Patil, S., & Shrivastava, J. (2017). Tectonomagmatic setting of lava packages in the mandla lobe of the eastern deccan volcanic province, india: palaeomagnetism and magnetostratigraphic evidence. *Geological Society, London, Special Publications*, *445*(1), 69–94.

Patil, S. K., Gadpallu, P., Monteiro, A., Sepahi, M. N., & Duraiswami, R. A. (2020). Characterising the bushe-poladpur contact across the western deccan traps and implications for mapping the k-pg boundary? *Journal of the Geological Society of India*, *95*(3), 227–240.

Patro, P. K., Raju, K., & Sarma, S. (2018). Some insights into the lithospheric electrical structure in the western ghat region from magnetotelluric studies. *Journal of the Geological Society of India*, *92*(5), 529–532.

Patro, P. K., & Sarma, S. (2016a, oct). Evidence for an extensive intrusive component of the deccan large igneous province in the narmada son lineament region, india from three dimensional magnetotelluric studies. *Earth and Planetary Science Letters*, *451*, 168–176. doi: 10.1016/j.epsl.2016.07.005

Patro, P. K., & Sarma, S. (2016b, oct). Evidence for an extensive intrusive component of the deccan large igneous province in the narmada son lineament region, india from three dimensional magnetotelluric studies. *Earth and Planetary Science Letters*, *451*, 168–176. doi: 10.1016/j.epsl.2016.07.005

Pattanayak, S., & Shrivastava, J. (1999). Petrography and major-oxide geochemistry of basalts from the eastern deccan volcanic province, india. *Memoirs-Geological Society of India*(2), 233–270.

Paul, D. K., Ray, A., Das, B., Patil, S. K., & Biswas, S. K. (2008). Petrology, geochemistry and paleomagnetism of the earliest magmatic rocks of deccan volcanic province, kutch, northwest india. *Lithos*, *102*(1-2), 237–259.

Pavlov, V. E., Fluteau, F., Latyshev, A. V., Fetisova, A. M., Elkins-Tanton, L. T., Black, B. A., ... Veselovskiy, R. V. (2019). Geomagnetic secular variations at the permian-triassic boundary and pulsed magmatism during eruption of the siberian traps. *Geochemistry, Geophysics, Geosystems*, *20*(2), 773–791.

Pawar, N. R., Katikar, A. H., Vaddadi, S., Shinde, S. H., Rajaguru, S. N., Joshi, S. V., & Eksambekar, S. P. (2015). The genesis of a lava cave in the deccan volcanic province (maharashtra, india). *International Journal of Speleology*, *45*(1), 6.

Peace, A., McCaffrey, K., Imber, J., van Hunen, J., Hobbs, R., & Wilson, R. (2018). The role of pre-existing structures during rifting, continental breakup and transform system development, offshore west greenland. *Basin Research*, *30*(3), 373–394.

Peate, D. W., Barker, A. K., Riishuus, M. S., & Andreasen, R. (2008). Temporal variations in crustal assimilation of magma suites in the east greenland flood basalt province: Tracking the evolution of magmatic plumbing systems. *Lithos*, *102*(1-2), 179–197.

Peate, D. W., & Hawkesworth, C. J. (1996). Lithospheric to asthenospheric transition in low-ti flood basalts from southern parana, brazil. *Chemical Geology*, *127*(1-3), 1–24.

Peng, Z., & Mahoney, J. (1995). Drillhole lavas from the northwestern deccan traps, and the evolution of réunion hotspot mantle. *Earth and Planetary Science Letters*, *134*(1-2), 169–185.

Peng, Z., Mahoney, J., Hooper, P., Harris, C., & Beane, J. (1994). A role for lower continental crust in flood basalt genesis? isotopic and incompatible element study of the lower six formations of the western deccan traps. *Geochimica et Cosmochimica Acta*, *58*(1), 267–288.

Peng, Z., Mahoney, J., Hooper, P., Macdougall, J., & Krishnamurthy, P. (1998). Basalts of the northeastern deccan traps, india: isotopic and elemental geochemistry and relation to southwestern deccan stratigraphy. *Journal of Geophysical Research: Solid Earth*, *103*(B12), 29843–29865.

Peng, Z., Walter, J., Aster, R., & Nyblade, A. (2014). Antarctic icequakes triggered by the 2010 Maule earthquake in Chile. *Nature ...*, *7*(August), 1–5. doi: 10.1038/NGEO2212

Peng, Z. X., Mahoney, J. J., Vanderkluysen, L., & Hooper, P. R. (2014). Sr, nd and pb isotopic and chemical compositions of central deccan traps lavas and relation to southwestern deccan stratigraphy. *Journal of Asian Earth Sciences*, *84*, 83–94.

Percival, L. M., Jenkyns, H. C., Mather, T. A., Dickson, A. J., Batenburg, S. J., Ruhl, M., ... others (2018). Does large igneous province volcanism always perturb the mercury cycle? comparing the records of oceanic anoxic event 2 and the end-cretaceous to other mesozoic events. *American Journal of Science*, *318*(8), 799–860.

Petcovic, H., & Grunder, A. (2003). Textural and thermal history of partial melting in tonalitic wallrock at the margin of a basalt dike, wallowa mountains, oregon. *Journal of Petrology*, *44*(12), 2287–2312.

Petcovic, H. L., & Dufek, J. D. (2005). Modeling magma flow and cooling in dikes: Implications for emplacement of columbia river flood basalts. *Journal of Geophysical Research: Solid Earth*, *110*(B10).

Peters, B. J., Day, J. M., Greenwood, R. C., Hilton, D. R., Gibson, J., & Franchi, I. A. (2017). Helium–oxygen–osmium isotopic and elemental constraints on the mantle sources of the deccan traps. *Earth and Planetary Science Letters*, *478*, 245–257.

Petford, N., & Mirhadizadeh, S. (2017). Image-based modelling of lateral magma flow: the basement sill, antarctica. *Royal Society open science*, *4*(5), 161083.

Philpotts, A. R. (1998). Nature of a flood-basalt-magma reservoir based on the compositional variation in a single flood-basalt flow and its feeder dike in the mesozoic hartford basin, connecticut. *Contributions to mineralogy and petrology*, *133*(1-2), 69–82.

Pitra, P., & De Waal, S. (2001). High-temperature, low-pressure metamorphism and development of prograde symplectites, marble hall fragment, bushveld complex (south africa). *Journal of Metamorphic Geology*, *19*(3), 311–325.

Potter, K. E., Shervais, J. W., Christiansen, E. H., & Vetter, S. K. (2018). Evidence for cyclical fractional crystallization, recharge, and assimilation in basalts of the kimama drill core, central snake river plain, idaho: 5.5-million-years of petrogenesis in a mid-crustal sill complex. *Frontiers in Earth Science*, *6*, 10.

Prasad, K., Singh, A., & Tiwari, V. (2018, aug). 3d upper crustal density structure of the deccan syneclise, central india. *Geophysical Prospecting*, *66*(8), 1625–1640. doi: 10.1111/1365-2478.12675

Prasanth, M. M., Hari, K., & Santosh, M. (2019, mar). Tholeiitic basalts of deccan large igneous province, india: An overview. *Geological Journal*. doi: 10.1002/gj.3497

Rabinowicz, M., & Ceuleneer, G. (2005). The effect of sloped isotherms on melt migration in the shallow mantle: A physical and numerical model based on observations in the Oman ophiolite. *Earth and Planetary Science Letters*, *229*(3-4), 231–246. doi: 10.1016/j.epsl.2004.09.039

Rader, E., Vanderkluysen, L., & Clarke, A. (2017). The role of unsteady effusion rates on inflation in long-lived lava flow fields. *Earth and Planetary Science Letters*, *477*, 73–83.

Rajaram, M., Anand, S., Erram, V. C., & Shinde, B. (2017). Insight into the structures below the deccan trap-covered region of maharashtra, india from geopotential data. *Geological Society, London, Special Publications*, *445*(1), 219–236.

Raju, S. (2016). Geological survey of india. *Proceedings of the Indian National Science Academy*, *82*(3), 1061–1081.

Ramakrishnan, M., & Vaidyanadhan, R. (2010). Geology of india (vol. 1 & 2). *GSI Publications*, *2*(1).

Rao, G. S., Kumar, M., & Radhakrishna, M. (2018, feb). Structure, mechanical properties and evolution of the lithosphere below the northwest continental margin of india. *International Journal of Earth Sciences*, *107*(6), 2191–2207. doi: 10.1007/s00531-018-1594-x

Rao, Y. B., Sreenivas, B., Kumar, T. V., Khadke, N., Krishna, A. K., & Babu, E. (2017). Evidence for neoarchean basement for the deccan volcanic flows around

koyna-warna region, western india: Zircon u-pb age and hf-isotopic results. *Journal of the Geological Society of India*, *90*(6), 752–760.

Ray, A., Paul, D., Patil, S., Das, B., & Biswas, S. (2010). Petrology, geochemistry and petrogenesis of the magmatic rocks of pachcham island, kutch, northwestern india. *Origin and Evolution of Deep Continental Crust. Narosa Publishing House Pvt. Ltd, New Delhi*, 217–236.

Ray, J. S., & Parthasarathy, G. (2019). Recent advancement in studies of deccan trap and its basement; carbonatites and kimberlites–an indian perspective in last five years. *Proceedings of the Indian National Science Academy*, *85*(2), 481–492.

Ray, L., Nagaraju, P., Singh, S., Ravi, G., & Roy, S. (2016). Radioelemental, petrological and geochemical characterization of the bundelkhand craton, central india: implication in the archaean geodynamic evolution. *International Journal of Earth Sciences*, *105*(4), 1087–1107.

Ray, R., Sheth, H. C., & Mallik, J. (2007). Structure and emplacement of the nandurbar–dhule mafic dyke swarm, deccan traps, and the tectonomagmatic evolution of flood basalts. *Bulletin of Volcanology*, *69*(5), 537.

Ray, R., Shukla, A. D., Sheth, H. C., Ray, J. S., Duraiswami, R. A., Vanderkluysen, L., ... Mallik, J. (2008). Highly heterogeneous precambrian basement under the central deccan traps, india: direct evidence from xenoliths in dykes. *Gondwana Research*, *13*(3), 375–385.

Reichow, M. K., Saunders, A., White, R., Al'Mukhamedov, A., & Medvedev, A. Y. (2005). Geochemistry and petrogenesis of basalts from the west siberian basin: an extension of the permo–triassic siberian traps, russia. *Lithos*, *79*(3-4), 425–452.

Reidel, S., Tolan, T., & Camp, V. (2018). Columbia river flood basalt flow emplacement rates—fast, slow, or variable. *Field Volcanology: A Tribute to the Distinguished Career of Don Swanson: Geological Society of America Special Paper*, *538*, 1–19.

Reidel, S. P. (1998). Emplacement of columbia river flood basalt. *Journal of Geophysical Research: Solid Earth*, *103*(B11), 27393–27410.

Reidel, S. P. (2005). A lava flow without a source: The cohassett flow and its compositional components, sentinel bluffs member, columbia river basalt group. *The Journal of geology*, *113*(1), 1–21.

Reidel, S. P., Camp, V. E., Tolan, T. L., & Martin, B. S. (2013). The columbia river flood basalt province: Stratigraphy, areal extent, volume, and physical volcanology. *The Columbia River flood basalt province: geological society of America special paper*, *497*, 1–43.

Renne, P. R., Balco, G., Ludwig, K. R., Mundil, R., & Min, K. (2011). Response to the comment by wh schwarz et al. on "joint determination of 40k decay constants and 40ar/40k for the fish canyon sanidine standard, and improved accuracy for 40ar/39ar geochronology" by pr renne et al.(2010). *Geochimica et Cosmochimica Acta*, *75*(17), 5097–5100.

Renne, P. R., Sprain, C. J., Richards, M. A., Self, S., Vanderkluysen, L., & Pande, K. (2015). State shift in deccan volcanism at the cretaceous-paleogene boundary, possibly induced by impact. *Science*, *350*(6256), 76–78.

Richards, M., Contreras-Reyes, E., Lithgow-Bertelloni, C., Ghiorso, M., & Stixrude, L. (2013). Petrological interpretation of deep crustal intrusive bodies beneath oceanic hotspot provinces. *Geochemistry, Geophysics, Geosystems*, *14*(3), 604–619. doi: 10.1029/2012GC004448

Richards, M. A., Alvarez, W., Self, S., Karlstrom, L., Renne, P. R., Manga, M., ... Gibson, S. A. (2015). Triggering of the largest Deccan eruptions by the Chicxulub impact. *Bulletin of the Geological Society of America*, *127*(11-12), 1507–1520. doi: 10.1130/B31167.1

Richards, M. A., Duncan, R. A., & Courtillot, V. E. (1989). Flood basalts and hot-spot tracks: plume heads and tails. *Science*, *246*(4926), 103–107.

Ridley, V. A., & Richards, M. A. (2010). Deep crustal structure beneath large igneous provinces and the petrologic evolution of flood basalts. *Geochemistry, Geophysics, Geosystems*, *11*(9), 1–21. doi: 10.1029/2009GC002935

Riisager, J., Riisager, P., & Pedersen, A. K. (2003). Paleomagnetism of large igneous provinces: case-study from west greenland, north atlantic igneous province. *Earth and Planetary Science Letters*, *214*(3-4), 409–425.

Rivalta, E., Taisne, B., Bunger, A. P., & Katz, R. F. (2015). A review of mechanical models of dike propagation: Schools of thought, results and future directions. *Tectonophysics*, *638*(C), 1–42. doi: 10.1016/j.tecto.2014.10.003

Robb, S. J., & Mungall, J. E. (2020). Testing emplacement models for the rustenburg layered suite of the bushveld complex with numerical heat flow models and plagioclase geospeedometry. *Earth and Planetary Science Letters*, *534*, 116084.

Roman, A., & Jaupart, C. (2016, nov). The fate of mafic and ultramafic intrusions in the continental crust. *Earth and Planetary Science Letters*, *453*, 131–140. doi: 10.1016/j.epsl.2016.07.048

Roman, A., & Jaupart, C. (2017). Postemplacement dynamics of basaltic intrusions in the continental crust. *Journal of Geophysical Research: Solid Earth*, *122*(2), 966–987.

Rowland, S. K., & Walker, G. P. (1990). Pahoehoe and aa in hawaii: volumetric flow rate controls the lava structure. *Bulletin of Volcanology*, *52*(8), 615–628.

Rubin, A. M. (1995). Propagation of magma-filled cracks. *Annual Review of Earth and Planetary Sciences*, *23*(1), 287–336.

Saha, G. K., Prakasam, K., & Rai, S. (2020). Diversity in the peninsular indian lithosphere revealed from ambient noise and earthquake tomography. *Physics of the Earth and Planetary Interiors*, 106523.

Sahoo, S., Rao, N. C., Monié, P., Belyatsky, B., Dhote, P., & Lehmann, B. (2020). Petro-geochemistry, srnd isotopes and 40ar/39ar ages of fractionated alkaline lamprophyres from the mount girnar igneous complex (nw india): Insights into the timing of magmatism and the lithospheric mantle beneath the deccan large igneous province. *Lithos*, *374*, 105712.

Samant, H., Patel, V., Pande, K., Sheth, H., & Jagadeesan, K. (2019). 40ar/39ar dating of tholeiitic flows and dykes of elephanta island, panvel flexure zone, western deccan traps: A five-million-year record of magmatism preceding india-laxmi ridge-seychelles breakup. *Journal of Volcanology and Geothermal Research*, *379*, 12–22.

Sano, T., Fujii, T., Deshmukh, S., Fukuoka, T., & Aramaki, S. (2001). Differentiation processes of deccan trap basalts: contribution from geochemistry and experimental petrology. *Journal of Petrology*, *42*(12), 2175–2195.

Sant, D., & Karanth, R. (1990). Emplacement of dyke swarms in lower narmada valley, western india. In *International dyke conference. 2* (pp. 383–389).

Schiemenz, A., Liang, Y., & Parmentier, E. M. (2011). A high-order numerical study of reactive dissolution in an upwelling heterogeneous mantle-I. Channelization, channel lithology and channel geometry. *Geophysical Journal International*, *186*(2), 641–664. doi: 10.1111/j.1365-246X.2011.05065.x

Schmeling, H., Marquart, G., & Grebe, M. (2018). A porous flow approach to model thermal non-equilibrium applicable to melt migration. *Geophysical Journal International*, *212*(1), 119–138.

Schmeling, H., Marquart, G., Weinberg, R., & Wallner, H. (2019, jan). Modelling melting and melt segregation by two-phase flow: new insights into the dynamics of magmatic systems in the continental crust. *Geophysical Journal International*, *217*(1), 422–450. doi: 10.1093/gji/ggz029

Schöbel, S., de Wall, H., Ganerød, M., Pandit, M. K., & Rolf, C. (2014). Magnetostratigraphy and 40ar–39ar geochronology of the malwa plateau region (northern deccan traps), central western india: Significance and correlation with the main deccan large igneous province sequences. *Journal of Asian Earth Sciences*, *89*, 28–45.

Schoene, B., Eddy, M. P., Samperton, K. M., Keller, C. B., Keller, G., Adatte, T., & Khadri, S. F. (2019). U-pb constraints on pulsed eruption of the deccan traps across the end-cretaceous mass extinction. *Science*, *363*(6429), 862–866.

Schoene, B., Samperton, K. M., Eddy, M. P., Keller, G., Adatte, T., Bowring, S. A., ... Gertsch, B. (2015). U-pb geochronology of the deccan traps and relation to the end-cretaceous mass extinction. *Science*, *347*(6218), 182–184.

Schofield, N., Brown, D. J., Magee, C., & Stevenson, C. T. (2012). Sill morphology and comparison of brittle and non-brittle emplacement mechanisms. *Journal of Structural Geology*, *169*(Baer 1995), 127–141. doi: 10.1144/0016-76492011-078 .Sill

Scoon, R. N., & Costin, G. (2018). Chemistry, morphology and origin of magmatic-reaction chromite stringers associated with anorthosite in the upper critical zone at winnaarshoek, eastern limb of the bushveld complex. *Journal of Petrology*, *59*(8), 1551–1578.

Scoon, R. N., Costin, G., Mitchell, A., & Moine, B. (2020). Non-sequential injection of pge-rich ultramafic sills in the platreef unit at akanani, northern limb of the bushveld complex: Evidence from sr and nd isotopic systematics. *Journal of Petrology*.

Self, S., Jay, A. E., Widdowson, M., & Keszthelyi, L. P. (2008). Correlation of the deccan and rajahmundry trap lavas: Are these the longest and largest lava flows on earth? *Journal of Volcanology and Geothermal Research*, *172*(1-2), 3–19.

Self, S., Keszthelyi, L., & Thordarson, T. (1998). The importance of pāhoehoe. *Annual Review of Earth and Planetary Sciences*, *26*(1), 81–110.

Self, S., Schmidt, A., & Mather, T. (2014). Emplacement characteristics, time scales, and volcanic gas release rates of continental flood basalt eruptions on earth. *Geological Society of America Special Papers*, *505*.

Self, S., Thordarson, T., & Keszthelyi, L. (1997). Emplacement of continental flood basalt lava flows. *Geophysical Monograph - American Geophysical Union*, *100*, 381–410.

Sen, A., Pande, K., Hegner, E., Sharma, K. K., Dayal, A., Sheth, H. C., & Mistry, H. (2012). Deccan volcanism in rajasthan: 40ar–39ar geochronology and geochemistry of the tavidar volcanic suite. *Journal of Asian Earth Sciences*, *59*, 127–140.

Sen, B. (2017). Lava flow transition in pāhoehoe-dominated lower pile of deccan traps from manmad-chandwad area, western maharashtra. *Journal of the Geological Society of India*, *89*(3), 281–290.

Sen, G. (2001). Generation of deccan trap magmas. *Journal of Earth System Science*, *110*(4), 409–431.

Sen, G., Bizimis, M., Das, R., Paul, D. K., Ray, A., & Biswas, S. (2009). Deccan plume, lithosphere rifting, and volcanism in kutch, india. *Earth and Planetary Science Letters*, *277*(1-2), 101–111.

Sen, G., & Chandrasekharam, D. (2011). Deccan traps flood basalt province: An evaluation of the thermochemical plume model. In *Topics in igneous petrology* (pp. 29–53). Springer.

Sengupta, P., & Ray, A. (2006). Primary volcanic structures from a type section of deccan trap flows around narsingpur-harrai-amarwara, central india: Implications for cooling history. *Journal of earth system science*, *115*(6), 631–642.

Sengupta, P., & Ray, J. (2011). Petrology of the mafic sill of narshingpur-lakhnadon section, eastern deccan volcanic province. *Journal of the Geological Society of*

India, *77*(4), 309–327.

Seshu, D., Rao, P. R., & Naganjaneyulu, K. (2016, jan). Three-dimensional gravity modelling of kutch region, india. *Journal of Asian Earth Sciences*, *115*, 16–28. doi: 10.1016/j.jseaes.2015.09.015

Sharma, J., Kumar, M. R., Roy, K. S., & Roy, P. (2018). Seismic imprints of plume-lithosphere interaction beneath the northwestern deccan volcanic province. *Journal of Geophysical Research: Solid Earth*, *123*(12), 10–831.

Shaw, H., & Swanson, D. A. (1970). Eruption and flow rates of flood basalts. In *Proceedings of the second columbia river basalt symposium* (pp. 271–299).

Sheikh, J. M., Sheth, H., Naik, A., & Keluskar, T. (2020). Physical volcanology of the pavagadh rhyolites, northern deccan traps: Stratigraphic, structural, and textural record of explosive and effusive eruptions. *Journal of Volcanology and Geothermal Research*, *404*, 107024.

Sheldon, N. D. (2003). Pedogenesis and geochemical alteration of the picture gorge subgroup, columbia river basalt, oregon. *Geological Society of America Bulletin*, *115*(11), 1377–1387.

Shellnutt, J. G., Yeh, M.-W., Suga, K., Lee, T.-Y., Lee, H.-Y., & Lin, T.-H. (2017). Temporal and structural evolution of the early palaeogene rocks of the seychelles microcontinent. *Scientific reports*, *7*(1), 1–7.

Sheth, H. (2016). Giant plagioclase basalts: Continental flood basalt–induced remobilization of anorthositic mushes in a deep crustal sill complex. *Bulletin*, *128*(5-6), 916–925.

Sheth, H., & Chandrasekharam, D. (1997). Early alkaline magmatism in the deccan traps: implications for plume incubation and lithospheric rifting. *Physics of the Earth and Planetary Interiors*, *104*(4), 371–376.

Sheth, H., Mahoney, J., & Chandrasekharam, D. (2004). Geochemical stratigraphy of deccan flood basalts of the bijasan ghat section, satpura range, india. *Journal of Asian Earth Sciences*, *23*(1), 127–139.

Sheth, H., Pande, K., Vijayan, A., Sharma, K. K., & Cucciniello, C. (2017). Recurrent early cretaceous, indo-madagascar (89–86 ma) and deccan (66 ma) alkaline magmatism in the sarnu-dandali complex, rajasthan: 40ar/39ar age evidence and geodynamic significance. *Lithos*, *284*, 512–524.

Sheth, H., Vanderkluysen, L., Demonterova, E. I., Ivanov, A. V., & Savatenkov, V. M. (2018, mar). Geochemistry and 40 ar/39 ar geochronology of the nandurbar-dhule mafic dyke swarm: Dyke-sill-flow correlations and stratigraphic development across the deccan flood basalt province. *Geological Journal*, *54*(1), 157–176. doi: 10.1002/gj.3167

Sheth, H., Vanderkluysen, L., Demonterova, E. I., Ivanov, A. V., & Savatenkov, V. M. (2019). Geochemistry and 40ar/39ar geochronology of the nandurbar-dhule mafic dyke swarm: Dyke-sill-flow correlations and stratigraphic development across the deccan flood basalt province. *Geological Journal*, *54*(1), 157–176.

Sheth, H. C. (2005). Were the deccan flood basalts derived in part from ancient oceanic crust within the indian continental lithosphere? *Gondwana Research*, *8*(2), 109–127.

Sheth, H. C., & Cañón-Tapia, E. (2015). Are flood basalt eruptions monogenetic or polygenetic? *International Journal of Earth Sciences*, *104*(8), 2147–2162.

Sheth, H. C., & Melluso, L. (2008). The mount pavagadh volcanic suite, deccan traps: geochemical stratigraphy and magmatic evolution. *Journal of Asian Earth Sciences*, *32*(1), 5–21.

Sheth, H. C., Pande, K., & Bhutani, R. (2001a). 40 ar-39 ar age of a national geological monument: the gilbert hill basalt, deccan traps, bombay. *Current Science (Bangalore)*, *80*(11), 1437–1440.

Sheth, H. C., Pande, K., & Bhutani, R. (2001b). 40ar-39ar ages of bombay trachytes: Evidence for a palaeocene phase of deccan volcanism. *Geophysical Re-*

search Letters, *28*(18), 3513–3516.

Sheth, H. C., Ray, J. S., Ray, R., Vanderkluysen, L., Mahoney, J. J., Kumar, A., ... Jana, B. (2009). Geology and geochemistry of pachmarhi dykes and sills, satpura gondwana basin, central india: problems of dyke-sill-flow correlations in the deccan traps. *Contributions to Mineralogy and Petrology*, *158*(3), 357.

Sheth, H. C., Zellmer, G. F., Demonterova, E. I., Ivanov, A. V., Kumar, R., & Patel, R. K. (2014). The deccan tholeiite lavas and dykes of ghatkopar–powai area, mumbai, panvel flexure zone: geochemistry, stratigraphic status, and tectonic significance. *Journal of Asian Earth Sciences*, *84*, 69–82.

Sheth, H. C., Zellmer, G. F., Kshirsagar, P. V., & Cucciniello, C. (2013). Geochemistry of the palitana flood basalt sequence and the eastern saurashtra dykes, deccan traps: clues to petrogenesis, dyke–flow relationships, and regional lava stratigraphy. *Bulletin of Volcanology*, *75*(4), 701.

Shrivastava, J., Duncan, R. A., & Kashyap, M. (2015). Post-k/pb younger 40ar–39ar ages of the mandla lavas: implications for the duration of the deccan volcanism. *Lithos*, *224*, 214–224.

Shrivastava, J., Kumar, R., & Rani, N. (2017). Feeder and post deccan trap dyke activities in the northern slope of the satpura mountain: Evidence from new 40ar-39ar ages. *Geoscience Frontiers*, *8*(3), 483–492.

Shrivastava, J., Mahoney, J., & Kashyap, M. (2014). Trace elemental and nd-sr-pb isotopic compositional variation in 37 lava flows of the mandla lobe and their chemical relation to the western deccan stratigraphic succession, india. *Mineralogy and Petrology*, *108*(6), 801–817.

Shrivastava, J., MUKTA, G., & RAJU, K. (2008). Petrography, composition and petrogenesis of basalts from chakhla-delakhari intrusive complex, eastern deccan volcanic province, india. indian dykes: Geochemistry. *Geophysics and Geochronology*, 83–108.

Shrivastava, J., & Pattanayak, S. (2002). Basalts of the eastern deccan volcanic province, india. *Gondwana Research*, *5*(3), 649–665.

Shukla, A., Bhandari, N., Kusumgar, S., Shukla, P., Ghevariya, Z., Gopalan, K., & Balaram, V. (2001). Geochemistry and magnetostratigraphy of deccan flows at anjar, kutch. *Journal of Earth System Science*, *110*(2), 111–132.

Sial, A., Lacerda, L., Ferreira, V., Frei, R., Marquillas, R., Barbosa, J., ... Pereira, N. (2013). Mercury as a proxy for volcanic activity during extreme environmental turnover: The cretaceous–paleogene transition. *Palaeogeography, Palaeoclimatology, Palaeoecology*, *387*, 153–164.

Singh, A., Singh, C., & Kennett, B. L. N. (2015). Tectonophysics A review of crust and upper mantle structure beneath the Indian subcontinent. *Tectonophysics*, *644-645*, 1–21. doi: 10.1016/j.tecto.2015.01.007

Singh, B., Rao, M. P., Prajapati, S., & Swarnapriya, C. (2014a). Combined gravity and magnetic modeling over pavagadh and phenaimata igneous complexes, gujarat, india: Inference on emplacement history of deccan volcanism. *Journal of Asian Earth Sciences*, *80*, 119–133.

Singh, B., Rao, M. P., Prajapati, S., & Swarnapriya, C. (2014b, feb). Combined gravity and magnetic modeling over pavagadh and phenaimata igneous complexes, gujarat, india: Inference on emplacement history of deccan volcanism. *Journal of Asian Earth Sciences*, *80*, 119–133. doi: 10.1016/j.jseaes.2013.11.005

Sobolev, S. V., Sobolev, A. V., Kuzmin, D. V., Krivolutskaya, N. a., Petrunin, A. G., Arndt, N. T., ... Vasiliev, Y. R. (2011). Linking mantle plumes, large igneous provinces and environmental catastrophes. *Nature*, *477*(7364), 312–316. doi: 10.1038/nature10385

Solano, J. M. S., Jackson, M. D., Sparks, R. S. J., Blundy, J. D., & Annen, C. (2012). Melt segregation in deep crustal hot zones: A mechanism for chemical differentiation, crustal assimilation and the formation of evolved magmas.

Journal of Petrology, *53*(10), 1999–2026. doi: 10.1093/petrology/egs041

Song, X.-Y., Zhou, M.-F., Keays, R. R., Cao, Z.-M., Sun, M., & Qi, L. (2006). Geochemistry of the emeishan flood basalts at yangliuping, sichuan, sw china: implications for sulfide segregation. *Contributions to Mineralogy and Petrology*, *152*(1), 53–74.

Spera, F. J., & Bohrson, W. A. (2001). Energy-constrained open-system magmatic processes i: General model and energy-constrained assimilation and fractional crystallization (ec-afc) formulation. *Journal of Petrology*, *42*(5), 999–1018.

Spera, F. J., & Bohrson, W. A. (2002). Energy-constrained open-system magmatic processes 3. energy-constrained recharge, assimilation, and fractional crystallization (ec-rafc). *Geochemistry, Geophysics, Geosystems*, *3*(12), 1–20.

Sprain, C. J., Renne, P. R., Clemens, W. A., & Wilson, G. P. (2018). Calibration of chron c29r: New high-precision geochronologic and paleomagnetic constraints from the hell creek region, montana. *Bulletin*, *130*(9-10), 1615–1644.

Sprain, C. J., Renne, P. R., Vanderkluysen, L., Pande, K., Self, S., & Mittal, T. (2019). The eruptive tempo of deccan volcanism in relation to the cretaceous-paleogene boundary. *Science*, *363*(6429), 866–870.

Srivastava, R. K., Wang, F., & Shi, W. (2020). Substantiation of réunion plume induced prolonged magmatic pulses (ca. 70.5–65.5 ma) of the deccan lip in the chhotanagpur gneissic complex, eastern india: Constraints from 40 ar/39 ar geochronology. *Journal of Earth System Science*, *129*(1), 1–10.

Subbarao, K., Bodas, M., Hooper, P., & Walsh, J. (1988). Petrogenesis of jawhar and igatpuri formations, western deccan basalt province. *Memoir-Geological Society of India*(10), 253–280.

Subbarao, K. V. (1988). *Deccan flood basalts* (Vol. 10). Geological Society of India.

Sukheswala, R. (1981). Deccan basalt volcanism. *Memoir-Geological Society of India*(3), 8–18.

Svensen, H., Corfu, F., Polteau, S., Hammer, Ø., & Planke, S. (2012). Rapid magma emplacement in the karoo large igneous province. *Earth and Planetary Science Letters*, *325*, 1–9.

Svensen, H., Torsvik, T., Callegaro, S., Augland, L., Heimdal, T., Jerram, D., ... Pereira, E. (2018). Gondwana large igneous provinces: plate reconstructions, volcanic basins and sill volumes. *Geological Society, London, Special Publications*, *463*(1), 17–40.

Svensen, H. H., Frolov, S., Akhmanov, G. G., Polozov, A. G., Jerram, D. A., Shiganova, O. V., ... Planke, S. (2018). Sills and gas generation in the siberian traps. *Philosophical Transactions of the Royal Society A: Mathematical, Physical and Engineering Sciences*, *376*(2130), 20170080.

Talusani, R. V. (2010). Bimodal tholeiitic and mildly alkalic basalts from bhir area, central deccan volcanic province, india: Geochemistry and petrogenesis. *Journal of Volcanology and Geothermal Research*, *189*(3-4), 278–290.

Talusani, R. V. (2012). Giant plagioclase basalts from northeastern deccan volcanic province, india: Implications for their origin and petrogenetic significance.

Tegner, C., Michelis, S. A., McDonald, I., Brown, E. L., Youbi, N., Callegaro, S., ... Marzoli, A. (2019). Mantle dynamics of the central atlantic magmatic province (camp): Constraints from platinum group, gold and lithophile elements in flood basalts of morocco. *Journal of Petrology*, *60*(8), 1621–1652.

Tewari, H. C., Prasad, B. R., & Kumar, P. (2018a). Central indian region. In *Structure and tectonics of the indian continental crust and its adjoining region* (pp. 147–174). Elsevier. doi: 10.1016/b978-0-12-813685-0.00006-6

Tewari, H. C., Prasad, B. R., & Kumar, P. (2018b). Deccan volcanic province near the west coast. In *Structure and tectonics of the indian continental crust and its adjoining region* (pp. 115–145). Elsevier. doi: 10.1016/b978-0-12-813685-0.00005-4

Thordarson, T., Miller, D., Larsen, G., Self, S., & Sigurdsson, H. (2001). New estimates of sulfur degassing and atmospheric mass-loading by the 934 ad eldgjá eruption, iceland. *Journal of Volcanology and Geothermal Research*, *108*(1-4), 33–54.

Thordarson, T., & Self, S. (1993). The laki (skaftár fires) and grímsvötn eruptions in 1783–1785. *Bulletin of Volcanology*, *55*(4), 233–263.

Thordarson, T., & Self, S. (1998). The roza member, columbia river basalt group: A gigantic pahoehoe lava flow field formed by endogenous processes? *Journal of Geophysical Research: Solid Earth*, *103*(B11), 27411–27445.

Thybo, H., & Artemieva, I. M. (2013). Moho and magmatic underplating in continental lithosphere. *Tectonophysics*, *609*, 605–619.

Tolan, T. L. (1989). Revision on the extent and volume of the columbia river basalt group. *Geol. Soc. Am. Spec. Paper*, *239*, 1–20.

Tolia, N., & Sethna, S. (1990). Lopolithic intrusion of basalt in the intertrappeans at amboli hill, jogeshwari, bombay. *J. Geol. Soc. India*, *35*, 524–528.

Tomshin, M., Kopylova, A., & Tyan, O. (2005). Petrochemical variability of traps at the eastern periphery of the tungus basin. *Russ. Geol. Geophys*, *46*, 72–82.

Tomshin, M., Kopylova, A., Vasilyeva, A., & Zaitsev, A. (2014). Geochemical and isotope characteristics of intrusive traps in the eastern siberian platform. *International Multidisciplinary Scientific GeoConference: SGEM: Surveying Geology & mining Ecology Management*, *1*, 113.

Torsvik, T. H. (2020). Connecting the deep earth and the atmosphere.

Townsend, M., Huber, C., Degruyter, W., & Bachmann, O. (2019). Magma chamber growth during inter-caldera periods: insights from thermo-mechanical modeling with applications to laguna del maule, campi flegrei, santorini, and aso. *Geochemistry, Geophysics, Geosystems*.

Turner, S., & Hawkesworth, C. (1995). The nature of the sub-continental mantle: constraints from the major-element composition of continental flood basalts. *Chemical Geology*, *120*(3-4), 295–314.

Vanderkluysen, L., Mahoney, J. J., Hooper, P. R., Sheth, H. C., & Ray, R. (2011). The feeder system of the Deccan Traps (India): Insights from dike geochemistry. *Journal of Petrology*, *52*(2), 315–343. doi: 10.1093/petrology/egq082

Vedanti, N., Malkoti, A., Pandey, O. P., & Shrivastava, J. P. (2018, mar). Ultrasonic p- and s-wave attenuation and petrophysical properties of deccan flood basalts, india, as revealed by borehole studies. *Pure and Applied Geophysics*, *175*(8), 2905–2930. doi: 10.1007/s00024-018-1817-x

Verma, O., & Khosla, A. (2019). Developments in the stratigraphy of the deccan volcanic province, peninsular india. *Comptes Rendus Geoscience*, *351*(7), 461–476.

Vye-Brown, C., Barry, T., & Self, S. (2018). Revealing emplacement dynamics of a simple flood basalt eruption unit using systematic compositional heterogeneities. *Field Volcanology: A Tribute to the Distinguished Career of Don Swanson*, *538*, 21.

Vye-Brown, C., Gannoun, A., Barry, T., Self, S., & Burton, K. (2013). Osmium isotope variations accompanying the eruption of a single lava flow field in the columbia river flood basalt province. *Earth and Planetary Science Letters*, *368*, 183–194.

Vye-Brown, C., Self, S., & Barry, T. (2013). Architecture and emplacement of flood basalt flow fields: case studies from the columbia river basalt group, nw usa. *Bulletin of Volcanology*, *75*(3), 697.

Wager, L., & Brown, G. (1968). Layered igneous intrusions. *Edinburgh and London: Oliver and Boyd*, 1–588.

Waichel, B. L., de Lima, E. F., Lubachesky, R., & Sommer, C. A. (2006). Pahoehoe flows from the central paraná continental flood basalts. *Bulletin of Volcanology*, *68*(7-8), 599–610.

White, C. M. (2007). The graveyard point intrusion: An example of extreme differentiation of snake river plain basalt in a shallow crustal pluton. *Journal of Petrology*, *48*(2), 303–325.

White, J. D., Bryan, S. E., Ross, P.-S., Self, S., & Thordarson, T. (2009). Physical volcanology of continental large igneous provinces: update and review. *Studies in volcanology: the legacy of George Walker. Special Publications of IAVCEI*, *2*, 291–321.

White, R., & McKenzie, D. (1989). Magmatism at rift zones: The generation of volcanic continental margins and flood basalts. *Journal of Geophysical Research*, *94*(B6), 7685. doi: 10.1029/JB094iB06p07685

White, R., & McKenzie, D. (1995). Mantle plumes and flood basalts. *Journal of Geophysical Research: Solid Earth*, *100*(B9), 17543–17585.

Widdowson, M., Pringle, M., & Fernandez, O. (2000). A post k–t boundary (early palaeocene) age for deccan-type feeder dykes, goa, india. *Journal of Petrology*, *41*(7), 1177–1194.

Wignall, P. B. (2001). Large igneous provinces and mass extinctions. *Earth-science reviews*, *53*(1-2), 1–33.

Wilkinson, C. M., Ganerød, M., Hendriks, B. W., & Eide, E. A. (2017). Compilation and appraisal of geochronological data from the north atlantic igneous province (naip). *Geological Society, London, Special Publications*, *447*(1), 69–103.

Wolff, J., & Ramos, F. (2013). Source materials for the main phase of the Columbia River Basalt Group: Geochemical evidence and implications for magma storage and transport. *Geological Society of America Special Papers*, *497*(11), 273–291. doi: 10.1130/2013.2497(11)

Wrona, T., Magee, C., Fossen, H., Gawthorpe, R. L., Bell, R., Jackson, C.-L., & Faleide, J. I. (2019). 3-d seismic images of an extensive igneous sill in the lower crust. *Geology*, *47*(8), 729–733.

Yarushina, V. M., Podladchikov, Y. Y., & Connolly, J. a. D. (2015, jul). (De)compaction of porous viscoelastoplastic media: Solitary porosity waves. *Journal of Geophysical Research: Solid Earth*, *120*(7), 4843–4862. doi: 10.1002/2014JB011260

Yu, X., Lee, C.-T. A., Chen, L.-H., & Zeng, G. (2015). Magmatic recharge in continental flood basalts: Insights from the chifeng igneous province in inner mongolia. *Geochemistry, Geophysics, Geosystems*, *16*(7), 2082–2096.

Zieg, M., & Marsh, B. (2012). Multiple reinjections and crystal-mush compaction in the beacon sill, mcmurdo dry valleys, antarctica. *Journal of Petrology*, *53*(12), 2567–2591.

Zieg, M. J., & Wallrich, B. M. (2018). Emplacement and differentiation of the black sturgeon sill, nipigon, ontario: A principal component analysis. *Journal of Petrology*, *59*(12), 2385–2412.